Title
Elucidating Mechanisms and Improving Models of Traumatic Brain Injury for Treatment

Permalink
https://escholarship.org/uc/item/94z07896

Author
Chou, Austin C.

Publication Date
2017

Peer reviewed|Thesis/dissertation

Elucidating Mechanisms and Improving Models of Traumatic Brain
Injury for Treatment

by

Austin C Chou

DISSERTATION

Submitted in partial satisfaction of the requirements for the degree of

DOCTOR OF PHILOSOPHY

in

Neuroscience

in the

GRADUATE DIVISION

of the

UNIVERSITY OF CALIFORNIA, SAN FRANCISCO

Dedication

To my parents especially with their unconditional support.

To my friends and family to whom I attribute a statistically significant part of my growth.

And to Dr. Susanna Rosi for her unending mentorship, guidance, and force of will.

Acknowledgements

I'd like to first acknowledge my friends and family. To my friends, from high school to Berkeley and finally UCSF, I owe a great deal for their encouragement and care. I also had the great fortune of having close family – the Chang gang – in California and the bay area that were a constant source of comfort. Beyond maintaining my sanity, every single one of my friends and family have played a great part in my personal growth. These relationships that I was fortunate have had are by far one of the best parts of my last seven years.

Of course, I'd like to particularly acknowledge my parents, Dr. Chen-Shih Chou and Hsien-Fen Chang, who have sacrificed much. I will always be grateful to them for giving me the opportunities I have had.

I also want to recognize Elaine Tay and her immense patience in all the time we have been together. My time at UCSF was likely more trying for her than for I, and yet she has stood by me.

I would like to thank everyone in the scientific community that have guided me and provided sage advice. More specifically, Dr. Louis Reichardt and Dr. Roger Nicoll have offered words of wisdom and genuine kindness during some rather tumultuous times. Dr. Wanda Kwan, Dr. Josh Morganti, and Dr. Karen Krukowski have become co-mentors at various stages of my graduate student career and considerably shaped my scientific perspective, and I am continually in awe of their scientific acumen. I also want to extend my gratitude to my thesis committee: Dr. Linda Noble, Dr. Saul Villeda, and Dr. Vikaas Sohal. They have all been incredibly supportive and reasonable beyond words, and I could not have asked for a better committee. And to all members of my

previous and current labs, thank you for creating such welcoming environments; I had no lack of people I could depend upon because of you all.

And of course, of course, I must thank Dr. Susanna Rosi, my advisor, mentor, and a close confidant. The sentiment "I would never have finished graduate school without her" cannot be stressed enough. She is not only an upstanding and brilliant scientist but also an indominable force of nature, and I have come this far because of her unrelenting inspiration.

Lastly, I would like to explicitly thank the contributors and collaborators in this dissertation. In Chapter 2: Dr. Saul Villeda and Patrick Ventura. In Chapter 3, published in the Proceedings of the National Academy of Sciences of the United States of America in 2017 (doi: 10.1073/pnas.1707661114): Dr. Karen Krukowski, Timothy Jopson, Dr. Ping Jun Zhu, Dr. Mauro Costa-Mattioli, and Dr. Peter Walter. Lastly, in Chapter 4, published in PLoS ONE in 2016 (doi: 10.1371/journal.pone.0151418): Dr. Josh Morganti. The two latter chapters have been reformatted from the publications, but the content remains unchanged.

Abstract

Traumatic brain injury (TBI) is the leading cause of neurological disability and the primary risk factor for development of neurodegenerative diseases and dementia in the United States. Over 2 million TBI-related incidents occur each year, and 3-5 million people currently suffer from chronic TBI-related disabilities. With the incidence of TBI on the rise, it is increasingly important to understand the underlying injury mechanisms and develop treatments for current and future patients. This dissertation investigates two such mechanisms contributing to TBI-induced cognitive decline, broadens the scope of TBI research to understand the effect of aging, and describes a new mouse model for frontal lobe TBI.

In chapter 1, I investigated the effect of aging on TBI-induced cognitive deficits and inflammatory response with emphasis on the contribution of peripheral, infiltrating monocytes. Our mouse model of TBI showed significantly greater chronic impairment of spatial memory in aging mice. Aging also exacerbated the infiltration of the peripheral monocytes while impairing expression of anti-inflammatory markers in peripheral monocytes and resident microglia. Furthermore, I observed that a subpopulation of the peripheral monocytes regained proliferative capabilities after infiltrating the injured brain, and the effect was significantly more pronounced in the old mice. In chapter 2, I targeted the integrated stress response (ISR) pathway using a novel small molecule at a chronic timepoint after injury. Inhibition of the ISR during behavioral testing fully restored spatial learning and memory in two different mouse models of TBI. The treatment additionally rescued deficits in long-term potentiation in the hippocampus at the chronic timepoint. In chapter 3, I applied the controlled cortical impact method to

develop a frontal lobe injury mouse model to better mimic TBIs commonly observed among human patients. Markedly, mice that had received the frontal lobe TBI displayed deficits in prefrontal cortex-driven behavior similar to symptoms seen in human TBI patients. These chapters collectively add to our understanding of the biology of TBIs with the hope that we are a step closer to providing effective treatment for a major health crisis in the future.

Table of Contents

List of Figures

Chapter 2

Chapter 3

Chapter 4

Chapter 1: General Introduction

TBI epidemiology

Traumatic brain injury (TBI) is a fast growing health care crisis with estimates of 2 million reported TBI-related incidents each year and 3-5 million people in the United States currently living with TBI-related disabilities (1). Furthermore, it is one of the principal environmental risk factors for development of neurodegenerative diseases and dementia (2, 3). Though the mortality rate of TBIs has declined since 2007, the overall incidence of TBI continues to rise each year (4). The CDC broadly defines TBI as disruption of normal brain functions caused by a bump, blow, or jolt to the head or a penetrating head injury (1, 4). TBI can occur in a variety of circumstances including traffic accidents, falls, sports, violence/assault, and blasts experienced by active-duty military personnel (5, 6). The wide spectrum of injuries are clinically classified as mild, moderate, or severe based on presentation of symptoms with a respective distribution of approximately 80%, 10%, and 10% (1, 7). However, even mild TBIs can produce long-term dysfunction of motor behaviors, cognition, and emotion processes in patients (6) Predicting patient outcome is complicated; chronic symptoms are dependent upon a multitude of variables, including location and extent of injury, preexisting conditions, psychosocial factors, and possible post-injury treatments (8). The diversity of causes and complexity of injury responses have ultimately hindered the development of effective treatments by researchers trying to model and study mechanisms of TBI (9, 10).

Mouse models of TBI

TBI consists of two phases of injury. The first phase is the primary injury during and immediately after impact. The mechanical trauma leads to gross tissue deformation, hemorrhaging, sheering of brain cells, and activation of apoptotic pathways in damaged cells (11, 12). TBI also activates various signaling cascades that produce inflammation, free radical production, mitochondrial damage, and excitotoxicity which can contribute to further neuronal death and dysfunction (11, 13-15). These pathways can be active for weeks after the initial injury event and are collectively labeled as the secondary injury phase of TBI. Secondary injuries are the focus of most TBI research as they present broader temporal windows for potential treatment compared to the immediate primary injury (12).

There are a variety of animal models that attempt to mimic the secondary injuries of TBI seen in human patients. The four most common techniques are controlled cortical impact (CCI) (16, 17), fluid percussion injury (FPI) (18), weight drop/impact acceleration models (19, 20), and blast injury models. These models were each originally developed to mimic a subset of human injuries, for example CCI for focal contusion and weight drop for diffuse injuries (12, 21). In the following studies, we utilized the CCI model which is well established for simulating focal contusion mechanisms observed in human patients (16, 17, 22).

The CCI model involves driving an impactor through a craniectomy to injure the brain. The craniectomy is just large enough to fit the impactor tip, and the skull is removed without disrupting the dura between the bone and brain (12, 23). The model induces cortical tissue loss, acute hematoma, blood brain barrier dysfunction, and axonal injury (16, 17). The injury is typically delivered unilaterally over the parietal cortex

using coordinates defined from bregma and lambda (12, 16). The CCI is thus easily reproducible due to the well-defined location of the injury site and use of a stereotaxic frame to prevent movement of the animal's head during the procedure. The velocity, depth, and dwell time parameters of the CCI can also be adjusted to model different injury severities (17, 24).

In all variants, CCI produces cortical contusion and corresponding tissue loss at the site of impact (16, 22). The size and depth of the resulting cavitation have been used to loosely categorize the injury severity (mild, moderate, and severe) across studies and is affected by changing any of the three impact parameters (16, 17, 25). More importantly, CCI is well established as a model for secondary injury pathways as it reliably produces neuronal death distal to the immediate injury site. For example, CCI injuries that spare the hippocampus from anatomical tissue loss still result in significant hippocampal neuronal death (25-27). Severe CCI injuries can even affect neuronal survival in the contralateral hippocampus (28). Similarly, significant cell death has been observed in the corpus callosum and thalamus within 2-7 days after moderate-to-severe CCI without any lesioning of the regions by the impactor (29).

Mice and rats subjected to CCI injuries correspondingly exhibit behavioral deficits both acutely and chronically after TBI. Post-TBI recovery in animals is often evaluated through a neurological severity score (NSS), which is a battery of various motor tests such as limb flexing, gait, and reflexes. These motor functions are notably impaired up to three weeks post-TBI after a mild-to-moderate CCI (30, 31). The same pattern of recovery is reflected on fine motor assays such as the balance beam and rotarod that better mirror balance and coordination problems seen in patients (30, 32). Likewise,

3

cognition has been studied in the CCI model. The two most notable cognitive assays used are the Morris Water Maze and radial arm water maze (RAWM), both of which measure spatial learning and memory (33). Unlike motor deficits, spatial learning and memory remain impaired even at several weeks and months post-injury for rats and mice with mild-to-moderate TBIs (22, 23, 34, 35). CCI injury thus serves as a reliable, reproducible and widely used model for assessing secondary injury mechanisms that produce long-lasting cognitive deficits. Furthermore, we also expanded the use of CCI by developing a frontal lobe injury model and a closed head injury model with the technique to reproduce frontal cortex injuries and diffuse concussive injuries respectively as experienced by human patients.

Inflammation after TBI

Inflammation is broadly recognized as a secondary injury mechanism after TBI, and notable work has been done to study the role of innate immune cells and corresponding proinflammation/anti-inflammation. Microglia, the resident immune cells of the brain, are quickly activated after injury (11, 36, 37). They not only actively extend and move towards the site of injury but also proliferate in number (38, 39). In addition to the local microglial response, chemotactic signaling and disruption of the BBB recruit leukocytes into the injured brain (40, 41). Neutrophils, for instance, infiltrate within the first 24 hours after experimental TBI and contribute to edema and tissue loss (42-45). Monocytes likewise are recruited after TBI though their kinetics are slower and prolonged compared to that of neutrophils (23, 46). Monocytes differentiate to activated

macrophages after infiltration and take on microglia-like phenotype and function, though more recent work has begun to distinguish the two populations (23, 47).

Neutrophils and microglia/macrophages contribute to neuronal death and dysfunction through several mechanisms. For example, all three populations express inducible nitric oxide synthase (iNOS) and NADPH oxidase (NOX2) subunits after injury (48-51). NOX2 and iNOS produce reactive oxygen species (ROS) that can lead to neuronal death. TBI notably upregulates NOX2 and iNOS and chronically increases ROS in the injured brain (49, 52-54). Furthermore, NOX2 activity promotes other inflammation pathways such as cytokine production and microglia/macrophage kinetics. Inhibition of NOX2 increases anti-inflammatory cytokine production while downregulating proinflammatory mediators and reducing microglia/macrophage accumulation after injury (55, 56). Yet despite the fact that NOX2 inhibition reduces neuronal death in animal TBI models (49), clinical trials with existing antioxidants were only effective within an extremely narrow treatment window – less than 24 hours – which presents a major hurdle for targeting ROS pathways in human patients (52).

Microglia/macrophages also release a multitude of proinflammatory and anti-inflammatory cytokines and chemokines after injury (15, 37). Proinflammatory cytokines such as IL-1 and TNF-α have been shown to promote neuronal death, BBB breakdown, and further recruitment of inflammatory cells (15, 57, 58). Administration of anti-IL-1 antibodies or antagonists improved neuronal health and survival after TBI (59, 60). Similarly, overexpression of IL-1 receptor agonist (IL-1ra) to reduce IL-1 signaling accelerated motor recovery after injury (61). TNF-α is likewise upregulated within hours post-injury, and inhibition of TNF transcription significantly improved acute functional

recovery after injury (62, 63). Targeting pro-inflammatory cytokines and pathways thus may seem ideal for TBI treatments; indeed, minocycline, an antibiotic that is commonly used as an anti-inflammatory molecule, has effectively decreased inflammatory cytokine production and reduced neurotoxicity in rodent TBI models (64, 65). However, complete knockout of TNF-α actually exacerbates chronic TBI-induced deficits and increases the size of the injury cavitation (32, 66). This potentially biphasic contribution of proinflammatory cytokines has complicated the approach of inhibiting proinflammatory pathways. Alternatively, promoting anti-inflammation pathways has also received attention as a potential treatment approach. Anti-inflammatory cytokines are expressed later than proinflammatory cytokines (11, 23) and function to modulate and eventually resolve the inflammatory response (48). However, preclinical trials and experiments with anti-inflammatory agents have not translated to clinical success (67, 68). Furthermore, there is a consensus that immune-modulatory treatments would be most effective at an acute and subacute window and would not benefit patients suffering from chronic disabilities.

Neuronal Dysfunction after TBI

Another approach for TBI treatment is through understanding how neuronal function is affected beyond cell death. Hippocampal neurons are particularly vulnerable to secondary injury; as mentioned previously, even mild CCI injuries result in hippocampal neuronal death and corresponding loss of synapses in the region within the first 48 hours post-injury (26). Though the hippocampus partially recovers through both neurogenesis (69) and synaptogenesis (70) in the first 30 days post-injury, the net

loss of neurons and synapses ultimately results in impaired cognition (35). However, surviving neurons also notably exhibit chronic changes in their function which can compound the development of cognitive deficits. Most notably, long-term potentiation (LTP), a phenomenon of synaptic plasticity and a correlate for learning and memory (71, 72), is inhibited weeks after TBI (73, 74). Treating deficits in neuronal function presents another avenue for ameliorating TBI outcomes beyond preventing neuron and synapse loss.

Several TBI models including CCI have been used to investigate the effect of injury on the underlying biochemical and molecular pathways of LTP, though most studies have focused on acute effects. The expressions of AMPA and NMDA receptors involved in excitatory neuronal activity and the LTP process transiently fluctuate after injury but recover within a week (75, 76). Expression and activation of various kinases downstream of AMPA and NMDA signaling, such as extracellular signal-regulated kinase (ERK) 1/2 and the calcium/calmodulin-dependent protein kinase (CaMK), are dysregulated acutely after injury (77). Like the AMPA and NMDA receptors, these kinases also return to basal levels of expression and phosphorylation within 3 days of injury (78). In contrast, hippocampal slices from brain-injured animals exhibit less phosphorylation of ERK and CREB (cAMP response element binding protein, a downstream effector of ERK signaling) in response to stimulation even at 12 weeks post-injury (79). Similarly, TBI chronically impairs expression of activity-regulated cytoskeleton-associated (Arc) protein, an immediate early gene that is upregulated and required for learning and LTP induction (80, 81). In fact, inhibition of protein translation has been implicated even more broadly; TBI chronically activates the integrated stress

response which in turn inhibits general protein synthesis that is necessary for plasticity and memory (82-84). Unfortunately, these few studies showing TBI-induced impairment of stimulus-driven signaling in neurons have yet to provide a target for therapeutics, and further work is required to elucidate the chronic impact of TBI on neuronal function.

Summary

Each of the following chapters has a different approach to exploring possible targets of treatment for TBI patients using the CCI model in mice. In **Chapter 2**, we investigate the effect of age on TBI-driven peripheral monocyte response. The aging population is growing quickly, and aging increases incidence and severity of TBIs. Accordingly, studying how aging alters TBI response may highlight particular targets for treatment that studies in younger animals would not. We find that aging not only increases the number of peripheral monocytes in the injured parenchyma, but we also observe proliferation of this population in the injured brain. This is particularly novel given the longstanding perception that once peripheral monocytes exit the bone marrow into the blood or inflamed tissue, they no longer proliferate. In **Chapter 3**, we pursue the integrated stress response (ISR), an arm of the unfolded protein response which regulates global protein translation, as a chronically upregulated pathway that contributes to neuronal dysfunction after TBI. We find that brief treatment with an ISR inhibitor (ISRIB) during behavior a month after TBI is sufficient to restore spatial learning and memory in brain-injured mice. Furthermore, ISRIB also rescues the LTP inhibition observed in CCI animals. This provides an exciting therapeutic target for TBI patients who are suffering from chronic cognitive disabilities. Lastly, in **Chapter 4**, we develop a

8

frontal lobe model of injury using the CCI technique to better represent the site of injury experienced by the majority of patients. We find that the frontal focal contusion produces chronic deficits on a battery of behavioral assays for frontal cortex functions including attention and sociability. More strikingly, we find that orbitofrontal cortical function was affected while medial prefrontal cortical function was spared. This region-specificity provides a foundation for future studies to investigate how TBI affects the frontal lobe, and the model overall is a better representation of TBIs observed in human patients.

References

1. CDC (2015) Report to Congress: Traumatic Brain Injury in the United States: Epidemiology and Rehabilitation.

2. Fleminger S, Oliver DL, Lovestone S, Rabe-Hesketh S, & Giora A (2003) Head injury as a risk factor for Alzheimer's disease: the evidence 10 years on; a partial replication. *Journal of neurology, neurosurgery, and psychiatry* 74(7):857-862.

3. Sivanandam TM & Thakur MK (2012) Traumatic brain injury: a risk factor for Alzheimer's disease. *Neuroscience and biobehavioral reviews* 36(5):1376-1381.

4. Faul M & Coronado V (2015) Epidemiology of traumatic brain injury. *Handbook of clinical neurology* 127:3-13.

5. Butcher I*, et al.* (2007) Prognostic value of cause of injury in traumatic brain injury: results from the IMPACT study. *Journal of neurotrauma* 24(2):281-286.

6. Majdan M*, et al.* (2011) Severity and outcome of traumatic brain injuries (TBI) with different causes of injury. *Brain injury* 25(9):797-805.

7. Saatman KE*, et al.* (2008) Classification of traumatic brain injury for targeted therapies. *Journal of neurotrauma* 25(7):719-738.

8. Riggio S & Wong M (2009) Neurobehavioral sequelae of traumatic brain injury. *The Mount Sinai journal of medicine, New York* 76(2):163-172.

9. Margulies S & Hicks R (2009) Combination therapies for traumatic brain injury: prospective considerations. *Journal of neurotrauma* 26(6):925-939.

10. Vink R & Nimmo AJ (2009) Multifunctional drugs for head injury. *Neurotherapeutics : the journal of the American Society for Experimental NeuroTherapeutics* 6(1):28-42.

11. Loane DJ & Faden AI (2010) Neuroprotection for traumatic brain injury: translational challenges and emerging therapeutic strategies. *Trends in pharmacological sciences* 31(12):596-604.

12. Xiong Y, Mahmood A, & Chopp M (2013) Animal models of traumatic brain injury. *Nature reviews. Neuroscience* 14(2):128-142.

13. Raghupathi R (2004) Cell death mechanisms following traumatic brain injury. *Brain pathology (Zurich, Switzerland)* 14(2):215-222.

14. Raghupathi R, Graham DI, & McIntosh TK (2000) Apoptosis after traumatic brain injury. *Journal of neurotrauma* 17(10):927-938.

15. Ziebell JM & Morganti-Kossmann MC (2010) Involvement of pro- and anti-inflammatory cytokines and chemokines in the pathophysiology of traumatic brain injury. *Neurotherapeutics : the journal of the American Society for Experimental NeuroTherapeutics* 7(1):22-30.

16. Dixon CE, Clifton GL, Lighthall JW, Yaghmai AA, & Hayes RL (1991) A controlled cortical impact model of traumatic brain injury in the rat. *Journal of neuroscience methods* 39(3):253-262.

17. Lighthall JW (1988) Controlled cortical impact: a new experimental brain injury model. *Journal of neurotrauma* 5(1):1-15.

18. Dixon CE*, et al.* (1987) A fluid percussion model of experimental brain injury in the rat. *Journal of neurosurgery* 67(1):110-119.

19. Feeney DM, Boyeson MG, Linn RT, Murray HM, & Dail WG (1981) Responses to cortical injury: I. Methodology and local effects of contusions in the rat. *Brain research* 211(1):67-77.

20. Marmarou A*, et al.* (1994) A new model of diffuse brain injury in rats. Part I: Pathophysiology and biomechanics. *Journal of neurosurgery* 80(2):291-300.

21. Gennarelli TA (1994) Animate models of human head injury. *Journal of neurotrauma* 11(4):357-368.

22. Smith DH*, et al.* (1995) A model of parasagittal controlled cortical impact in the mouse: cognitive and histopathologic effects. *Journal of neurotrauma* 12(2):169-178.

23. Morganti JM*, et al.* (2015) CCR2 antagonism alters brain macrophage polarization and ameliorates cognitive dysfunction induced by traumatic brain injury. *The Journal of neuroscience : the official journal of the Society for Neuroscience* 35(2):748-760.

24. Mao H, Zhang L, Yang KH, & King AI (2006) Application of a finite element model of the brain to study traumatic brain injury mechanisms in the rat. *Stapp car crash journal* 50:583-600.

25. Goodman JC, Cherian L, Bryan RM, Jr., & Robertson CS (1994) Lateral cortical impact injury in rats: pathologic effects of varying cortical compression and impact velocity. *Journal of neurotrauma* 11(5):587-597.

26. Baldwin SA*, et al.* (1997) Neuronal cell loss in the CA3 subfield of the hippocampus following cortical contusion utilizing the optical disector method for cell counting. *Journal of neurotrauma* 14(6):385-398.

27. Saatman KE, Feeko KJ, Pape RL, & Raghupathi R (2006) Differential behavioral and histopathological responses to graded cortical impact injury in mice. *Journal of neurotrauma* 23(8):1241-1253.

28. Zhao Z, Loane DJ, Murray MG, 2nd, Stoica BA, & Faden AI (2012) Comparing the predictive value of multiple cognitive, affective, and motor tasks after rodent traumatic brain injury. *Journal of neurotrauma* 29(15):2475-2489.

29. Hall ED*, et al.* (2005) Spatial and temporal characteristics of neurodegeneration after controlled cortical impact in mice: more than a focal brain injury. *Journal of neurotrauma* 22(2):252-265.

30. Fujimoto ST*, et al.* (2004) Motor and cognitive function evaluation following experimental traumatic brain injury. *Neuroscience and biobehavioral reviews* 28(4):365-378.

31. Nakamura M*, et al.* (1999) Increased vulnerability of NFH-LacZ transgenic mouse to traumatic brain injury-induced behavioral deficits and cortical damage. *Journal of cerebral blood flow and metabolism : official journal of the International Society of Cerebral Blood Flow and Metabolism* 19(7):762-770.

32. Scherbel U*, et al.* (1999) Differential acute and chronic responses of tumor necrosis factor-deficient mice to experimental brain injury. *Proceedings of the National Academy of Sciences of the United States of America* 96(15):8721-8726.

33. Morris RG, Garrud P, Rawlins JN, & O'Keefe J (1982) Place navigation impaired in rats with hippocampal lesions. *Nature* 297(5868):681-683.

34. Dixon CE*, et al.* (1999) One-year study of spatial memory performance, brain morphology, and cholinergic markers after moderate controlled cortical impact in rats. *Journal of neurotrauma* 16(2):109-122.

35. Scheff SW, Baldwin SA, Brown RW, & Kraemer PJ (1997) Morris water maze deficits in rats following traumatic brain injury: lateral controlled cortical impact. *Journal of neurotrauma* 14(9):615-627.

36. d'Avila JC*, et al.* (2012) Microglial activation induced by brain trauma is suppressed by post-injury treatment with a PARP inhibitor. *Journal of neuroinflammation* 9:31.

37. Morganti-Kossmann MC, Satgunaseelan L, Bye N, & Kossmann T (2007) Modulation of immune response by head injury. *Injury* 38(12):1392-1400.

38. Davalos D*, et al.* (2005) ATP mediates rapid microglial response to local brain injury in vivo. *Nature neuroscience* 8(6):752-758.

39. Sandhir R, Onyszchuk G, & Berman NE (2008) Exacerbated glial response in the aged mouse hippocampus following controlled cortical impact injury. *Experimental neurology* 213(2):372-380.

40. Chodobski A, Zink BJ, & Szmydynger-Chodobska J (2011) Blood-brain barrier pathophysiology in traumatic brain injury. *Translational stroke research* 2(4):492-516.

41. Kumar A & Loane DJ (2012) Neuroinflammation after traumatic brain injury: opportunities for therapeutic intervention. *Brain, behavior, and immunity* 26(8):1191-1201.

42. Kenne E, Erlandsson A, Lindbom L, Hillered L, & Clausen F (2012) Neutrophil depletion reduces edema formation and tissue loss following traumatic brain injury in mice. *Journal of neuroinflammation* 9:17.

43. Roth TL*, et al.* (2014) Transcranial amelioration of inflammation and cell death after brain injury. *Nature* 505(7482):223-228.

44. Soares HD, Hicks RR, Smith D, & McIntosh TK (1995) Inflammatory leukocytic recruitment and diffuse neuronal degeneration are separate pathological processes resulting from traumatic brain injury. *The Journal of neuroscience : the official journal of the Society for Neuroscience* 15(12):8223-8233.

45. Whalen MJ*, et al.* (1999) Neutrophils do not mediate blood-brain barrier permeability early after controlled cortical impact in rats. *Journal of neurotrauma* 16(7):583-594.

46. Semple BD, Bye N, Rancan M, Ziebell JM, & Morganti-Kossmann MC (2010) Role of CCL2 (MCP-1) in traumatic brain injury (TBI): evidence from severe TBI patients and CCL2-/- mice. *Journal of cerebral blood flow and metabolism : official journal of the International Society of Cerebral Blood Flow and Metabolism* 30(4):769-782.

47. Saederup N*, et al.* (2010) Selective chemokine receptor usage by central nervous system myeloid cells in CCR2-red fluorescent protein knock-in mice. *PloS one* 5(10):e13693.

48. Barrett JP*, et al.* (2017) NOX2 deficiency alters macrophage phenotype through an IL-10/STAT3 dependent mechanism: implications for traumatic brain injury. *Journal of neuroinflammation* 14(1):65.

49. Dohi K*, et al.* (2010) Gp91phox (NOX2) in classically activated microglia exacerbates traumatic brain injury. *Journal of neuroinflammation* 7:41.

50. Liao Y, Liu P, Guo F, Zhang ZY, & Zhang Z (2013) Oxidative burst of circulating neutrophils following traumatic brain injury in human. *PloS one* 8(7):e68963.

51. Niesman IR*, et al.* (2014) Traumatic brain injury enhances neuroinflammation and lesion volume in caveolin deficient mice. *Journal of neuroinflammation* 11:39.

52. Bains M & Hall ED (2012) Antioxidant therapies in traumatic brain and spinal cord injury. *Biochimica et biophysica acta* 1822(5):675-684.

53. Byrnes KR, Loane DJ, Stoica BA, Zhang J, & Faden AI (2012) Delayed mGluR5 activation limits neuroinflammation and neurodegeneration after traumatic brain injury. *Journal of neuroinflammation* 9:43.

54. Zhang QG*, et al.* (2012) Critical role of NADPH oxidase in neuronal oxidative damage and microglia activation following traumatic brain injury. *PloS one* 7(4):e34504.

55. Choi SH, Aid S, Kim HW, Jackson SH, & Bosetti F (2012) Inhibition of NADPH oxidase promotes alternative and anti-inflammatory microglial activation during neuroinflammation. *Journal of neurochemistry* 120(2):292-301.

56. Kumar A, Alvarez-Croda DM, Stoica BA, Faden AI, & Loane DJ (2016) Microglial/Macrophage Polarization Dynamics following Traumatic Brain Injury. *Journal of neurotrauma* 33(19):1732-1750.

57. Ramilo O*, et al.* (1990) Tumor necrosis factor alpha/cachectin and interleukin 1 beta initiate meningeal inflammation. *The Journal of experimental medicine* 172(2):497-507.

58. Rothwell NJ (1999) Annual review prize lecture cytokines - killers in the brain? *The Journal of physiology* 514 (Pt 1):3-17.

59. Lu KT, Wang YW, Yang JT, Yang YL, & Chen HI (2005) Effect of interleukin-1 on traumatic brain injury-induced damage to hippocampal neurons. *Journal of neurotrauma* 22(8):885-895.

60. Toulmond S & Rothwell NJ (1995) Interleukin-1 receptor antagonist inhibits neuronal damage caused by fluid percussion injury in the rat. *Brain research* 671(2):261-266.

61. Tehranian R*, et al.* (2002) Improved recovery and delayed cytokine induction after closed head injury in mice with central overexpression of the secreted isoform of the interleukin-1 receptor antagonist. *Journal of neurotrauma* 19(8):939-951.

62. Shohami E, Bass R, Wallach D, Yamin A, & Gallily R (1996) Inhibition of tumor necrosis factor alpha (TNFalpha) activity in rat brain is associated with cerebroprotection after closed head injury. *Journal of cerebral blood flow and metabolism : official journal of the International Society of Cerebral Blood Flow and Metabolism* 16(3):378-384.

63. Shohami E, Gallily R, Mechoulam R, Bass R, & Ben-Hur T (1997) Cytokine production in the brain following closed head injury: dexanabinol (HU-211) is a novel TNF-alpha inhibitor and an effective neuroprotectant. *Journal of neuroimmunology* 72(2):169-177.

64. Homsi S*, et al.* (2010) Blockade of acute microglial activation by minocycline promotes neuroprotection and reduces locomotor hyperactivity after closed head injury in mice: a twelve-week follow-up study. *Journal of neurotrauma* 27(5):911-921.

65. Sanchez Mejia RO, Ona VO, Li M, & Friedlander RM (2001) Minocycline reduces traumatic brain injury-mediated caspase-1 activation, tissue damage, and neurological dysfunction. *Neurosurgery* 48(6):1393-1399; discussion 1399-1401.

66. Sullivan PG*, et al.* (1999) Exacerbation of damage and altered NF-kappaB activation in mice lacking tumor necrosis factor receptors after traumatic brain injury. *The Journal of neuroscience : the official journal of the Society for Neuroscience* 19(15):6248-6256.

67. Bergold PJ (2016) Treatment of traumatic brain injury with anti-inflammatory drugs. *Experimental neurology* 275 Pt 3:367-380.

68. Simon DW*, et al.* (2017) The far-reaching scope of neuroinflammation after traumatic brain injury. *Nature reviews. Neurology* 13(3):171-191.

69. Wang X, Gao X, Michalski S, Zhao S, & Chen J (2016) Traumatic Brain Injury Severity Affects Neurogenesis in Adult Mouse Hippocampus. *Journal of neurotrauma* 33(8):721-733.

70. Scheff SW*, et al.* (2005) Synaptogenesis in the hippocampal CA1 field following traumatic brain injury. *Journal of neurotrauma* 22(7):719-732.

71. Bliss TV & Lomo T (1973) Long-lasting potentiation of synaptic transmission in the dentate area of the anaesthetized rabbit following stimulation of the perforant path. *The Journal of physiology* 232(2):331-356.

72. Nicoll RA (2017) A Brief History of Long-Term Potentiation. *Neuron* 93(2):281-290.

73. Schwarzbach E, Bonislawski DP, Xiong G, & Cohen AS (2006) Mechanisms underlying the inability to induce area CA1 LTP in the mouse after traumatic brain injury. *Hippocampus* 16(6):541-550.

74. Titus DJ*, et al.* (2016) Chronic Cognitive Dysfunction after Traumatic Brain Injury Is Improved with a Phosphodiesterase 4B Inhibitor. *The Journal of neuroscience : the official journal of the Society for Neuroscience* 36(27):7095-7108.

75. Atkins CM*, et al.* (2007) Modulation of the cAMP signaling pathway after traumatic brain injury. *Experimental neurology* 208(1):145-158.

76. Kumar A, Zou L, Yuan X, Long Y, & Yang K (2002) N-methyl-D-aspartate receptors: transient loss of NR1/NR2A/NR2B subunits after traumatic brain injury in a rodent model. *Journal of neuroscience research* 67(6):781-786.

77. Atkins CM (2011) Decoding hippocampal signaling deficits after traumatic brain injury. *Translational stroke research* 2(4):546-555.

78. Hu B*, et al.* (2004) Changes in trkB-ERK1/2-CREB/Elk-1 pathways in hippocampal mossy fiber organization after traumatic brain injury. *Journal of cerebral blood flow and metabolism : official journal of the International Society of Cerebral Blood Flow and Metabolism* 24(8):934-943.

79. Atkins CM, Falo MC, Alonso OF, Bramlett HM, & Dietrich WD (2009) Deficits in ERK and CREB activation in the hippocampus after traumatic brain injury. *Neuroscience letters* 459(2):52-56.

80. Bramham CR*, et al.* (2010) The Arc of synaptic memory. *Experimental brain research* 200(2):125-140.

81. Rosi S*, et al.* (2012) Trauma-induced alterations in cognition and Arc expression are reduced by previous exposure to 56Fe irradiation. *Hippocampus* 22(3):544-554.

82. Begum G, Harvey L, Dixon CE, & Sun D (2013) ER stress and effects of DHA as an ER stress inhibitor. *Translational stroke research* 4(6):635-642.

83. Costa-Mattioli M*, et al.* (2007) eIF2alpha phosphorylation bidirectionally regulates the switch from short- to long-term synaptic plasticity and memory. *Cell* 129(1):195-206.

84. Petrov T, Underwood BD, Braun B, Alousi SS, & Rafols JA (2001) Upregulation of iNOS expression and phosphorylation of eIF-2alpha are paralleled by suppression of protein synthesis in rat hypothalamus in a closed head trauma model. *Journal of neurotrauma* 18(8):799-812.

Chapter 2: Proliferation of Infiltrating Macrophages in the Aging Brain after Trauma

Introduction

Traumatic brain injury (TBI) is a leading cause of neurological disability and a major risk factor for neurodegenerative diseases and dementia (1, 2). The elderly population in particular has higher incidence of TBIs which presents a rapidly emergent health issue as the world population and average human lifespan increases (3). Not only are the mortality and hospitalization rates higher for the elderly after TBI, this population also suffers worse cognitive recovery and poorer quality of life post-injury (4-6). The disparity between elderly and younger populations is true even for mild TBIs (7). Thus beyond recognizing age as a prognostic factor for TBI outcome (8), research to identify mechanisms of TBI affected by age is imperative as the number of elderly TBI patients inevitably grows.

Little work has been done to investigate mechanisms underlying the effect of aging on TBI outcome. However, a few studies have established the efficacy of rodent TBI models for the purpose (9, 10). For example, old (21+ months old) mice subjected to a controlled cortical impact (CCI), a rodent model of focal contusion TBI, exhibited exacerbated acute edema, neurodegeneration along with worsened motor recovery compared to younger adult (5-6 months old) mice (10, 11). Furthermore, age-associated increases of injury cavitation size and neuronal death post-TBI are correlated with an amplified acute inflammatory cytokine response (dpi) (11-13). There is a corresponding increase of microglia/macrophage activation that persists several weeks post-injury as exhibited by upregulated activation markers and amoeboid morphology (14-16).

Infiltrated macrophages – peripheral monocytes that have entered the injured brain and differentiated to activated macrophages – contribute to TBI-induced inflammation and cognitive deficits in adult animals (17-19). The CCR2 receptor and its ligand CCL2 are the primary signaling pathway of peripheral monocyte infiltration, and CCL2 is upregulated in both human patients and rodent models after TBI (19-21). Knocking out or inhibiting CCR2 prevents 80-90% of peripheral monocyte infiltration, reduces inflammatory cytokine expression, preserves neuronal density, and reduces development of chronic learning impairments in the CCI mouse model (17, 18). Furthermore, our lab has shown that old animals have seven times more TBI-induced peripheral monocyte recruitment within 24 hours of injury compared to young animals (15). Accordingly, we hypothesize that the peripheral monocyte and macrophage population contributes to age-driven differences after injury.

While resident microglia and infiltrated macrophages express similar markers and are often indistinguishable from one another, the two populations differ notably in their origin (22, 23). Microglia originate from the yolk sac during development and self-renew in the brain over the organism's lifetime (24-26). Conversely, infiltrated macrophages originate from bone marrow hematopoietic progenitors and circulate in the blood as monocytes until drawn to sites of inflammation (21, 27). After infiltration, peripherally-derived macrophages take on a microglia-like state including the downregulation of CCR2 (not expressed on microglia) and upregulation of the fractalkine receptor CX3CR1 (highly expressed on microglia) (18, 28). As of yet, there is no evidence of peripheral macrophage proliferation after they infiltrate the brain, injured

or uninjured, despite the similarities in function and phenotype between them and the resident microglia.

In this study, we show that aging increases the peripheral monocyte ($CD11b^+CD45^{hi}$ or $CD11b^+CCR2^+$) population in the injured brain. Simultaneously, there is a significant expansion of the peripheral monocyte population in the blood of the old animals. Furthermore, the aging brain contains more proliferation of activated ($F4/80^{hi}$ or $CX3CR1^{hi}$) macrophages after TBI. We validated this phenomenon through parabiosis, and we observed macrophages that proliferated after infiltration into the injured brain in both young and old mice. This not only highlights an effect of age on the peripheral monocyte response after TBI but is also the first observation that peripheral monocytes can infiltrate the injured brain, differentiate to an activated phenotype, and regain proliferative capabilities. Unfortunately, preventing peripheral monocyte infiltration through CCR2 knockout did not rescue age-exacerbated TBI-induced cognitive loss.

Results

Aging increases peripheral monocyte infiltration to the injured brain at 4 and 7 days post-TBI

We have previously shown that at 24 hours after injury, old mice had more peripheral monocytes infiltrating the brain than in young mice (18). To investigate whether this effect of aging persists beyond 24 hours post-TBI, we employed the same controlled-cortical impact (CCI) TBI model in young (3-6mo) and old (20-25mo) mice (15, 29). The peripheral monocyte count, defined as $CD45^{hi}$ in wildtype animals or RFP-positive in $CX3CR1^{GFP/+}CCR2^{RFP/+}$ transgenic animals, was expressed as a percentage of the

CD11b⁺ myeloid population (Fig. 1A). We found that aging increases the percentage of peripheral monocytes in the injured brain at 4 and 7 dpi in both wildtype (Fig. 1B) and transgenic (Fig. 1C) animals, indicating an extended, exacerbated peripheral monocyte response with age. We also observed differences in the expression of CCR2 ligands – CCR2, CCR7, CCR8, and CCR12 – in the ipsilateral hippocampus. Specifically, CCL8 and CCL12 levels are higher in the old animals at both 4 and 7 dpi. Furthermore, there is a trend that old animals maintain CCL2 and CCL7 upregulation whereas young animals begin to downregulate the two ligands by 7 dpi (Supplementary Fig. 2). The higher expression of CCR2 ligands may explain the difference in peripheral monocyte infiltration observed in the old animals. To verify that CD45 and CCR2 define the same peripheral monocyte population, we validated that the majority of CD45^{hi} cells are CCR2⁺ and vice versa (Supplementary Fig. 1). Thus CD45 and CCR2 expression can be used interchangeably to distinguish peripheral monocytes.

Aging increases the CCR2⁺ monocyte population in the blood after injury

To investigate if aging increases the number of peripheral CCR2⁺ monocytes in circulation, we ran flow cytometry with blood samples of mice after injury and gated for CD11b⁺, CCR2⁺ monocytes (Fig. 2A). We found that aging significantly increased the monocyte population in the blood at 4 dpi compared to young animals (Fig. 2B).

Aging increases proliferation of infiltrated macrophages and resident microglia after TBI

Next we determined whether proliferation of resident microglia and peripheral monocytes after TBI was affected by aging by BrdU pulsing animals after injury to label proliferating cells. Animals were given three injections of 100 mg/kg BrdU between 3-4 dpi and then euthanized for flow cytometry at 4 dpi (Fig. 3A). BrdU$^+$ labeling was determined from the CD45^{hi} peripheral macrophage and CD45^{lo} resident microglia populations (Fig. 3B). We observed that aging animals have an increase in proliferation of both peripheral macrophages (Fig. 3C) and resident microglia (Fig. 3D) between 3-4 dpi. Interestingly, the effect of age on proliferation of the peripheral population was significant only when considering F4/80^{hi} macrophages. Peripheral monocytes – specifically the inflammatory monocytes in circulation (Supplementary Fig. 3A) – differentiate to activated macrophages and upregulate F4/80 expression after infiltration into inflamed tissue (30, 31). As has been reported, we confirmed that these F4/80^{hi} macrophages also upregulate CX3CR1 compared to the F4/80^{lo} and F4/80$^-$ monocytes which are CX3CR1^{lo} (Supplementary Fig. 4A, B) (18, 28). High expression of both CX3CR1 and F4/80 are phenotypically similar to microglia (CX3CR1^{hi}CCR2$^-$; Supplementary Fig. 4B). Thus, aging specifically increases the proliferation of microglia-like, infiltrated macrophages in the brain after TBI. However, the BrdU experiment alone does not differentiate between infiltrated macrophages that proliferate in the brain and macrophages that proliferated from bone marrow progenitors then infiltrated and differentiated within the 3-4 dpi window.

Macrophages from the periphery can proliferate after infiltration of the injured brain

We hypothesized that a population of the infiltrated macrophages were proliferating in the injured brain. To investigate the possibility, we utilized the parabiosis model and paired CCR2$^{rfp/+}$ and wildtype animals to generate blood chimeras with a RFP-labeled monocyte subpopulation in the blood of a wildtype host. We then induced a TBI in the wildtype animal and pulsed the animal with BrdU between 3-4 dpi (Fig. 4A). Since BrdU-labeling of proliferated macrophages could only occur in the bone marrow or, given our hypothesis, the injured brain, the observation of the observation of RFP-positive, BrdU-labeled macrophages in the brain would validate the hypothesis; the wildtype host lacked RFP-labeled progenitors in the bone marrow, and the only source of RFP-positive monocytes were the ones in circulation (Fig. 4B). By immunostaining, we detected a significant number of RFP, BrdU-labeled cells (Fig. 4C-E). The data thus suggest that a peripheral monocyte is indeed capable of proliferation after they infiltrate the injured brain and differentiate into activated macrophages.

Aging impairs anti-inflammatory response after TBI

To further determine whether microglia/macrophage function was affected by age, we isolated the myeloid population by percoll gradient at 7 dpi and ran qPCR for inflammatory markers. We found that pro-inflammatory markers Tnf-α, IL-1β, and iNOS were similarly upregulated between old and young animals after TBI (Supplementary Fig. 5A). However, we found that expression of anti-inflammatory markers Ym1, CD206, TGF-β, and IL4Ra were all lower in the old animals at 7 dpi (Supplementary Fig. 5B). Thus, while the microglia/macrophages were equally pro-inflammatory between age

groups, the immune populations were significantly less anti-inflammatory in the old animals.

Knocking out CCR2 to prevent peripheral monocyte infiltration does not rescue age-exacerbated TBI-induced deficits in spatial learning and memory

We additionally investigated the effect of age on long-term cognitive outcome post-injury and whether inhibiting peripheral monocyte infiltration with a CCR2 knockout could rescue any differences (17, 18). Utilizing the radial arm water maze (RAWM) to characterize spatial learning and memory at 30 dpi, we found a significant age and TBI effect (Fig. 5A). Furthermore, aging significantly exacerbates the TBI-induced deficit on spatial memory assessed during the memory probe of the RAWM (Fig. 5B).

To verify the worsened spatial memory deficit after TBI in old animals, we tested another cohort at 30+ dpi on the novel object recognition assay (NOR) which also tests hippocampal-dependent spatial memory. During the training session when animals are exposed to two identical objects, only the young animals with TBIs showed a slight preference for one of the objects (Fig. 5C). However, young sham-surgery animals, young TBI animals, and old sham-surgery animals all preferred exploring the novel object presented 24 hours later during the testing trial. In comparison, the old animals with TBIs did not distinguish between the novel and familiar objects, thus further highlighting the effect of aging on cognitive outcome after TBI (Fig. 5D). We then examined the performance of CCR2$^{-/-}$ animals after TBI on the NOR. As expected, we found no preferences between the two identical objects during training (Fig. 5E). On the test trial, however, the brain-injured CCR2$^{-/-}$ animals also did not differentiate between

novel and familiar objects (Fig. 5F), suggesting that preventing peripheral monocyte infiltration by knocking out CCR2 is insufficient for reducing the impact of age on TBI cognitive outcome.

Discussion

Our results indicate that aging exacerbates peripheral monocyte response after TBI. There was an age-driven increase of peripheral monocytes both in circulation and the injured brain, the latter of which persists at 7 dpi. This corresponds with an elevation of CCR2 chemotactic ligands in the aging brain after TBI. However, knocking out CCR2 to prevent TBI-induced infiltration of the peripheral monocytes did not prevent the worsened spatial memory deficits in aging animals. Surprisingly though, we observed the ability of peripheral monocytes to proliferate after infiltrating the injured parenchyma and differentiating into activated macrophages. Aging furthermore increases the number of proliferated, infiltrated macrophages in the brain after TBI.

We have previously shown a seven-fold increase in the number of peripheral monocytes (CCR2$^+$) in the injured brain of old animals compared to that of young animals at 1 dpi (15). Preventing CCR2$^+$ monocyte infiltration significantly reduces both pro- and anti-inflammatory markers and NADPH oxidase (NOX2) subunit expression (18, 32), and ultimately reduces secondary injury and improves cognitive outcome after TBI (17). Accordingly, prolonged infiltration may further exacerbate inflammation, leading to worse secondary injury and cognitive deficits observed in old TBI animals (14). In this study, we not only corroborated the age-driven increase of peripheral monocytes (CD45^{hi}) in wildtype animals 24 hours post-injury but also expanded our

27

findings to 4 and 7 dpi using wildtype and CX3CR1$^{GFP/+}$CCR2$^{RFP/+}$ transgenic animals. Indeed, at all timepoints, old animals had significantly more peripheral monocytes in the injured brain. This was correlated with more circulating monocytes in the blood of the old animals 4 days after TBI. In young animals, TBI induces expansion of the circulating monocyte population (33), and our data suggest that this proliferation is further amplified by age. Additionally, we found that old animals further upregulate and maintain expression of CCR2 ligands in the injured brain as compared to young animals. Altogether, the larger pool of available circulating monocytes and persistent chemotactic signaling could explain the difference in peripheral monocyte populations between young and old animals.

Most remarkably, we found that activated macrophages – differentiated from peripheral monocytes after infiltrating the injured brain – are capable of proliferation. To verify this, we parabiosed a CCR2$^{RFP/+}$ animal to an isochronic wildtype. Once blood chimerism is achieved, the wildtype animal's peripheral monocyte population essentially consists of 40-50% RFP-labeled monocytes (donor) and 50-60% wildtype (host) (34). More importantly, the bone marrow progenitors of the wildtype host remain RFP-negative; the source of RFP-positive cells that infiltrate the brain of the wildtype animal after TBI would be those in circulation. Given that circulating monocytes do not proliferate in the blood (21), the BrdU-labeled, RFP-positive cells we observed in the brain must first have infiltrated the brain then integrated BrdU as they proliferated in the parenchyma.

It is established that many resident macrophage populations, including microglia, self-renew over the course of the host's lifetime rather than replenish by constant influx

and replacement by bone marrow-derived monocytes (26, 35). In contrast, peripheral monocytes that originate from bone marrow progenitors circulate in the blood, infiltrate inflamed tissues, differentiate into macrophages, participate in inflammation, and then are removed from the system (21, 36). However, sites such as the brain with a resident macrophage population may present a permissive environment to allow for proliferation of a differentiated macrophage. In fact, infiltrated macrophages can take on a microglia-like phenotype after injury; our lab has used the CX3CR1$^{GFP/+}$CCR2$^{RFP/+}$ transgenic line to show that peripheral monocytes in the injured brain upregulate the fractalkine receptor CX3CR1, which is highly expressed on microglia (18, 28). This is matched by a corresponding increase of F4/80, an activation marker that is also highly expressed on microglia (30, 31). Infiltrating monocytes eventually downregulate CCR2, thus making infiltrated macrophages and resident microglia indistinguishable during injury and other neuroinflammatory events (28). The microglia-like phenotype may relate to the ability for infiltrated macrophages to proliferate in the TBI brain.

There has been one study showing proliferation of peripherally-derived monocytes/macrophages after infiltrating an inflammation site. As inflammation is resolved, infiltrated macrophages are typically removed from the injured tissue, leaving resident tissue macrophages such as microglia to reinstate the homeostatic state (37). However, in a peritonitis model, a small percentage of infiltrating monocytes were observed undergoing dna-replication and mitosis in the peritoneum (38). Both the brain and peritoneum have self-replicating resident macrophages, so a common microenvironment factor during inflammation may drive the infiltrated macrophage proliferation. In particular, M-CSF – monocyte colony stimulating factor that affects

monocytic differentiation and survival – promotes the inflammatory macrophage proliferation during peritonitis (38). M-CSF, also known as CSF1, is also necessary for microglia survival and proliferation; application of CSF1R inhibitor effectively eliminates the microglia population (39). Conversely, CSF1 overexpression significantly increases microglia proliferation (40). In the context of TBI, CSF1 is moderately upregulated acutely after injury (41, 42), but additional validation will be required due to the lack of confirmatory studies in TBI mouse models. Regardless, future investigations into similarities between tissue niches that house self-renewing resident macrophages may identify underlying mechanisms of the phenomenon.

Previous studies have shown that aging increases both pro- and anti-inflammation gene expression within the first 24 hours after injury (11, 14, 15). Our data suggest that pro-inflammatory gene expression evens out between young and old animals, but anti-inflammatory gene expression is lower in the myeloid cells of the old animals at 7 dpi. The two profiles also broadly indicate the microglia/macrophage polarization into M1 and M2 phenotypes (43, 44). While it is important to note that microglia/macrophages can express M1 (pro-inflammatory) and M2 (anti-inflammatory) phenotypes simultaneously (44, 45), the decrease in M2 markers Ym1 and CD206 in the old TBI animals would suggest less overall M2-like functionality (46). This result would imply impairment in immune regulation and resolution as a result of age. Indeed, the aging brain already predisposes microglia/macrophages towards M1 and away from M2 gene expression when directly stimulated with cytokine cocktails (47). Furthermore, our observed decrease in TGF-β and IL-4Ra, a cytokine and receptor that promote the M2 phenotype, suggest at least an upstream impairment for M2 polarization (43, 48). In

fact, IL-4 is normally a M2 stimulating cytokine but in aging macrophages appears to promote M1polarization (49). It is possible that this bias away from M2 may exacerbate the chronic inflammation after TBI that we have previously characterized in young animals (18).

Persistent expansion of microglia/macrophage populations after TBI is also known to be affected by age. Specifically, there is prolonged upregulation of myeloid markers CD11b and Iba1 in old animals at 28 dpi. In comparison, CD11b and Iba1 expression in young animals normalize to sham levels by then (16). It is not yet known whether this chronic increase of microglia/macrophages is due solely to increases in peripheral monocyte infiltration and microglia proliferation (14, 15) or if processes responsible for returning microglia/macrophages to homeostatic numbers are also affected by age. Evidence that the phagocytic ability of microglia/macrophages, critical for removing excess immune and apoptotic cells after inflammation, are negatively affected age (50-52) would suggest the latter. Regardless, we hypothesized that reducing the number of peripheral monocytes altogether by CCR2 knockout would decrease inflammation and ultimately age-exacerbated secondary injury and TBI-induced cognitive deficits. Unfortunately, such a broad approach did not reduce the impairment on spatial memory we observed in old animals after TBI. Further investigation will be required as to whether the aging resident microglia population compensates for the lack of infiltrating monocytes or if another avenue of monocyte infiltration exists in aging animals.

Materials and Methods

Animals. All experiments were conducted in accordance with National Institutes of Health *Guide for the Care and Use of Laboratory Animals* and were approved by the Institutional Animal Care and Use Committee of University of California (San Francisco). Adult 3-6mo (young) and 20-25mo (old) male C57B6/J were purchased from Jackson Laboratory (Bar Harbor, ME) and the National Institute on Aging animal colony respectively. Similarly aged young and old $CX3CR1^{GFP/+}CCR2^{RFP/+}$ (double heterozygous (Dbl-Het)), $CCR2^{RFP/+}$, and CCR2$^{-/-}$ mice were bred and aged as previously described (28) and genotyped using a commercial service (Transnetyx). Mice were group housed in environmentally controlled conditions with reverse light cycle (12:12 h light:dark cycle at 21 ± 1 °C) and provided food and water ad libitum.

TBI surgical procedure. Animals were anesthetized and maintained at 2% isoflurane and secured to a stereotaxic frame with non-traumatic ear bars. The hair on the scalp was removed by shaving with an electric razor. Eye lubricant was applied to their eyes and betadine and 70% alcohol was applied to the scalp. A midline incision was made to expose the skull.

A unilateral TBI was induced via the controlled cortical impact (CCI) model in the parietal lobe (15, 29). Mice received a craniectomy ~3.5 mm in diameter using an electric microdrill at the coordinates: -2.00 mm anteroposterior and +2.00 mm mediolateral with respect to bregma. Any animal with excessive bleeding due to disruption of the dura was removed from the study. After the craniectomy, a contusion was delivered using a 3 mm convex tip attached to an electromagnetic impactor (Leica).

The impact parameters were set to a contusion depth of 0.95 mm (from dura) at a velocity of 4.0 m/s sustained for 300 msec. After the CCI, the scalp was either sutured for survival past a week or closed with wound clips for experiments at seven days post-injury (dpi) or shorter. Sham animals received a similar procedure but with only slight drilling without removal of the skull.

Post-surgery, animals were placed in a cage on top of a heatpad until they were fully ambulatory and recovered. After recovery, animals were returned to their home cage and monitored for normal behavior and weight maintenance throughout the duration of the experiments.

BrdU/EdU injection. A 10mg/ml solution of BrdU (Sigma-Aldrich) or EdU (ThermoFisher) was prepared fresh in sterile PBS (Gibco) for each injection timepoint. Animals were injected intraperitoneally at 100 mg/kg per injection. For the CD45-gated brain-proliferation experiment, animals were injected starting at 3 dpi every 8 hours and sacrificed 24hours after the first injection (4 dpi). Animals in all other proliferation experiments were given injections every 12 hours starting at 3 dpi for a total of two injections.

Parabiosis surgery. Parabiosis surgery was performed between isochronic, same-sex pairs of one wildtype and one $CCR2^{RFP/+}$ animal as previously described (34, 53). Mirrored incisions through the skin were made at the right and left flanks respectively. The peritoneal openings of the two parabionts were sutured together along with the elbow and knee joints from the same side. The skin of the parabionts were then stapled

together. The animals were given antibiotics and analgesics for pain and monitored for recovery for 2.5-3 weeks before the TBI procedure and subsequent BrdU or EdU treatment at 3 dpi. All parabiosis pairs were euthanized at 4 dpi.

Tissue collection. All mice were euthanized with a mixture of ketamine (150 mg/kg)/xylazime (15 mg/kg) in accordance with standard animal protocols. For flow cytometry endpoints, blood was drawn via cardiac puncture and mixed with EDTA to prevent coagulation (1.5 ul 0.5M EDTA per 100 ul blood). Animals were then perfused transcardially with cold Hank's balanced salt solution without calcium and magnesium (HBSS; Gibco). Immediately after perfusion, mice were decapitated and the brain was extracted into HBSS and kept on ice for flow cytometry. For qRT-PCR endpoints, mice were perfused with with phosphate buffered saline without calcium chloride and magnesium chloride (PBS; Gibco) and the hippocampi were dissected out and snap frozen on dry ice. For immunohistochemistry, after perfusion with HBSS, mice were further perfused with 4% paraformaldehyde (PFA; Sigma-Aldrich). The brains were removed and post-fixed overnight in 4% PFA before being transferred to 30% sucrose.

Flow cytometry. The olfactory bulbs and cerebellums were removed prior to processing brain tissue. For $CX3CR1^{GFP/+}CCR2^{RFP/+}$ experiments, only the injured hemisphere was processed. All other experiments utilized both hemispheres. The brains were diced in plastic weigh boats with a razor blade and mechanically homogenized with glass dounce tissue grinders (Kimble Kontes). The cell suspension

34

was then filtered through 70 um cell strainers (Fisherbrand). Myelin cleanup or leukocyte isolation was performed via percoll gradients (Sigma) (15).

Blood samples were processed by adding 1.5 ml lysing buffer (BD Pharm Lyse) and incubating on ice for one minute before centrifugation. The lysis step was repeated with another 0.5 ml lysing buffer to remove most of the red blood cells.

All washes and antibody dilutions were done in staining buffer made of 2% fetal bovine serum (FBS; Gibco) in PBS. Fc receptor blocking was performed before all staining procedures using an anti-CD16/32 antibody (BD Pharmingen). The following reagents were used for labeling the monocytic populations across all experiments: CD11b Alexafluor 700 (BD Pharmingen) and F4/80 APC (Invitrogen). CD45 FITC (BD Pharmingen) and CD45 Brilliant Violet 711 (BD Horizon) were used to differentiate resident microglia and peripheral monocytes in non-BrdU and BrdU experiments respectively. ZombieViolet (BD Biolegend) or 7AAD (Sigma-Aldrich) was used to label live/dead populations. Ly6G V450 (BD Horizon) was used to further characterize CCR2$^{RFP/+}$ cells. BrdU staining was performed utilizing a FITC BrdU Flow Kit (BD Pharmingen). EdU staining was performed with a ClickIt Plus Alexa Fluor 488 Flow Cytometry Kit (Invitrogen). Spectral compensation was achieved using polystyrene microparticles (BD Pharmingen) in combination with the listed antibodies. Analysis was done on a FACS Aria III cell sorter (BD Biosciences). Flow cytometric data was analyzed using FlowJo (Treestar, v10.3).

qRT-PCR. Gene expression analyses were performed on dissected ipsilateral hippocampi or isolated myeloid cells from the injury hemispheres. Myeloid cell isolation

was performed by mechanically homogenizing the tissue with glass dounce tissue grinders (Kimble Kontes), filtering through 70 um cell strainers (Fisherbrand), and separating the population in a percoll gradient (Sigma) (15). RNA isolation and cDNA conversion were performed as previously described with Qiazol reagent and RNEasy mini-columns (QIAGEN) (18). RNA concentration was determined via NanoDrop (Thermo Scientific). For each sample, 300 ng of total RNA was reverse transcribed using the High-Capacity cDNA Reverse Transcription Kit (Applied Biosystems). The genes of interest were analyzed using SYBR Green Master Mix (Applied Biosystems) on a Stratagene Mx3005P Real-Time PCR system. The relative target gene expression was determined by the $2^{-\Delta\Delta Ct}$ method normalized to beta-actin expression. The primer sequences used were as previously described (15).

Immunohistochemistry. Brains collected for immunohistochemistry were sectioned on a Microm cryostat at 20 um thickness onto Superfrost Plus slides (Fisher) and stored at -20°C until staining. Slices were first amplified for RFP signal with 1:100 rabbit anti-RFP (Abcam) overnight followed by 1:100 anti-rabbit IgG 633 secondary (Invitrogen). DAPI was applied prior to BrdU staining steps. Slices were then fixed with 4% PFA and permeabilized with 2N HCl and 0.1M Boric Acid. The slices were incubated overnight with 1:200 rat BrdU IgG (AccueChem) followed by 1:100 anti-rat IgG 488 secondary (Invitrogen). Sections were preserved with VectaShield soft mount and kept at -20°C until imaging.

The injury site and hippocampus at 0 um, -120 um, and +120 um from the center of injury were imaged at 20x magnification with a Zeiss Imager.Z1 Apotome microscope

controlled by Zen software (Zeiss 2014). Seven z-planes were imaged at 1.5 um intervals with identical exposure durations across all slices. The z-stacks were then flattened to a single plane. Quantification of RFP[+]-only and RFP[+], GFP[+]-colocalized events were done in the Zen software.

Radial Arm Water Maze. At 28dpi, animals were tested on the radial arm water maze (RAWM) as previously described to test spatial learning and memory (54). The maze consisted of a circular pool with a diameter of 118.5 cm with eight arms of 41 cm each in length. An escape platform could be moved to the end of any of the arms. The pool was filled with water and paint (Crayola, 54-2128-053) was added to make the water opaque. Visual cues were placed around the room such that they were visible to animals in the maze. Animals ran 15 trials for two days of training (blocks 1-10) and then 3 trials during the memory test (block 11). On the first day of training, the escape platform was made visible every other trial by placing a flag on the platform. The escape platform alternated between visible and hidden for the first 12 trials and was hidden for trials 13-15. For the rest of the assay, the escape platform remained hidden.

During a trial, animals were placed in a pseudo-random arm not containing the escape platform. Animals were given one minute to explore the maze and locate the escape platform. If they successfully swam to the platform, they were returned to their holding cage after a 10 second interval. On a failed trial, animals were guided to the escape platform then returned to the holding cage 10 second later. The escape platform location was the same for each individual animal. The start arm was randomized such that each non-escape arm was used before any repetition. The escape platform location

was randomly assigned for each animal to account for potential preferences of exploration in the maze.

RAWM data was collected through a video tracking and analysis setup (Ethovision XT 8.5, Noldus Information Technology). The program automatically analyzed the number of errors – an entry into an arm not containing the escape platform – per trial. The results of every three trials were averaged into a block to account for the large variability in performance; a training day thus consisted of 15 trials averaged into 5 blocks and the memory probe consisted of 3 trials averaged into 1 block.

Novel Object Recognition. At 30+ dpi, animals were tested for hippocampal-dependent spatial memory on the novel object recognition (NOR) assay. The test arena consisted of a square box (30 cm x 30 cm x 30cm) in a dimly lit behavior test room. For two consecutive days, animals were individually placed into the arena and allowed to explore for 10 min. On the third day, two identical objects were placed into the arena and secured into place with magnets. The mice were given 5 min to explore the arena with the objects. On the fourth day, one of the objects from day three was replaced with a novel object; the object that was replaced was pseudo-randomized across animals to account for place preference in the arena. Animals were again given 5 min to explore. Trials were recorded and analyzed by a video tracking and analysis setup (Ethovision XT 8.5, Noldus Information Technology) and verified via manual scoring for exploratory behavior. Animals were considered to be exploring the objects when they direct their nose towards an object within a 2 cm distance or less. The arena and objects were cleaned with 70% ethanol between trials to eliminate odors.

Statistical Analysis. All statistical analyses were performed on Graphpad Prism (Graphpad Software). Flow cytometry data for peripheral monocyte timecourse were analyzed by two-way analysis of variance (ANOVA), and the main effects and interactions were reported. Two-way ANOVA was used for the blood monocyte flow cytometry with post hoc Bonferroni's multiple comparison. BrdU proliferation experiment data was analyzed via unpaired Student's t-test. RAWM memory probe data was analyzed via two-way ANOVA and post hoc Bonferroni's multiple comparison. NOR data was analyzed as unpaired Student's t-test between objects for each experiment group. All data presented are means ± standard error of mean (SEM) with significance set at $p < 0.05$.
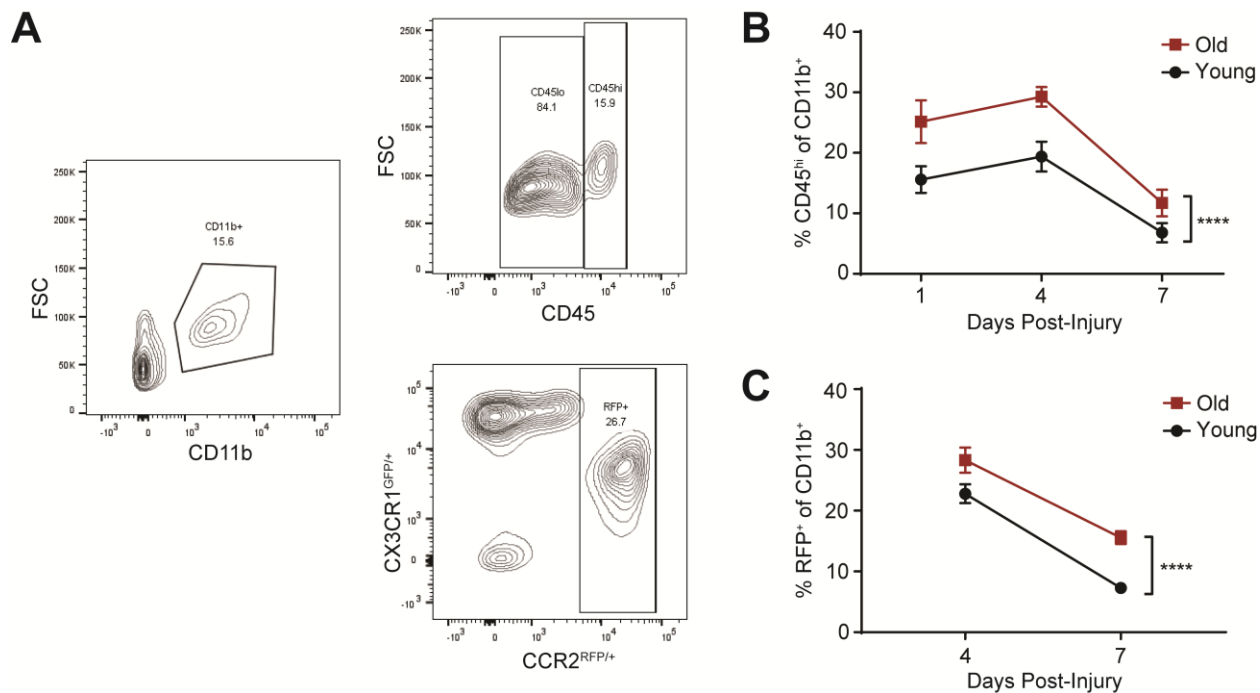
Figures

Fig 1. Aging increases peripheral monocyte (CD11b+CD45hi or CD11b+CCR2+) infiltration at 1, 4, and 7 days post-TBI.

(A) Example flow cytometry gating profiles for peripheral monocyte population in the brain. CD11b+ is gated from the live, single cell population (left). Peripheral monocytes are gated as either CD45hi (top right) or CCR2rfp/+ (Q2 and Q3, bottom right). Example images are from a young animal at 4 days post-injury (dpi).

(B) Percent CD45hi of the CD11b+ population at 1, 4, and 7 dpi. Aging increases infiltration of CD45hi cells at all timepoints after TBI. Data are means ± SEM (two-way ANOVA, ****p<0.0001, main effects of Age and Time, no significant Interaction).

(C) Percent CCR2rfp/+ of the CD11b+ population at 4 and 7 dpi. Aging increases infiltration of CCR2 cells at 4 and 7 dpi. Data are means ± SEM (two-way ANOVA, ****p<0.0001, main effects of Age and Time, no significant Interaction).
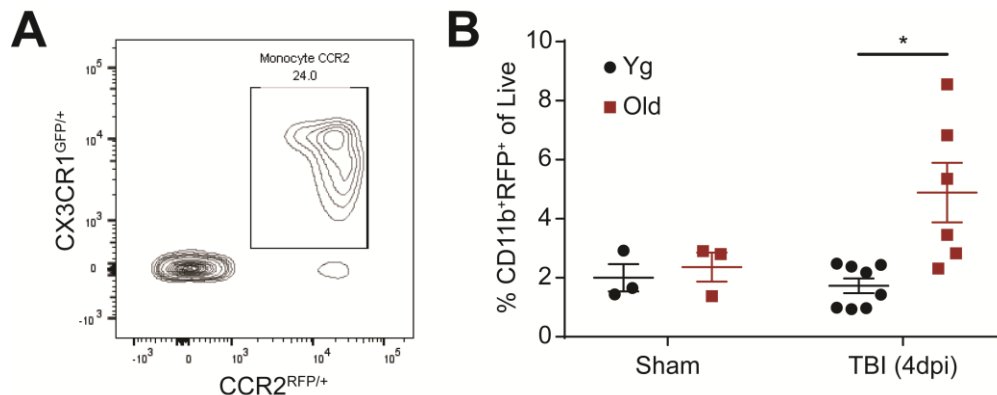

Fig 2. Aging increases CCR2+ monocytes in the blood after TBI.

(A) Example flow cytometry profile of CD11b+ population from blood sample showing gating of CCR2+ monocyte population at 4 dpi.

(B) Percent CD11b+, CCR2+ monocytes of all single, live cells in 100 ul of blood. Aging increases the CCR2+ monocyte population at 4 dpi (Bonferroni's post hoc test, *p<0.05).
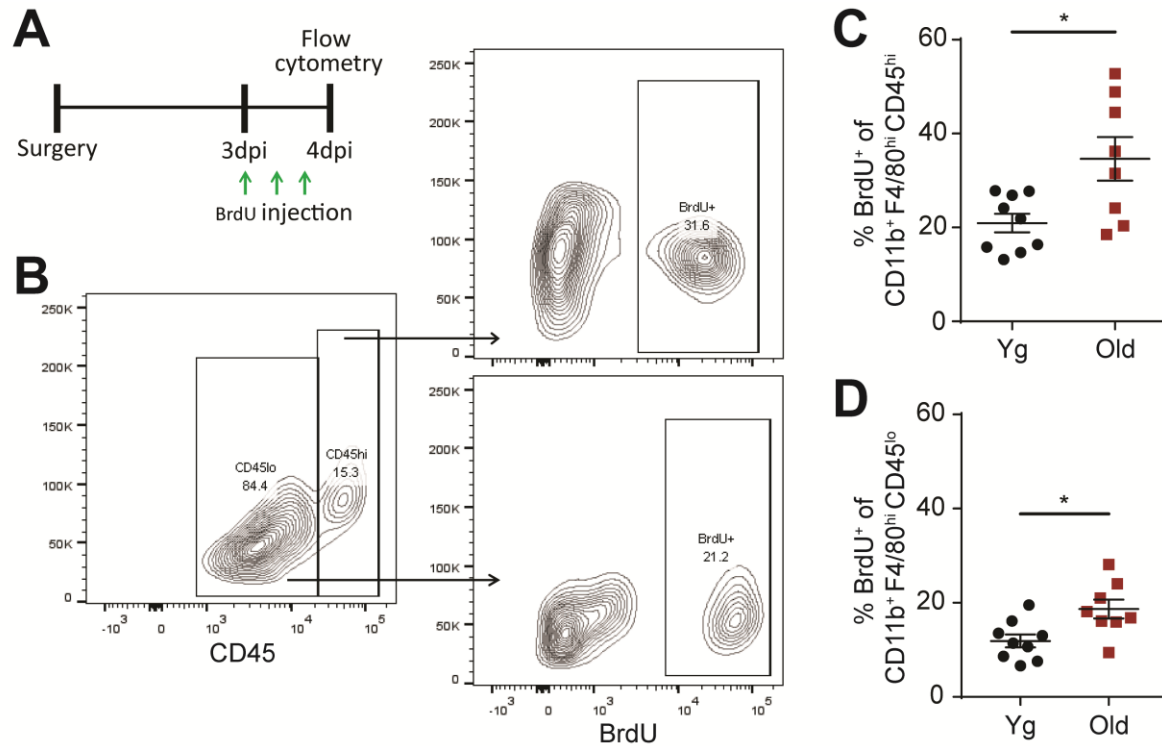
Fig 3. Aging increases proliferation of peripheral macrophages (CD45^{hi}) and microglia (CD45^{lo}) observed in the injured brain.

(A) Experiment layout for BrdU injections. Animals were given three injections of 100 mg/kg BrdU every 8 hours starting at 3 dpi. The animals were then euthanized and the brains collected for flow cytometry at 4 dpi.

(B) Example flow cytometry gating profiles for proliferated infiltrated macrophage and resident microglia populations in the TBI brain. First CD45^{hi} (infiltrated macrophage) or CD45^{lo} (resident microglia) are gated from CD11b$^+$F4/80^{hi} population (left). BrdU signal is then gated in each of the two myeloid populations (top and bottom right). Example images are from an old animal.

41

(C) Percent of CD45^{hi} infiltrated macrophages with BrdU signal. Aging significantly increases the number of infiltrated macrophages that proliferated between 3 and 4 dpi. Data are means ± SEM (Student's t-test, *p<0.05).

(D) Percent of CD45^{lo} resident microglia with BrdU signal. Aging significantly increases the number of resident microglia that proliferated between 3 and 4 dpi. Data are means ± SEM (Student's t-test, *p<0.05).
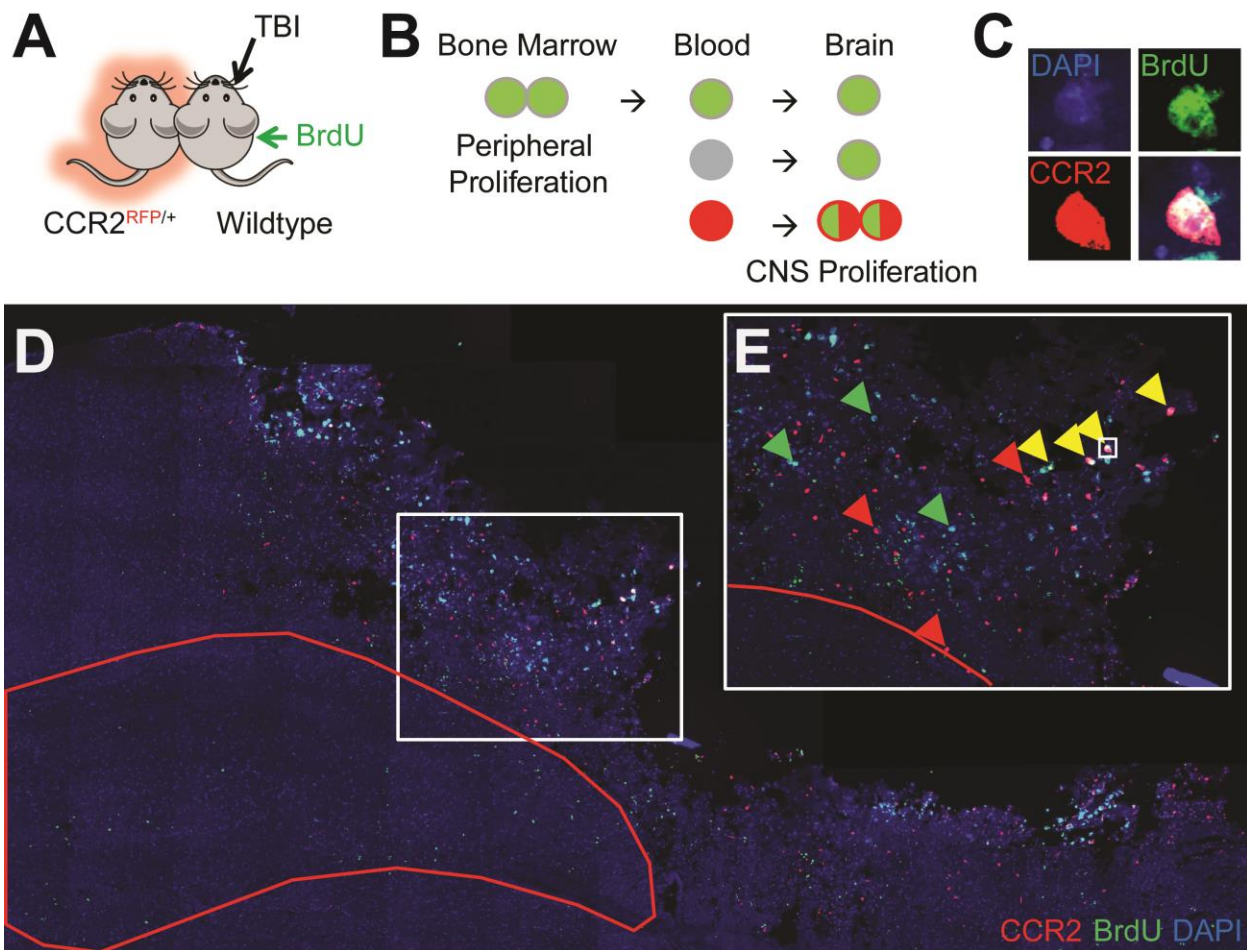

Fig 4. Parabiosis experiment showing peripheral monocytes that proliferate after infiltrating the injured parenchyma.

(A) Schematic of parabiosis pairing. An isochronic pair consisting of one CCR2$^{rfp/+}$ and one wildtype were parabiosed together. After 2-3 weeks of recovery to establish blood chimerism, the wildtype animal was given a TBI. Starting at 3 dpi, the wildtype animal was given two injections of 100 mg/kg BrdU spaced 12 hours apart. At 4 dpi, the animals were euthanized, and the brains were collected for immunohistochemical detection of BrdU signal in the injured brain.

(B) Possible sources of BrdU-labeled peripheral monocytes in the injured brain of the wildtype animal. Monocytes that proliferated in the bone marrow then infiltrated to the injured parenchyma will be BrdU-positive and RFP-negative since there are no CCR2$^{rfp/+}$ progenitors in the bone marrow of the wildtype animal. Conversely, a subpopulation of monocytes that infiltrated the brain prior to proliferation will be RFP-positive due to the blood chimerism established by parabiosis.

(C) Example image of a BrdU-positive, RFP-positive cell. A cell is labeled as a positive if there is a DAPI signal with colocalization of BrdU and RFP signals.

(D) Example slice showing distribution of RFP and BrdU signals are mainly close to the injury site at 4 dpi. The hippocampal is outlined in red.

(E) Magnification of the region outlined in white from (D). Red arrows emphasize RFP-only cells, green arrows emphasize BrdU-only cells, and yellow arrows highlight BrdU-positive, RFP-positive cells.
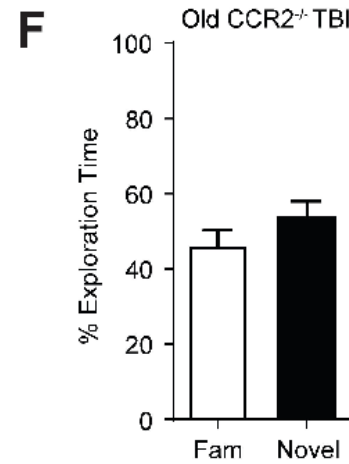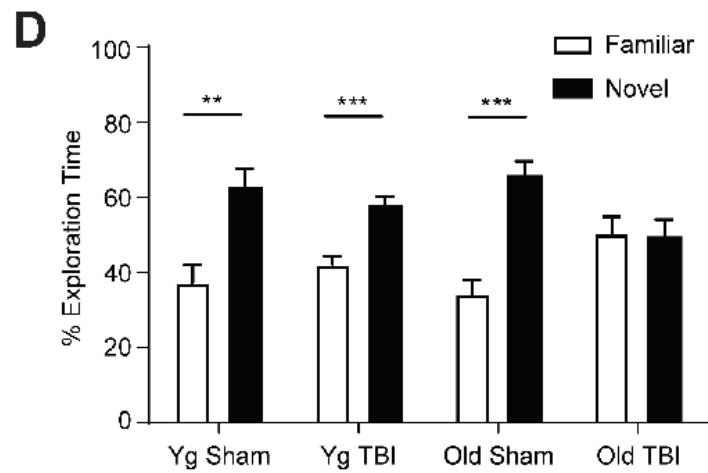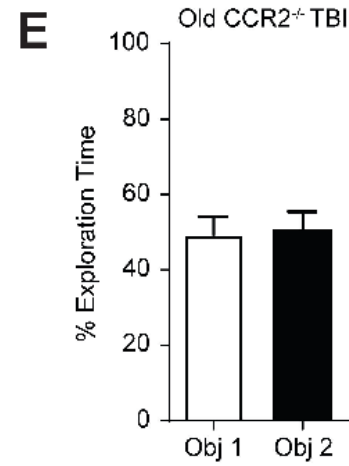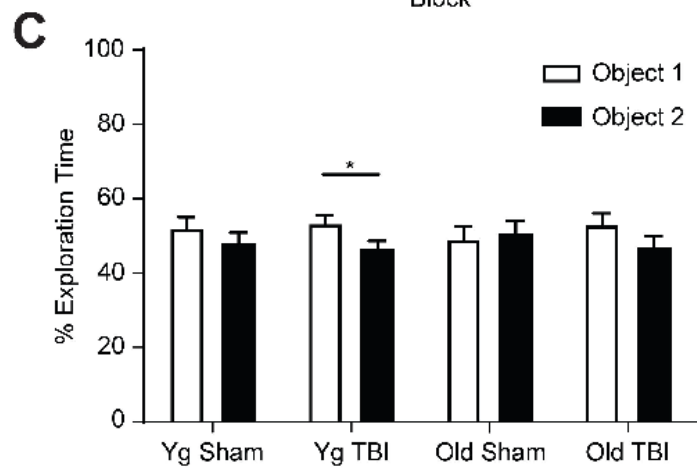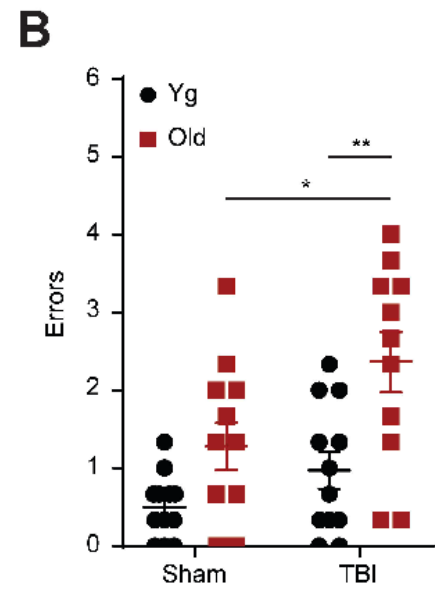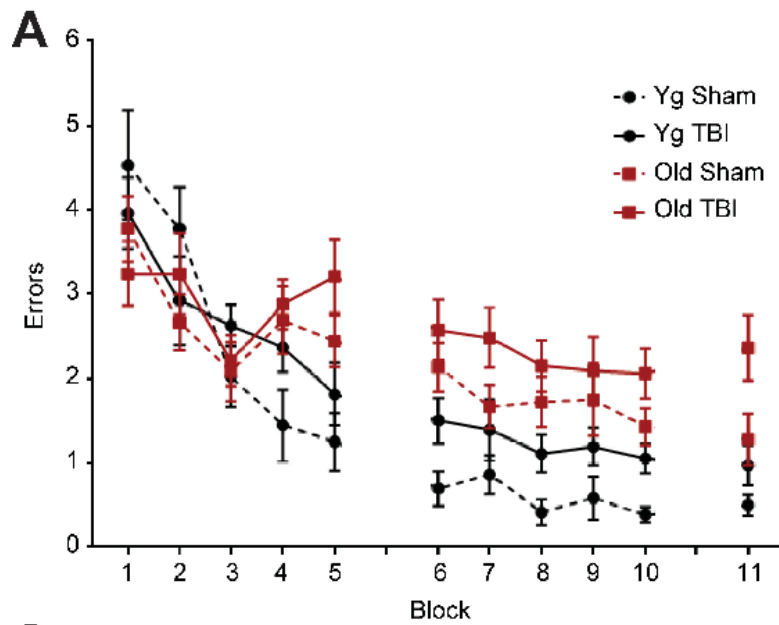
Fig 5. Aging exacerbates spatial learning and memory deficits on the radial arm water maze (RAWM) and novel object recognition assay (NOR). Knockout of CCR2 does not prevent spatial memory impairment on NOR.

(A) Animals were trained on 15 trials (averaged every 3 trials as a block for a total of 5 blocks each training day) of RAWM starting at 28 dpi through 29 dpi. At 30 dpi, animals were tested for their memory of the escape platform location. There was an age effect across both TBI and Sham surgeries.

(B) Individual animal performance during the memory test (block 11; 30 dpi). Aging significantly exacerbates the memory impairment caused by TBI (Bonferroni's post hoc, *p<0.05, **p<0.01).

(C) Preferences for two identical objects during the training trial of the NOR assay. Only the young TBI group showed a slight preference for one object over the others. (Student's t-test, *p<0.05).

(D) Preferences for one novel and one familiar object during the test trial of the NOR assay. Every group except for the old TBI group significantly preferred to explore the novel object over the familiar object. TBI thus impairs spatial memory function on the NOR only in old animals.

(E) Preference of CCR2$^{-/-}$ animals with TBIs for two identical objects during the training trial of the NOR assay. There were no preferences for either of the identical objects.

(F) Preference of CCR2$^{-/-}$ animals with TBIs for one familiar object and one novel object during the test trial of the NOR assay. The animals did not distinguish between novel or familiar; knockout of CCR2 thus did not rescue the spatial memory impairment caused by TBI in old animals.
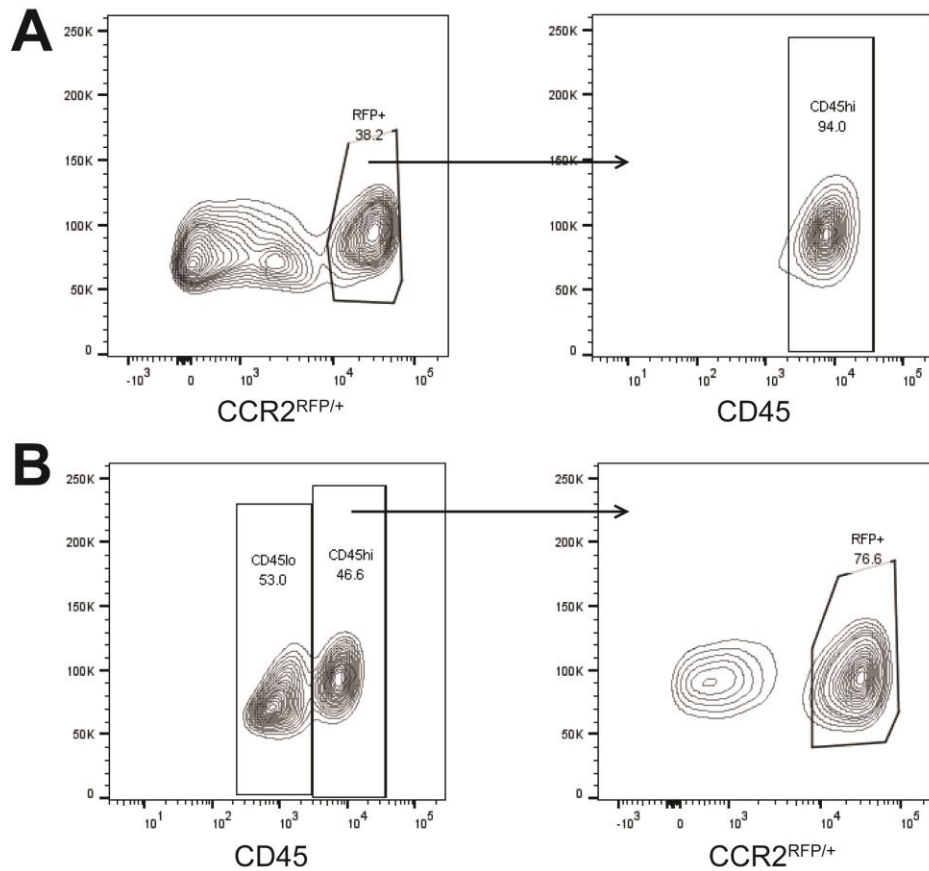
Supplementary Figure 1. Majority of CCR2+ cells are CD45hi and vice versa, and the two markers can be used interchangeably for the peripheral monocyte population.

(A) Example flow cytometry profile showing that majority of CCR2$^+$ (gated from live, single, CD11b$^+$ population) are CD45^{hi}.

(B) Example flow cytometry profile showing that majority of CD45^{hi} (gated from live, single, CD11b$^+$ population) are CCR2$^+$. Example images are from an old CCR2$^+$ animal brain at 4dpi.
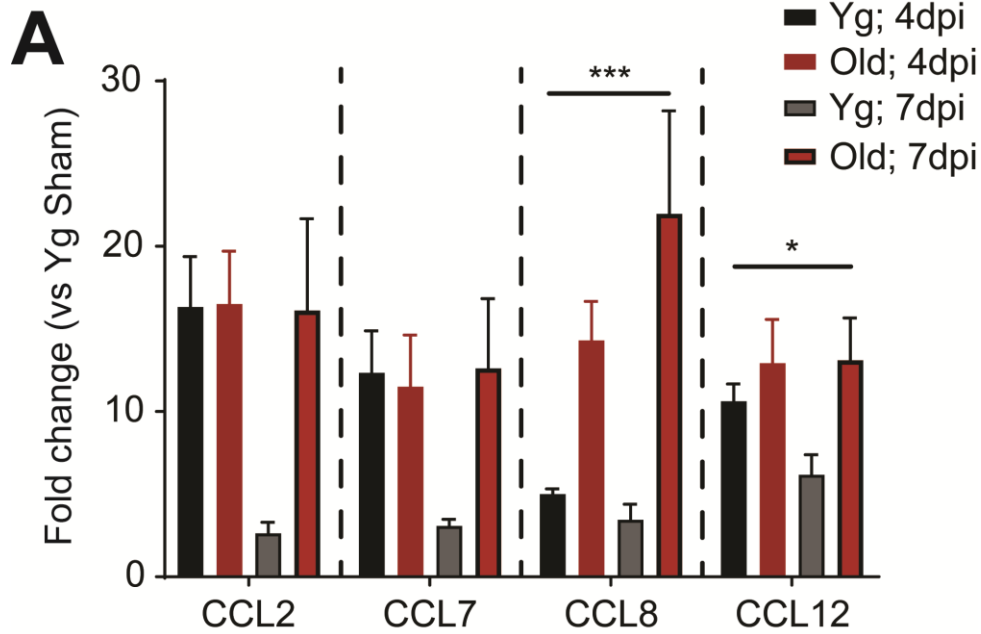
Supplementary Figure 2. Old animals have more CCR2 ligand expression at 7 days post-injury (dpi) than young animals.

(A) Quantitative PCR data for CCL2, CCL7, CCL8, and CCL12 expression. At 7 dpi, old animals have a trend of more CCL2 and CCL7 expression as compared to young animals which downregulate the ligands. Old animals have more CCL8 and CCL12 expression at both 4 and 7 dpi compared to young animals (two-way ANOVA, *p<0.05, ***p<0.001, main effect of Age, no effect of Time, no Interaction).
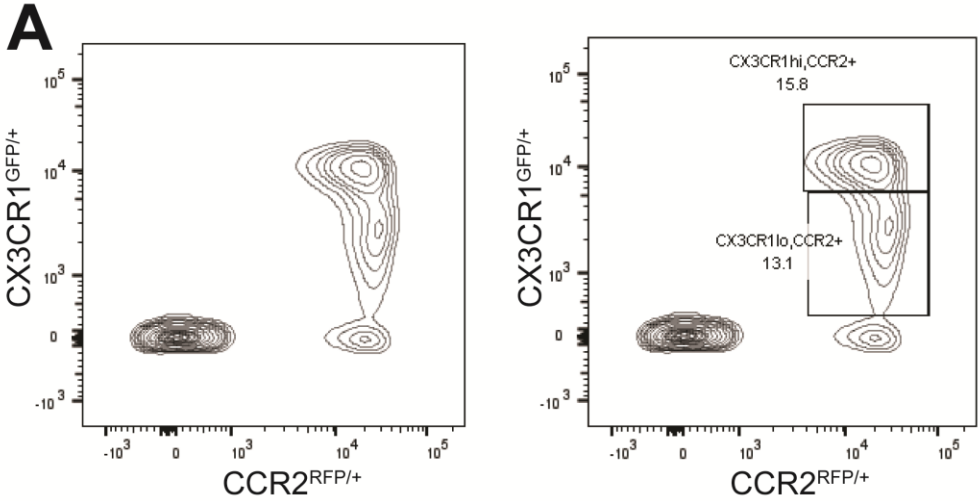
Supplementary Figure 3. Gating threshold of CX3CR1^{hi} and CX3CR1^{lo} are determined by inflammatory vs patrolling monocyte expression of CX3CR1.

(A) Example flow cytometry profiles with and without gating from blood CD11b$^+$ population. Distinct CX3CR1^{hi} (patrolling monocyte) and CX3CR1^{lo} (inflammatory monocyte) populations can be distinguished among the CCR2$^+$ population.
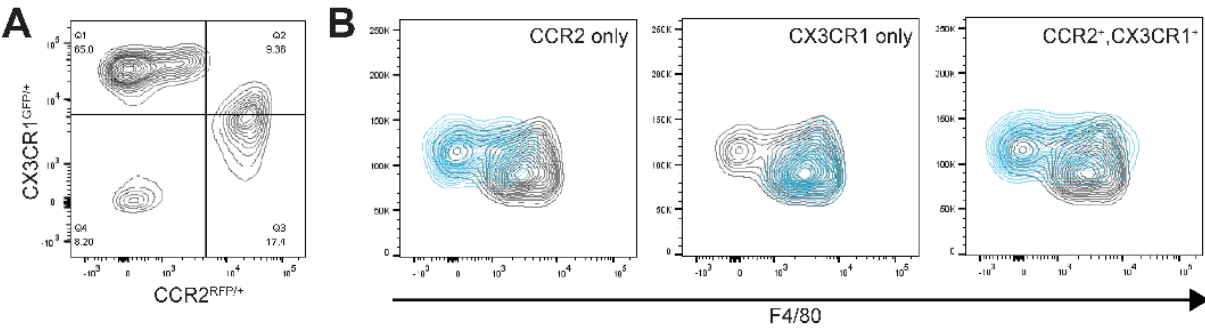
Supplementary Figure 4. A subpopulation of CCR2$^+$ peripheral monocytes take on an activated, microglia-like state by upregulating F4/80 and CX3CR1 at 4 dpi.

(A) Example flow cytometry profile for CCR2 and CX3CR1 expression in the CD11b$^+$ population isolated from an aging injured brain at 4 dpi. Gating scheme for determining

CX3CR1^{hi} and CX3CR1^{lo} was established by gating for patrolling and inflammatory monocyte populations in blood (SFig 3).

(B) Example flow cytometry profiles for F4/80 expression of peripheral monocytes (CCR2$^+$,CX3CR1^{lo}), resident microglia (CCR2$^-$, CX3CR1^{hi}), and microglia-like activated macrophages (CCR2$^+$, CX3CR1^{hi}). Peripheral monocytes are mostly F4/80$^-$ and F4/80^{lo}. Resident microglia are F4/80^{hi}. The microglia-like, activated macrophages have a F4/80^{hi} population not present on peripheral monocytes.
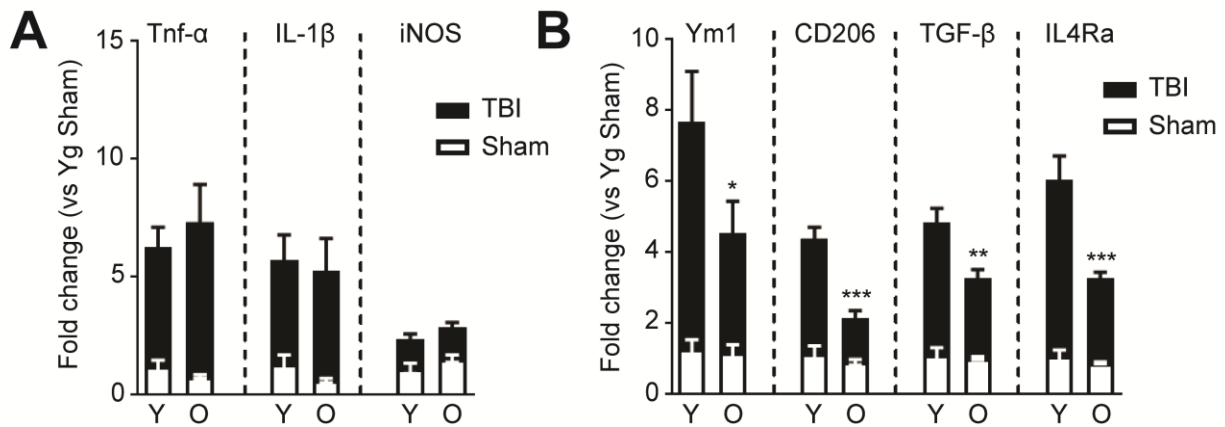
Supplementary Figure 5. Aging reduces anti-inflammatory marker expression at 7 dpi with no difference in pro-inflammation compared to young animals.

(A) Quantitative PCR data for Tnf-α, IL-1β, and iNOS as markers representative of pro-inflammation. TBI increases expression of the markers at 7 dpi with no difference due to aging.

(B) Quantitative PCR data for Ym1, CD206, TGF-β, and IL4Ra as markers representative of anti-inflammation. TBI increases expression of the markers at 7 dpi with significantly less expression in the old animals. (Bonferroni's post hoc test, *$p<0.05$, **$p<0.01$, ***$p<0.001$).

References

1. Johnson VE, Stewart W, & Smith DH (2010) Traumatic brain injury and amyloid-beta pathology: a link to Alzheimer's disease? *Nature reviews. Neuroscience* 11(5):361-370.

2. Smith C*, et al.* (2013) The neuroinflammatory response in humans after traumatic brain injury. *Neuropathology and applied neurobiology* 39(6):654-666.

3. Stocchetti N, Paterno R, Citerio G, Beretta L, & Colombo A (2012) Traumatic brain injury in an aging population. *Journal of neurotrauma* 29(6):1119-1125.

4. Himanen L*, et al.* (2006) Longitudinal cognitive changes in traumatic brain injury: a 30-year follow-up study. *Neurology* 66(2):187-192.

5. Hukkelhoven CW*, et al.* (2003) Patient age and outcome following severe traumatic brain injury: an analysis of 5600 patients. *Journal of neurosurgery* 99(4):666-673.

6. Schonberger M, Ponsford J, Reutens D, Beare R, & O'Sullivan R (2009) The Relationship between age, injury severity, and MRI findings after traumatic brain injury. *Journal of neurotrauma* 26(12):2157-2167.

7. Susman M*, et al.* (2002) Traumatic brain injury in the elderly: increased mortality and worse functional outcome at discharge despite lower injury severity. *The Journal of trauma* 53(2):219-223; discussion 223-214.

8. Mushkudiani NA*, et al.* (2007) Prognostic value of demographic characteristics in traumatic brain injury: results from the IMPACT study. *Journal of neurotrauma* 24(2):259-269.

9. Itoh T*, et al.* (2013) Increased apoptotic neuronal cell death and cognitive impairment at early phase after traumatic brain injury in aged rats. *Brain structure & function* 218(1):209-220.

10. Onyszchuk G, He YY, Berman NE, & Brooks WM (2008) Detrimental effects of aging on outcome from traumatic brain injury: a behavioral, magnetic resonance imaging, and histological study in mice. *Journal of neurotrauma* 25(2):153-171.

11. Timaru-Kast R*, et al.* (2012) Influence of age on brain edema formation, secondary brain damage and inflammatory response after brain trauma in mice. *PloS one* 7(8):e43829.

12. Kumar A & Loane DJ (2012) Neuroinflammation after traumatic brain injury: opportunities for therapeutic intervention. *Brain, behavior, and immunity* 26(8):1191-1201.

13. Sandhir R, Puri V, Klein RM, & Berman NE (2004) Differential expression of cytokines and chemokines during secondary neuron death following brain injury in old and young mice. *Neuroscience letters* 369(1):28-32.

14. Kumar A*, et al.* (2013) Traumatic brain injury in aged animals increases lesion size and chronically alters microglial/macrophage classical and alternative activation states. *Neurobiology of aging* 34(5):1397-1411.

15. Morganti JM*, et al.* (2016) Age exacerbates the CCR2/5-mediated neuroinflammatory response to traumatic brain injury. *Journal of neuroinflammation* 13(1):80.

16. Sandhir R, Onyszchuk G, & Berman NE (2008) Exacerbated glial response in the aged mouse hippocampus following controlled cortical impact injury. *Experimental neurology* 213(2):372-380.

17. Hsieh CL*, et al.* (2014) CCR2 deficiency impairs macrophage infiltration and improves cognitive function after traumatic brain injury. *Journal of neurotrauma* 31(20):1677-1688.

18. Morganti JM*, et al.* (2015) CCR2 antagonism alters brain macrophage polarization and ameliorates cognitive dysfunction induced by traumatic brain injury. *The Journal of neuroscience : the official journal of the Society for Neuroscience* 35(2):748-760.

19. Semple BD, Bye N, Rancan M, Ziebell JM, & Morganti-Kossmann MC (2010) Role of CCL2 (MCP-1) in traumatic brain injury (TBI): evidence from severe TBI patients and CCL2-/- mice. *Journal of cerebral blood flow and metabolism : official journal of the International Society of Cerebral Blood Flow and Metabolism* 30(4):769-782.

20. Liu S, Zhang L, Wu Q, Wu Q, & Wang T (2013) Chemokine CCL2 induces apoptosis in cortex following traumatic brain injury. *Journal of molecular neuroscience : MN* 51(3):1021-1029.

21. Shi C & Pamer EG (2011) Monocyte recruitment during infection and inflammation. *Nature reviews. Immunology* 11(11):762-774.

22. Cao T, Thomas TC, Ziebell JM, Pauly JR, & Lifshitz J (2012) Morphological and genetic activation of microglia after diffuse traumatic brain injury in the rat. *Neuroscience* 225:65-75.

23. Loane DJ & Kumar A (2016) Microglia in the TBI brain: The good, the bad, and the dysregulated. *Experimental neurology* 275 Pt 3:316-327.

24. Ajami B, Bennett JL, Krieger C, Tetzlaff W, & Rossi FM (2007) Local self-renewal can sustain CNS microglia maintenance and function throughout adult life. *Nature neuroscience* 10(12):1538-1543.

25. Alliot F, Godin I, & Pessac B (1999) Microglia derive from progenitors, originating from the yolk sac, and which proliferate in the brain. *Brain research. Developmental brain research* 117(2):145-152.

26. Ginhoux F*, et al.* (2010) Fate mapping analysis reveals that adult microglia derive from primitive macrophages. *Science (New York, N.Y.)* 330(6005):841-845.

27. Prinz M & Priller J (2010) Tickets to the brain: role of CCR2 and CX3CR1 in myeloid cell entry in the CNS. *Journal of neuroimmunology* 224(1-2):80-84.

28. Saederup N*, et al.* (2010) Selective chemokine receptor usage by central nervous system myeloid cells in CCR2-red fluorescent protein knock-in mice. *PloS one* 5(10):e13693.

29. Lighthall JW (1988) Controlled cortical impact: a new experimental brain injury model. *Journal of neurotrauma* 5(1):1-15.

30. Gordon S*, et al.* (1986) Localization and function of tissue macrophages. *Ciba Foundation symposium* 118:54-67.

31. Hume DA*, et al.* (2002) The mononuclear phagocyte system revisited. *Journal of leukocyte biology* 72(4):621-627.

32. Zhang QG*, et al.* (2012) Critical role of NADPH oxidase in neuronal oxidative damage and microglia activation following traumatic brain injury. *PloS one* 7(4):e34504.

33. Lee S, *et al.* (2016) A novel antagonist of p75NTR reduces peripheral expansion and CNS trafficking of pro-inflammatory monocytes and spares function after traumatic brain injury. *Journal of neuroinflammation* 13(1):88.

34. Villeda SA, *et al.* (2011) The ageing systemic milieu negatively regulates neurogenesis and cognitive function. *Nature* 477(7362):90-94.

35. Yona S, *et al.* (2013) Fate mapping reveals origins and dynamics of monocytes and tissue macrophages under homeostasis. *Immunity* 38(1):79-91.

36. Geissmann F, *et al.* (2010) Development of monocytes, macrophages, and dendritic cells. *Science (New York, N.Y.)* 327(5966):656-661.

37. Ajami B, Bennett JL, Krieger C, McNagny KM, & Rossi FM (2011) Infiltrating monocytes trigger EAE progression, but do not contribute to the resident microglia pool. *Nature neuroscience* 14(9):1142-1149.

38. Davies LC, *et al.* (2013) Distinct bone marrow-derived and tissue-resident macrophage lineages proliferate at key stages during inflammation. *Nature communications* 4:1886.

39. Elmore MR, *et al.* (2014) Colony-stimulating factor 1 receptor signaling is necessary for microglia viability, unmasking a microglia progenitor cell in the adult brain. *Neuron* 82(2):380-397.

40. De I, *et al.* (2014) CSF1 overexpression has pleiotropic effects on microglia in vivo. *Glia* 62(12):1955-1967.

41. Turtzo LC, *et al.* (2014) Macrophagic and microglial responses after focal traumatic brain injury in the female rat. *Journal of neuroinflammation* 11:82.

42. White TE, *et al.* (2013) Gene expression patterns following unilateral traumatic brain injury reveals a local pro-inflammatory and remote anti-inflammatory response. *BMC genomics* 14:282.

43. Gordon S (2003) Alternative activation of macrophages. *Nature reviews. Immunology* 3(1):23-35.

44. Kumar A, Alvarez-Croda DM, Stoica BA, Faden AI, & Loane DJ (2016) Microglial/Macrophage Polarization Dynamics following Traumatic Brain Injury. *Journal of neurotrauma* 33(19):1732-1750.

45. Morganti JM, Riparip LK, & Rosi S (2016) Call Off the Dog(ma): M1/M2 Polarization Is Concurrent following Traumatic Brain Injury. *PloS one* 11(1):e0148001.

46. Jablonski KA, *et al.* (2015) Novel Markers to Delineate Murine M1 and M2 Macrophages. *PloS one* 10(12):e0145342.

47. Lee DC, *et al.* (2013) Aging enhances classical activation but mitigates alternative activation in the central nervous system. *Neurobiology of aging* 34(6):1610-1620.

48. Gong D, *et al.* (2012) TGFbeta signaling plays a critical role in promoting alternative macrophage activation. *BMC immunology* 13:31.

49. Dimitrijevic M, *et al.* (2016) Aging affects the responsiveness of rat peritoneal macrophages to GM-CSF and IL-4. *Biogerontology* 17(2):359-371.

50. Linehan E & Fitzgerald DC (2015) Ageing and the immune system: focus on macrophages. *European journal of microbiology & immunology* 5(1):14-24.

51. Lynch AM, *et al.* (2010) The impact of glial activation in the aging brain. *Aging and disease* 1(3):262-278.

52. Streit WJ (2006) Microglial senescence: does the brain's immune system have an expiration date? *Trends in neurosciences* 29(9):506-510.

53. Conboy IM*, et al.* (2005) Rejuvenation of aged progenitor cells by exposure to a young systemic environment. *Nature* 433(7027):760-764.

54. Alamed J, Wilcock DM, Diamond DM, Gordon MN, & Morgan D (2006) Two-day radial-arm water maze learning and memory task; robust resolution of amyloid-related memory deficits in transgenic mice. *Nature protocols* 1(4):1671-1679.

Chapter 3: Inhibition of the Integrated Stress Response Reverses Cognitive Deficits after Traumatic Brain Injury

Abstract

Traumatic brain injury (TBI) is a leading cause of long-term neurological disability yet the mechanisms underlying the chronic cognitive deficits associated with TBI remain unknown. Consequently, there are no effective treatments for patients suffering from the long-lasting symptoms of TBI. Here, we show that TBI persistently activate the integrated stress response (ISR), a universal intracellular signaling pathway that responds to a variety of cellular conditions and regulates protein translation *via* phosphorylation of the translation initiation factor eIF2α. Treatment with ISRIB, a potent drug-like small-molecule inhibitor of the ISR, reversed the hippocampal-dependent cognitive deficits induced by TBI in two different injury mouse models—focal contusion and diffuse concussive injury. Surprisingly, ISRIB corrected TBI-induced memory deficits when administered weeks after the initial injury and maintained cognitive improvement after treatment was terminated. At the physiological level, TBI suppressed long-term potentiation in the hippocampus, which was fully restored with ISRIB treatment. Our results indicate that ISR-inhibition at time points late after injury can reverse memory deficits associated with TBI. As such, pharmacological inhibition of the ISR emerges as a promising avenue to combat head trauma induced chronic cognitive deficits.

Significance Statement

Traumatic brain injury (TBI) is a leading cause of long-term neurological disability and affects an ever-growing population. Currently, there are no effective treatments for patients suffering from chronic TBI-induced cognitive impairments. Here, we found that suppression of the integrated stress response (ISR) with a drug-like small-molecule inhibitor, ISRIB, rescued cognition in two TBI mouse models, even when administered weeks after injury. Consistent with the behavioral results, ISRIB restored long-term potentiation deficits observed in TBI mice. Our data suggests that targeting ISR activation could serve as a promising approach for the treatment of chronic cognitive dysfunction after TBI.

Introduction

Traumatic brain injury (TBI) represents a major mental health problem (1-4). Even a mild TBI can elicit cognitive deficits, including permanent memory dysfunction (2, 4). Moreover, TBI is one of the most predictive environmental risk factors for the development of Alzheimer's disease and other forms of dementia (5-9). Current treatments have focused primarily on reducing the risk of TBI incidence, immediate neurosurgical intervention, or broad behavioral rehabilitation (10, 11, 12 , 13). Despite posing a huge societal problem, there are currently no pharmacological treatment options for patients that suffer from TBI-induced cognitive deficits.

The integrated stress response (ISR) is an evolutionarily conserved pathway that controls cellular homeostasis and function (14). The central ISR regulatory step is the phosphorylation of the α-subunit of the eukaryotic translation initiation factor 2 (eIF2α)

by a family of four eIF2α kinases (15, 16). Phosphorylation of eIF2α leads to inhibition of general protein synthesis, but also, to the translational up-regulation of a select subset of mRNAs (17, 18). In the brain, phosphorylation of eIF2α regulates the formation of long-term memory (19-21). Briefly, animals with reduced phosphorylation of eIF2α show enhanced long-term memory storage (19, 22-24), and increased phosphorylation of eIF2α in the brain prevents the formation of long-term memory (19, 24, 25).

Similar to other chronic cognitive disorders (21, 26), TBI leads to a persistent activation of the ISR. TBI induces eIF2α phosphorylation even in brain regions that are distal to the injury site (27, 28). However, the direct impact of ISR activation on chronic TBI-induced behavioral deficits remains unknown.

We recently discovered a potent (in-cell EC_{50} = 5 nM) drug-like small molecule (ISRIB, for <u>ISR</u> Inhi<u>B</u>itor) that reverses the translational effects induced by ISR-mediated eIF2α phosphorylation and readily permeates the blood–brain barrier (29). ISRIB binds to eIF2's guanine nucleotide exchange factor eIF2B and induces its dimerization (30, 31). ISRIB-induced dimerization increases eIF2B-mediated guanine nucleotide exchange and desensitizes eIF2B activity to inhibition by p-eIF2α. As such, it blunts the effects of eIF2α phosphorylation on translation initiation. Strong parallels between *in vivo* genetic and pharmacological experiments support the notion that ISRIB exerts all its effect on-target by inhibiting the ISR induced by eIF2α phosphorylation (19, 32, 33).

We hypothesized that TBI-induced sustained eIF2α phosphorylation in the hippocampus, a brain region crucially involved in memory formation, could be a major contributor to the permanent cognitive dysfunction observed after TBI (34). To test this

notion, we investigated whether treatment with ISRIB, several weeks post-injury, could remedy TBI-induced impairments in cognitive function and associated changes in synaptic function.

Results

TBI induces acute and persistent phosphorylation of eIF2α in the hippocampus. To investigate whether TBI activates the ISR in the hippocampus, we induced focal contusion injury using controlled cortical impact in mice (34). This mouse model of TBI exhibits cognitive deficits similar to those commonly observed after contusion injuries in humans (35). Briefly, we surgically exposed the brain and induced a controlled impact injury with pneumatic piston on the right parietal cortex above the hippocampus. Sham controls received the same surgery but without a TBI. We collected and processed the hippocampus ipsilateral to the injury to quantify phosphorylation of eIF2α (p-eIF2α) levels at 1 and 28 days post injury ("dpi"; Fig. 1A). The phosphorylation of eIF2α was significantly increased in the hippocampus of animals with TBI at 1 dpi (Fig. 1B, C). Compared to sham controls, in mice with TBI, hippocampal p-eIF2α remained elevated even 28 days after injury (Fig. 1D, E), indicating that TBI triggers a persistent activation of the ISR in the hippocampus.

ISRIB rescues TBI-induced deficits in spatial learning and memory consolidation.
Next we investigated whether blockage of the TBI-induced ISR could reverse the learning and memory deficits in mice with TBI. To this end, we induced focal TBI (as described in Material and Methods), and allowed animals to recover for four weeks. We

then evaluated hippocampal-dependent long-term memory storage using a radial arm water maze (RAWM) (34). In this forced-swim behavioral test, animals learned to locate a hidden platform in one of the eight arms using navigational cues set in the room (Fig. 2A). Analysis tracking software was used to determine the number of incorrect arm entries (termed an "error"). The total number of errors before the animal finds the escape platform is used as a metric of learning and memory.

As expected, sham animals learned the location of the escape platform after multiple training blocks (Fig. 2B; 28-29 dpi; black solid circles). When memory was measured at 1 day and 7 days after training (Fig. 2B; 30 and 37 dpi), sham animals averaged less than one error before locating the escape platform. By contrast, learning was dramatically impaired in mice with TBI, even after multiple training blocks (Fig. 2B; 28 dpi; red circles, TBI mice averaged more than 3 errors). Consequently, when memory was tested on day 30 and day 37, injured mice made significantly more errors compared to sham animals (Fig. 2A, B; red solid circles). Thus, these data indicate that TBI impairs learning and memory.

To test whether pharmacological blockage of the ISR restores the lasting learning and memory deficits resulting from TBI, we injected the animals with ISRIB (at 2.5 mg/kg or vehicle) intra-peritoneally ("ip") into both sham and TBI animals. ISRIB treatment started at 27 dpi, the day before the first behavioral training (Fig. 2B, 27 dpi), and continued with daily injections throughout the duration of the training (3 injections in total; see Methods). Strikingly, during training ISRIB-treated injured animals (red open circles, dotted line; Fig. 2B; 28-29 dpi) performed better than vehicle-treated TBI animals (red solid circles, Fig. 2B; 28-29 dpi). More importantly, memory tested both 1

day (30 dpi) and 7 days (37 dpi) after training was dramatically improved in brain-injured mice treated with ISRB. As ISRIB was given only during training, the data demonstrate that the effect of ISRIB on memory lasts beyond the period of treatment.

ISRIB reverses TBI-induced deficits in hippocampal long-term potentiation. Sustained changes in synaptic efficacy that result from repeated neuronal activity are believed to constitute the cellular basis of learning and memory (36). The best-characterized form of synaptic plasticity in the mammalian brain is long-term potentiation (LTP), which is manifested as long-lasting increases in synaptic strength. Consistent with the deficits in hippocampal long-term memory, TBI has been previously reported to inhibit hippocampal LTP (37). To examine whether LTP was altered in our focal TBI model, we induced TBI as above, allowed the animals to recover for 4 weeks, and measured hippocampal LTP in hippocampal brain slices at Schaffer collateral-CA1 synapses. We observed that LTP was significantly impaired in hippocampal slices from TBI mice as compared to those of sham animals (Fig. 3A, B). Treatment with ISRIB reversed the deficient LTP in slices from TBI mice (Fig. 3A, B). It is noteworthy that ISRIB had no effect on LTP in sham animals (Fig. 3A, B), and did not significantly change basal synaptic transmission in TBI mice (Supplemental Fig. 1). Thus, ISRIB specifically restores LTP in mice with an injured brain. Taken together, these data show that ISRIB restored both hippocampal long-term memory and associated changes in synaptic function in TBI mice.

ISRIB restores TBI-induced deficits in working and episodic learning and memory in a concussive injury model.

To assess the robustness of our results, we next asked whether ISRIB might also be effective in another TBI model. We used a close head injury model (38-40), which mimics diffuse concussive injury commonly observed in human patients (35). Like the focal TBI model, concussive injury resulted in a chronic activation of the ISR in the hippocampus, as determined by increased phosphorylation of eIF2α at 26 dpi (Supplemental Fig. 2). We evaluated cognitive function using a delayed-matching-to-place paradigm (DMP) (41), a more challenging hippocampal-dependent behavioral task than RAWM. In DMP, deficits in both working and episodic-like learning and memory are assessed, while eliminating the potential stress-based caveats introduced by water exposure and forced swimming behavior, typically associated with RAWM. Animals on the DMP learn to locate an escape tunnel attached to one of 40 holes in a circular table using visual cues to evade loud noise in a brightly lit room (Fig. 4A). Importantly, the escape location was changed every day, forcing the animal to relearn the location of the tunnel. To quantify performance, analysis tracking software measured "escape latency", or the time taken by the mouse to enter the escape tunnel.

Both sham and concussive-injured animals were treated with ISRIB one day prior to behavior testing (14 dpi) and after the last trials of each testing day (15-17 dpi; Fig. 4B). Compared to sham, concussive-injured animals failed to learn the task and took significantly longer to reach the escape tunnel (Fig. 4B; TBI, vehicle: red solid circles; Sham, vehicle: black solid circles), a clear indication that their spatial memory is impaired. By contrast, ISRIB treatment ameliorated the concussive-injured animals'

performance by the third and fourth day of testing (17 and 18 dpi; Fig. 4B; TBI, ISRIB: red open circles, dotted line). Specifically, compared to vehicle-treated injured animals, ISRIB-treated concussive-injured animals, found the escape location faster, on the third and final day of the DMP (17 and 18 dpi; Fig. 4C and D). Thus, ISRIB effectively reversed cognitive deficits induced by a different TBI model and on an additional behavioral task.

Discussion

Our results demonstrate that pharmacological inhibition of the ISR with ISRIB can effectively reverse TBI-induced cognitive deficits in both focal and concussive rodent models. In both injury models, eIF2α phosphorylation was persistently increased, and hippocampus-dependent spatial learning and memory were severely impaired. Remarkably, ISRIB-treatment was sufficient to reverse the cognitive deficits in these TBI models. Likewise, LTP was restored in brain slices isolated from brain injured mice when treated with ISRIB. Since the long-term deficits induced by our TBI models last for at least 3-12 month ((42) and our unpublished results), these results demonstrate that pharmacological attenuation of the ISR can alleviate TBI-induced dementia and associated changes in synaptic function long after injury.

Unlike previous studies, our work focused on reversal of *chronic* deficits that develop after TBI. Previous work has been limited to acute injury responses immediately following injury where a robust inflammatory response characterized by immune-cell infiltration into the brain (34, 43-47), cytokine production (39, 40, 48-50), and reactive oxygen species release (51-53) lead to neuronal death. Thus, strategies to

64

counteract acute injury-mediated effects have aimed to dampen the inflammatory response (43, 44, 52, 54, 55). We and others have shown that blocking the acute inflammatory responses within 24 hours after injury prevented the development of TBI-induced cognitive deficits (34, 39, 40, 45, 50, 56, 57). However, attempts to translate the insights gleaned from acute TBI models have failed in preclinical studies. In addition, the development of potential treatments that can only be effective within an acute time window after injury poses limitations because their optimal treatment timing may not be feasible in many clinical settings.

In the present study, we demonstrate that treatment with ISRIB at *late* time points (2 and 4 weeks, respectively) rapidly reverses long-term TBI-induced cognitive deficits. Our findings rely on the study of two injury models and combine molecular biology, pharmacology, electrophysiology and behavioral studies to demonstrate that activation of the ISR is responsible, at least in part, for the memory deficits associated with TBI. As such, our results offer new hope that chronic cognitive defects resulting from TBI may be treatable.

Activation of the ISR impairs memory consolidation and activity-dependent changes in synaptic function. Phosphorylation of eIF2α inhibits the activity of eIF2's guanine nucleotide exchange factor eIF2B, and ISRIB counteracts this effect by activating eIF2B through dimerization, which renders it less sensitive to inhibition by p-eIF2. The consequences of ISR activation are a general down-regulation of translation of most cellular mRNAs that utilize eIF2 to initiate ribosomes at AUG start codons. In addition, proteins encoded by a small subset of mRNAs that contain strategically placed small open reading frames in their 5'-UTRs become selectively upregulated when the

ISR is activated. ISR-upregulated proteins include the broadly expressed transcription factor ATF4, a memory repressor gene (58, 59), and the neuronally expressed Rho GAP OPHN1 (33, 60). We have previously shown that eIF2α phosphorylation-mediated increase in OPHN1 leads to AMPA receptor down-regulation and mGluR-induced long-term depression (LTD) in the hippocampus and ventral tegmental area (VTA) (33, 61). We have also found that reduced phosphorylation of eIF2α (or treatment with ISRIB) blocks mGluR-LTD but enhances cocaine-induced LTP in the VTA (61, 62). While it remains unknown whether the principles described for the VTA also apply to the hippocampus, we speculate that ISRIB enhances cognitive abilities by blocking LTD and consequently enhancing LTP, thus keeping synaptic connections stronger. Indeed, reduction of eIF2α phosphorylation enhances hippocampal LTP (19, 22), but blocks mGluR-LTD (33). By contrast, induction of eIF2α phosphorylation in hippocampal neurons impairs LTP (19, 25) and induces mGluR-LTD (33). Thus, our finding that ISRIB treatment rescued long-term TBI-induced deficits in hippocampal LTP is entirely consistent with these studies linking the ISR to LTP.

Most surprisingly, we found that systemic treatment with ISRIB weeks after injury allowed mice to form stable spatial memories that lasted for at least a week even after ISRIB treatment was stopped. ISRIB's bioavailability has a half-life of approximately eight hours in mouse plasma and in the brain. It equilibrates readily between plasma and the brain and therefore it is entirely cleared from the system within a week (29). Thus it is highly unlikely that ISRIB is directly influencing memory recall (e.g., at 37 dpi in Figure 2), but rather that ISRIB has produced enduring changes to memory processes during the treatment period, such as dendritic spine remodeling.

Previous work has established that TBI acutely induces significant dendritic spine degeneration (63), and dendritic spine loss persists even a year after a severe TBI (64). In addition, pharmacological induction of eIF2α phosphorylation in chicks blocks training-induced increase in the number of spines in an auditory brain area (24). Given the close association between eIF2α phosphorylation, LTP, and spine formation, the observed lasting effects of ISRIB treatment on memory may point to changes in structural plasticity during learning that persist even in the absence of the ISRIB (65-67).

It remains unclear whether ISRIB is enhancing learning and memory through direct impact on neurons or if the potential therapeutic effects acts on other cell types such as microglia, astrocytes, and/or immune cells. Since activation of the ISR and eIF2α phosphorylation causes inflammatory cytokine production (68, 69) and ISRIB interferes with downstream effects of eIF2α, it is possible that ISRIB may be reversing TBI-initiated residual low-grade inflammation that remains after acute inflammation has subsided (34). We have previously shown that pharmacological or genetic blockade of peripherally-derived bone marrow macrophage infiltration to the brain ameliorates TBI-induced cognitive loss by preventing inflammatory cytokine production and reactive oxygen species release (34, 53). Whether ISRIB can influence immune cell-mediated cytokine production after TBI is not known. While our previous reports have shown that peripheral macrophage infiltration occurs only acutely after injury, we have observed low-level chronic inflammation after TBI (34). Hence, it is entirely plausible that ISRIB may impact immune function to alleviate cognitive decline.

The surprising results presented here have yet to be extended from mouse models to human physiology. It also remains unclear whether ISRIB treatment cures the

cognitive defects permanently or whether lingering pathologies necessitate the ISRIB treatment to be repeated for each new learning task. Chronic activation of the ISR and/or neuroinflammation are associated with numerous neurodegenerative disease states (reviewed in (70)). Therefore, increased understanding of these pathways characterized in TBI may have broader therapeutic potential, especially when the window for treating acute injuries has passed. These gaps in our knowledge notwithstanding, we are hopeful that our findings may open promising new therapeutic avenues for patients that are suffering from cognitive deficits associated with TBI and other neurodegenerative disorders.

Materials and Methods

Animals. All experiments were conducted in accordance with National Institutes of Health (NIH) *Guide for the Care and Use of Laboratory Animals* and were approved by the Institutional Animal Care and Use Committee of University of California (San Francisco). Male C57B6/J wildtype (WT) mice were purchased from Jackson Laboratory (Bar Harbor, ME) and used for experiments at approximately 12 weeks of age. Mice were group housed in environmentally controlled conditions with reverse light cycle (12:12h light:dark cycle at 21 ± 1°C) and provided food and water *ad libitum*.

Surgical Procedure. All animals were randomly assigned to TBI or sham surgeries. Animals were anesthetized and maintained at 2% isoflurane and secured to a stereotaxic frame with non-traumatic ear bars. The hair on their scalp was removed, and

eye ointment and betadine were applied to their eyes and scalp respectively. A midline incision was made to expose the skull.

Focal TBI: Controlled Cortical Impact. A unilateral TBI was induced in the right parietal lobe using the controlled cortical impact model (34). Mice received a ~3.5 mm diameter craniectomy, a removal of part of the skull, using an electric microdrill. The coordinates of the craniectomy were: anteroposterior, -2.00 mm and mediolateral, +2.00 mm with respect to bregma. Any animal that experienced excessive bleeding due to disruption of the dura was removed from the study. After the craniectomy, the contusion was induced using a 3 mm convex tip attached to an electromagnetic impactor (Leica). The contusion depth was set to 0.95 mm from dura with a velocity of 4.0 m/s sustained for 300 ms. These injury parameters were chosen to target, but not penetrate, the hippocampus. Sham animals received craniectomy surgeries but without the focal injury.

Concussive TBI: Closed Head Injury. TBI was induced along the midline of the parietal lobe using the closed head injury model (38). The head of the animal was supported with foam prior to injury. Contusion was induced using a 5 mm convex tip attached to an electromagnetic impactor (Leica) at the following coordinates: anteroposterior, -1.50 mm and mediolateral, 0 mm with respect to bregma. The contusion was produced with an impact depth of 1 mm from the surface of the skull with a velocity of 5.0 m/s sustained for 300 ms. Any animals that had a fractured skull after

injury were excluded from the study. Sham animals received the midline skin incision but no impact.

After focal or concussive TBI surgery, the scalp was sutured and the animal was allowed to recover in an incubation chamber set to 37°C. Animals were returned to their home cage after showing normal walking and grooming behavior. All animals fully recovered from the surgical procedures as exhibited by normal behavior and weight maintenance monitored throughout the duration of the experiments.

Drug Administration. ISRIB solution was made by dissolving 5 mg ISRIB in 1 mL Dimethyl Sulfoxide (DMSO; Fisher Scientific, Cat# D128-500) and 1 mL Polyethylene Glycol 400 (PEG400; EMD Millipore, Cat# PX1286B-2). The solution was gently heated in a 40°C waterbath and vortexed every 30 seconds until the solution became clear. The solution was kept in a warm environment throughout the experiment. Each solution was used for injections up to 4 days maximum. If the solution became visibly cloudy or precipitated, a new solution was prepared. ISRIB was delivered at 2.5 mg/kg dosage through intraperitoneal injections. The vehicle solution consisted of 1 mL DMSO and 1 mL PEG400.

Western Blotting. Hippocampi ipsilateral to the TBI in focal injury model animals were removed at 1 or 28 days post-surgery (dpi; days post-injury) while the right hippocampi from concussive injury model animals were removed at 26 dpi. Samples were processed for protein quantification using homogenization buffer consisting of RIPA Lysis and Extraction Buffer (Fisher Scientific, Cat#89900), PhosSTOP (Roche,

Cat#04906845001), and cOmplete ULTRA Tablets (Roche, Cat#05892970001). The nuclear and high molecular weight membrane fraction was removed and the remaining cytoplasmic and membrane fraction was quantified through use of a BCA assay (Pierce BCA Protein Assay Kit; Fisher Scientific, Cat#23227).

Total protein (50 microgram) per lane was loaded onto a 5-15% SDS-polyacrylamide gel (Bio-Rad, Cat#567-1084) for electrophoresis. Proteins were then transferred from gel onto a nitrocellulose membrane for immunodetection. Membranes were blocked for 1 hour in 5% nonfat dry milk (NFDM; Bio-Rad Cat#170-6404) in phosphate buffered saline with Tween20 (PBS-T; 0.1% Tween20). Antibodies specific for eIF2α (Cell Signaling, Cat#9722; 1:1000), p-eIF2α (Cell Signaling, Cat#9721; 1:1000), and GADPH (Sigma, Cat#G8795; 1:10000) were incubated overnight at 4C in 5% NFDM in PBS-T. After washes in PBS-T, the mebrane was incubated at room temperature for 1 hour in appropriate secondary antibodies (Li-Cor) diluted in 1% NFDM in PBST-T. Membranes were scanned using a Li-Cor Odyssey near-infrared imager. Raw intensity for each band was measured using Li-Cor Odyssey image analysis software. Target protein intensities were normalized to corresponding GADPH loading control intensities to account for amount of protein per well.

Behavioral Assays. For all behavioral assays the experimenters were blinded both to the injury regimen and therapeutic intervention. Behavioral tests were recorded and scored using a video tracking and analysis setup (Ethovision XT 8.5, Noldus Information Technology). Additionally, all behaviors were run on independent animal cohorts.

Radial Arm Water Maze: At 28 dpi, the focal TBI experiment groups (n=8 Sham+Vehicle, n=8 Sham+ISRIB, n=16 TBI+Vehicle, n=16 TBI+ISRIB) were tested on the radial arm water maze (RAWM) assay (34). The maze involved a pool 118.5 cm in diameter with 8 arms each 41 cm in length and an escape platform that could be moved (Fig. 1A). The pool was filled with water that was rendered opaque by adding white paint (Crayola, 54-2128-053). Visual cues were placed around the room such that they were visible to animals exploring the maze. Animals ran 15 trials a day during training and 3 trials during each memory test. On the first training day, the escape platform could be made visible by placing a flag that could be seen above water on the platform. The escape platform alternated between being visible and hidden for the first 12 trials. The final three trials of the first day were all presented with a hidden platform. During the second training day and the memory tests, the escape platform remained hidden. Animals were trained for two days and then tested on memory tests 24 hours and 7 days after training.

During a trial, animals were placed in a random arm that did not include the escape platform. Animals were allowed one minute to locate the escape platform. On successfully finding the platform, animals remained there for 10 seconds before being returned to their holding cage. On a failed trial, animals were guided to the escape platform and then returned to their holding cage 10 seconds later. The escape platform location was the same while the start arm varied between trials for each individual animal. The escape platform location was randomly assigned for each animal to account for any preferences of exploration in the maze.

Animals were i.p-injected either vehicle or ISRIB (2.5 mg/kg) starting the day prior to behavior (27 dpi) and after each of the final trials of the training days (28 and 29 dpi) for a total of three injections. No injections were given when memory was tested on days 30 and 37 dpi.

RAWM data was collected through a video tracking and analysis setup (Ethovision XT 8.5, Noldus Information Technology). The program automatically analyzed the number of errors made per trial. Every three trials were averaged into a block to account for large variability in performance; each training day thus consisted of five blocks while each memory test was one block each. Furthermore, the experimenter was blinded to the treatment groups during the behavioral assay.

Delayed-Matching-to-Place Paradigm: At 15 dpi, the concussive TBI experiment groups (n=12 Sham+Vehicle, n=11 Sham+ISRIB, n=11 TBI+Vehicle, n=12 TBI+ISRIB) were tested on delayed-matching-to-place paradigm (DMP) using a modified Barnes maze (41). The maze consisted of a round table 112 cm in diameter with 40 escape holes arranged in three concentric rings consisting of 8, 16, and 16 holes at 20, 35, and 50 cm from the center of the maze respectively. An escape tunnel was connected to one of the outer holes. Visual cues were placed around the room such that they were visible to animals on the table. Bright overhead lighting and a loud tone (2 KHz, 85 db) were used as aversive stimuli to motivate animals to locate the escape tunnel. The assay was performed for four days (15-18 dpi). The escape tunnel location was moved for each day and animals ran four trials per day.

During a trial, animals were placed onto the center of the table covered by an opaque plastic box so they are not exposed to the environment. After they had been

73

placed on the table for 10 seconds, the plastic box was removed and the tone started playing marking the start of the trial. Animals were given 90 seconds to explore the maze and locate the escape tunnel. Upon the animals successfully locating and entering the escape tunnel, the tone was stopped. If the animals failed to find the escape tunnel after 90 seconds, they were guided to the escape tunnel before the tone was stopped. Animals remained in the escape tunnel for 10 seconds before being returned to their home cage. The maze and escape tunnel were cleaned with ethanol between each trial.

Animals were i.p-injected with either vehicle or ISRIB (2.5 mg/kg) starting the day prior to behavior (14 dpi) and after the final trial of each day (15-17 dpi) for a total of four injections. The experimenter was blind to the treatment groups during the behavioral assay. Each trial was recorded using a video tracking and analysis setup (Ethovision XT 8.5, Noldus Information Technology) and the program automatically analyzed the amount of time required to locate the escape tunnel. The escape latencies of trials 2, 3, and 4 were averaged as a measure of ability to learn and perform the DMP task during the day.

Electrophysiology: Electrophysiological recordings were performed as previously described (22, 71, 72). Briefly, hippocampal slices (350 μm) were cut from brains of Sham and TBI (focal injury; n=7-9/group) mice in 4°C artificial cerebrospinal fluid (ACSF), kept in ACSF at room temperature for at least one hour before recording, and maintained in an interface-type chamber perfused with oxygenated ACSF (95% O_2 and 5% CO_2) containing in mM: 124 NaCl, 2.0 KCl, 1.3 $MgSO_4$, 2.5 $CaCl_2$, 1.2 KH_2PO_4, 25

NaHCO$_3$, and 10 glucose (2-3 ml/min). Bipolar stimulating electrodes were placed in the CA1 stratum radiatum to stimulate Schaffer collateral and commissural fibers. Field EPSPs were recorded using ACSF-filled micropipettes at 28-29 °C. The stimulus strength of the 0.1 ms pulses was adjusted to evoke 30-35% of maximum response. LTP was elicited by a train of high-frequency stimulation (100 Hz, 1 s). When indicated, slices were treated with ISRIB (50 nM) for at least 30 min before stimulation and throughout the entire recording.

Statistical Analysis: All statistical analyses were performed on Graphpad Prism 6 (Graphpad Software). Western blot quantification was analyzed by unpaired Student's t-test. Behavioral data was analyzed by two-way analysis of variance (ANOVA) with post hoc Bonferroni's multiple comparison. Electrophysiology data was analyzed by one-way ANOVA with post hoc Bonferroni's multiple comparison and "n" indicating the number of slices. All data presented are means ± SEM with significance set at $p < 0.05$.

Figures
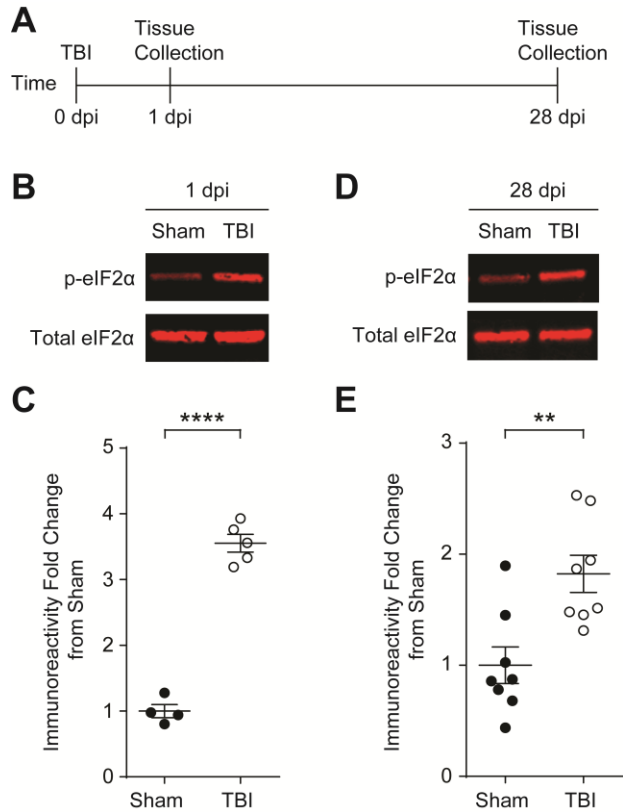
Fig. 1. TBI-induced increase in eIF2α phosphorylation persists four weeks after injury.

(A) Experimental design scheme. Animals were given a focal TBI by the controlled cortical impact method and the hippocampus ipsilateral to the injury was collected at either 1 dpi or 28 dpi. Sham controls received a craniectomy without a TBI and were analyzed at the same time points.

(B) Representative images of p-eIF2α and total-eIF2α Western blots from the hippocampi protein samples collected at 1 dpi.

(C) Quantification of p-eIF2α to total eIF2α ratio normalized to Sham. TBI increases phosphorylation of eIF2α at 24 hours post-injury. Data are means ± SEM (n=4-6/group, Student's t-test; ****$p<0.0001$).

(D) Representative images of p-eIF2α and total-eIF2α. Western blots from the hippocampi collected at 28 dpi.

(E) Quantification of p-eIF2α to total eIF2α ratio normalized to Sham. The increase in p-eIF2α in TBI animals persists at 28 dpi. Data are means ± SEM (n=8/group, Student's t-test; **p<0.01).

A

Vehicle   ISRIB

Sham

TBI

Block 1 (28 dpi)

Block 12 (37 dpi)

B

- SHAM, Vehicle
- SHAM, ISRIB
- TBI, Vehicle
- TBI, ISRIB

Errors

Block

ISRIB   ISRIB   ISRIB

28 dpi   29 dpi   30 dpi   37 dpi

C 30 dpi Memory Test

Errors

ISRIB
-    +   -   +
Sham   TBI

D 37 dpi Memory Test

Errors

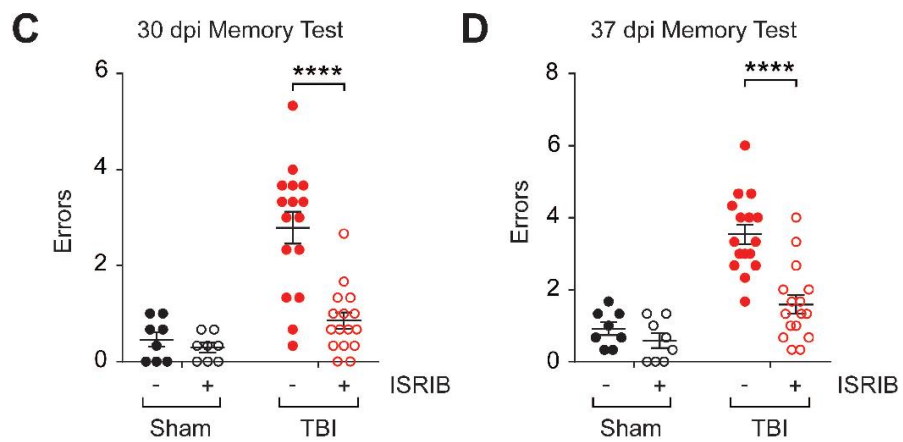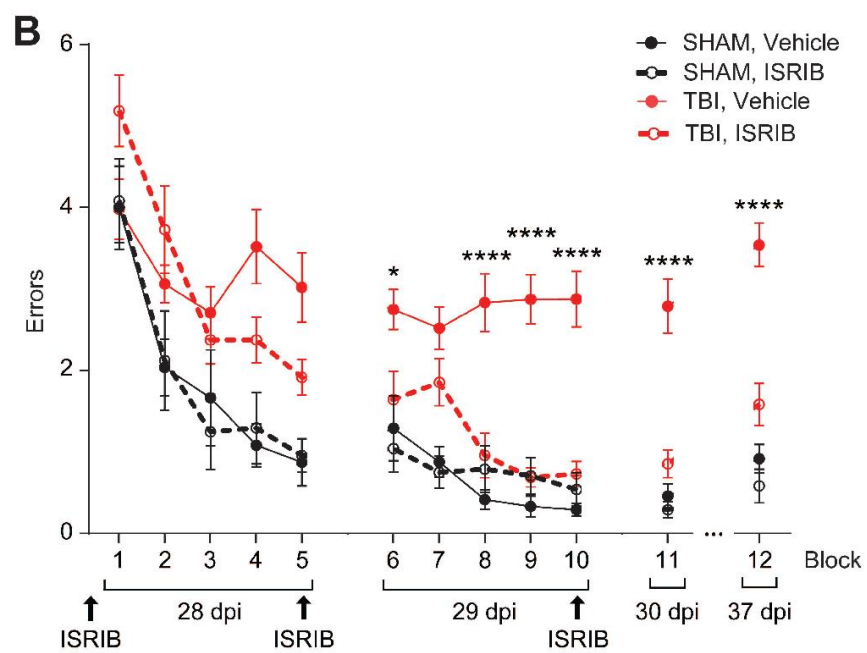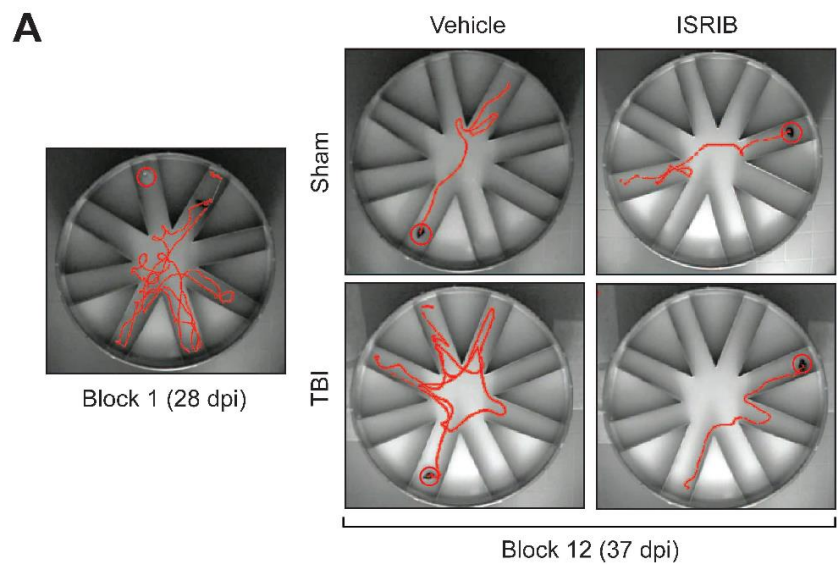ISRIB
-    +   -   +
Sham   TBI

Fig. 2. ISRIB treatment rescue TBI-induced behavioral deficits on the radial arm water maze 28 days after focal TBI.

(A) Representative track plots showing exploratory activity on the RAWM. While all animals initially made multiple errors while locating the escape platform (Block 1; left), sham and ISRIB-treated TBI animals learned the escape platform location and therefore made fewer errors during the memory test 7 days after training (Block 12; 37 dpi). Vehicle-treated TBI animals made more errors than animals in the other three experiment groups (right).

(B) Animals were i.p-injected either vehicle or ISRIB (2.5 mg/kg) the night prior to starting behavior (27 dpi) and after the last trials each day during training (28 and 29 dpi; n=8/Sham group, n=16/TBI group). Animals ran 15 trials on each training day with the performance of every 3 trials averaged as a single block. Compared to vehicle-treated group (red solid circle, solid line), ISRIB-treated animals (red open circle, dotted line) made significantly less errors over the course of training and when memory was tested on day 1 (30 dpi) and day 7 (37 dpi). Data are means ± SEM (Bonferroni post hoc test, TBI+vehicle vs TBI+ISRIB; *$p<0.05$, ****$p<0.0001$).

(C) Individual animal performance during the memory test 24 hours after training (Block 11; 30 dpi). Vehicle-treated TBI animals made significantly more errors than all other experimental cohorts. Data are means ± SEM (Bonferroni post hoc test; ****$p<0.0001$).

(D) Individual animal performance during the memory test 7 days after training (Block 12; 37 dpi). Improvement in RAWM performance persisted in ISRIB-treated TBI animals. Data are means ± SEM (Bonferroni post hoc test; ****$p<0.0001$).
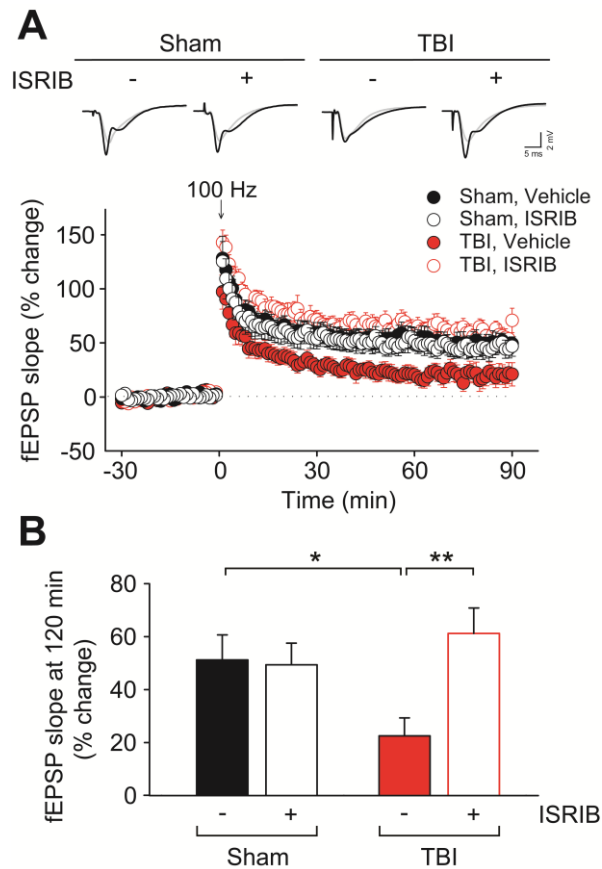
Fig. 3. ISRIB treatment reverses impaired hippocampal LTP in focal TBI mice.

(A) Top, Representative fEPSP traces at baseline and 90 min after high-frequency stimulation (100Hz, 1sec). Bottom, LTP was impaired in slices from TBI mice ($F_{(1,12)}$=7.549, p=0.018; n=7-9/group), compared to slices from sham mice. ISRIB treatment (50 nM) restored impaired LTP in TBI mice ($F_{(1,14)}$=10.556, p=0.006), but had no significant effect on LTP in slices from sham mice ($F_{(1,13)}$=0.555, p=0.470). Data are means ± SEM (Bonferroni post hoc test; *p < 0.05; **p < 0.01).

(B) Summary data shows the mean field excitatory postsynaptic potential fEPSP slope from 30 min before and 90 min after the stimulation. Data are means ± SEM (Bonferroni post hoc test; *p < 0.05; **p < 0.01).

A

Vehicle | ISRIB

Sham

TBI

Trial 1 (18 dpi)

Trial 4 (18 dpi)

B

- SHAM, Vehicle
- SHAM, ISRIB
- TBI, Vehicle
- TBI, ISRIB

Escape Latency (s)

15 dpi   16 dpi   17 dpi   18 dpi

ISRIB   ISRIB   ISRIB   ISRIB

Trial

C

17 dpi

Average Escape Latency (s)

ISRIB   −   +   −   +

Sham   TBI

D

18 dpi

Average Escape Latency (s)

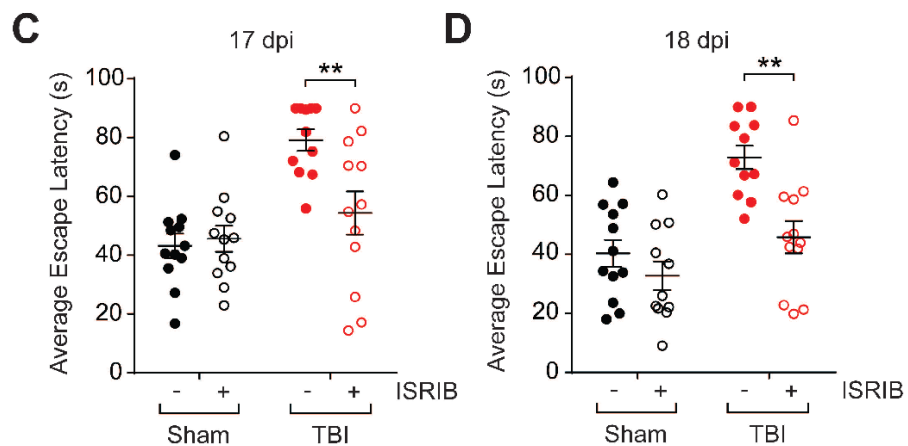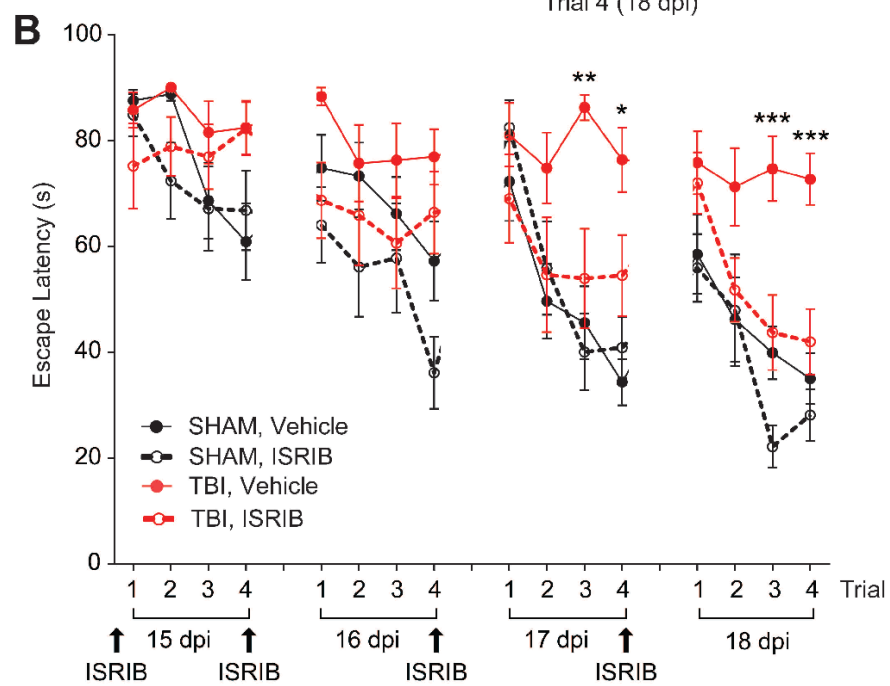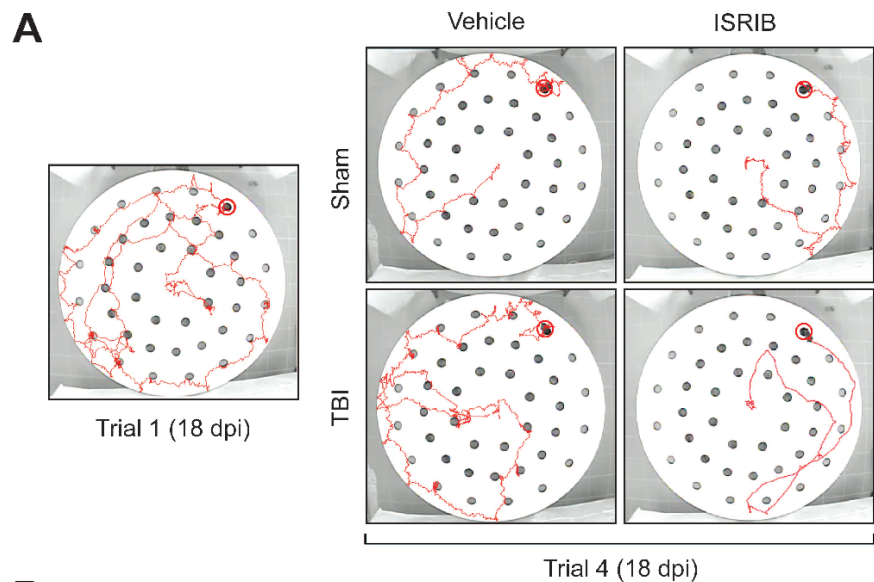ISRIB   −   +   −   +

Sham   TBI

81

Fig. 4. ISRIB treatment rescue TBI-induced behavioral deficits on the delayed-matching-to-place paradigm 14 days after concussive injury.

(A) Representative tracks of trials on the modified Barnes maze of the DMP assay. During Trial 1 of each day, animals did not know the escape tunnel location and did not find it quickly (Trial 1; left). By Trial 4, the animals had learned the location of the escape tunnel and took significantly less time on the trial. ISRIB-treated TBI mice showed similar performance as both sham groups on Day 4 whereas vehicle-treated TBI mice took longer to escape (right).

(B) Animals were injected the night before the first day of behavior (14 dpi) and after the last trial of each day (15-17 dpi; n=11-12/group). Animals that received sham surgeries were able to learn the location of the escape tunnel over the course of each day (vehicle: black solid circle, solid line; ISRIB-treated: black open circle, dotted line). TBI animals given vehicle injections (red solid circle, solid line) took longer to find the escape tunnel whereas TBI animals given ISRIB (red open circle, dotted line) did significantly better than their vehicle-treated counterparts. Data are means ± SEM (Bonferroni post hoc test; *p<0.05, **p<0.01, ***p<0.001).

(C) Individual animal performances averaged across trials 2, 3, and 4 on day 3 of the DMP (17 dpi). TBI animals treated with ISRIB were significantly faster at locating the escape location than their vehicle-treated, TBI counterparts. Data are means ± SEM (Bonferroni post hoc test; **p<0.01).

(D) Individual animal performances averaged across trials 2, 3, and 4 on day 4 of the DMP (18 dpi). ISRIB-treated TBI animals were significantly faster in locating the escape

82

tunnel than the vehicle-treated TBI group. Data are means ± SEM (Bonferroni post hoc test; **p<0.01).
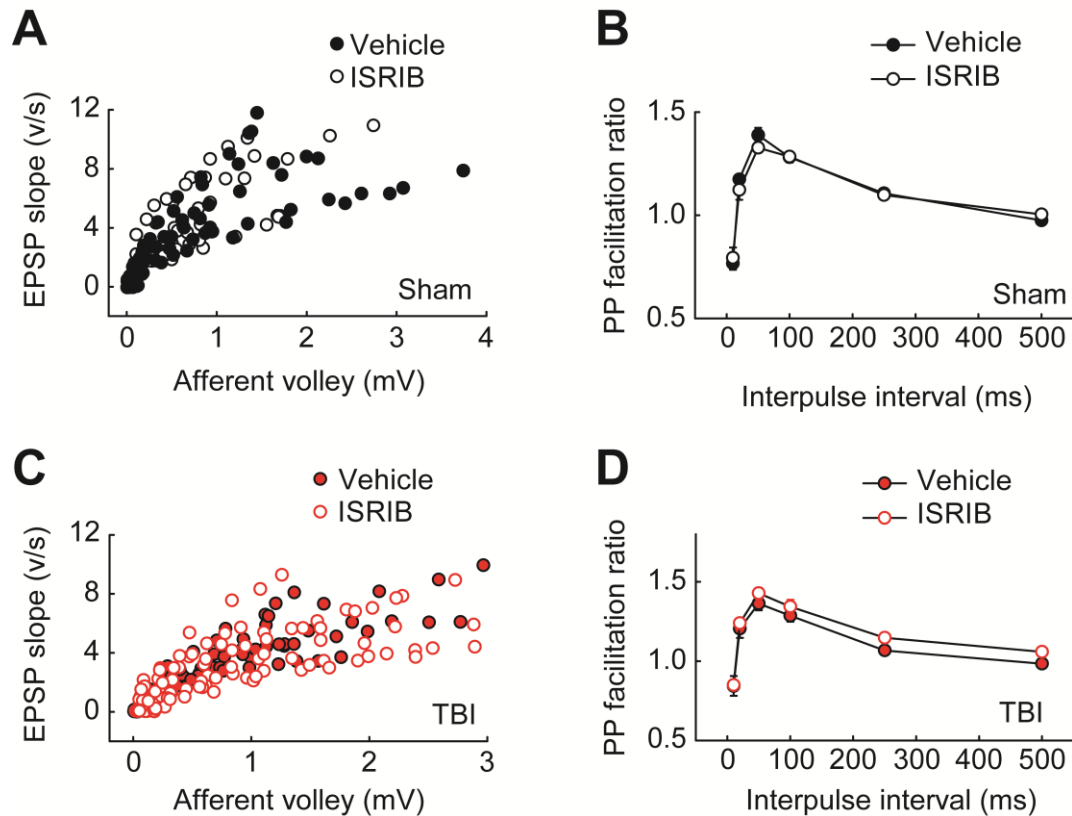
Fig. S1. ISRIB did not alter basal synaptic transmission in hippocampal slices from sham or TBI mice.

(A, C) Input-output plots show similar EPSPs as function of presynaptic fiber volley amplitude over a wide range of stimulus intensities in vehicle treated and ISRIB treated slices from sham (**A**; n=8-10/group) and TBI (**C**; n=11-13/group) mice.

(B, D) Paired-pulse facilitation of fEPSPs did not differ between vehicle and ISRIB-treated slices from sham (**B**; n=6-8/group) and TBI (**D**; n=8-9/group) mice, as shown by the plots of the PP ratio (fEPSP$_2$/ fEPSP$_1$) for various intervals of paired stimulation.
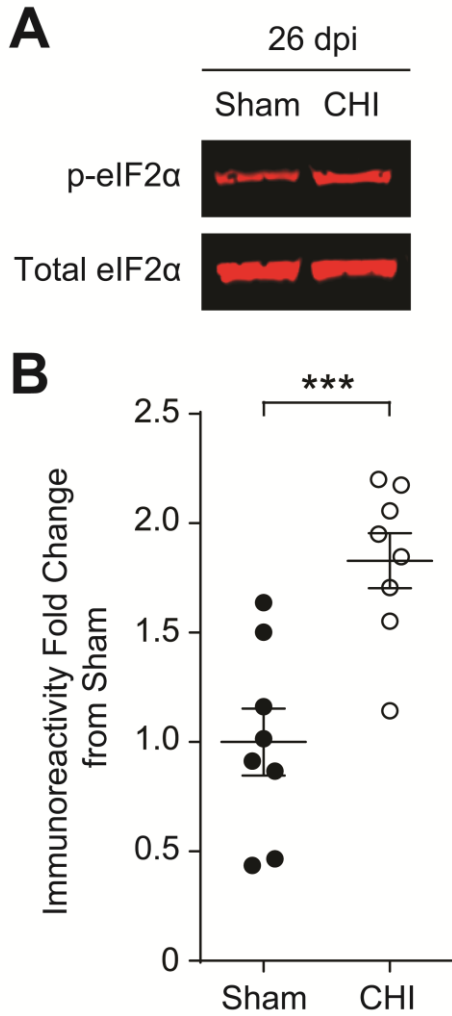
Fig. S2. Closed Head Injury induces an increase in eIF2α phosphorylation.

(A) Representative images of p-eIF2α and total-eIF2α. Western blots from the hippocampi protein samples collected at 26 dpi.

(B) Quantification of p-eIF2α to total eIF2α ratio normalized to Sham. CHI increases phosphorylation of eIF2α at 26 dpi. Data are means ± SEM (n=8/group; Student's t-test; ***p<0.001).

References

1. Smith DH, Johnson VE, & Stewart W (2013) Chronic neuropathologies of single and repetitive TBI: substrates of dementia? *Nat Rev Neurol* 9(4):211-221.

2. DeKosky ST, Ikonomovic MD, & Gandy S (2010) Traumatic brain injury--football, warfare, and long-term effects. *N Engl J Med* 363(14):1293-1296.

3. Sullivan P, Petitti D, & Barbaccia J (1987) Head trauma and age of onset of dementia of the Alzheimer type. *JAMA* 257(17):2289-2290.

4. Engberg AW & Teasdale TW (2004) Psychosocial outcome following traumatic brain injury in adults: a long-term population-based follow-up. *Brain Inj* 18(6):533-545.

5. Johnson VE, Stewart W, & Smith DH (2010) Traumatic brain injury and amyloid-beta pathology: a link to Alzheimer's disease? *Nat Rev Neurosci* 11(5):361-370.

6. Jellinger KA (2004) Traumatic brain injury as a risk factor for Alzheimer's disease. *J Neurol Neurosurg Psychiatry* 75(3):511-512.

7. Fleminger S, Oliver DL, Lovestone S, Rabe-Hesketh S, & Giora A (2003) Head injury as a risk factor for Alzheimer's disease: the evidence 10 years on; a partial replication. *J Neurol Neurosurg Psychiatry* 74(7):857-862.

8. Graves AB*, et al.* (1990) The association between head trauma and Alzheimer's disease. *Am J Epidemiol* 131(3):491-501.

9. Guo Z*, et al.* (2000) Head injury and the risk of AD in the MIRAGE study. *Neurology* 54(6):1316-1323.

10. Hernandez-Ontiveros DG*, et al.* (2013) Microglia activation as a biomarker for traumatic brain injury. *Front Neurol* 4:30.

11. Lozano D*, et al.* (2015) Neuroinflammatory responses to traumatic brain injury: etiology, clinical consequences, and therapeutic opportunities. *Neuropsychiatr Dis Treat* 11:97-106.

12. Adamides AA*, et al.* (2006) Current controversies in the management of patients with severe traumatic brain injury. *ANZ J Surg* 76(3):163-174.

13. Pearn ML*, et al.* (2016) Pathophysiology Associated with Traumatic Brain Injury: Current Treatments and Potential Novel Therapeutics. *Cell Mol Neurobiol*.

14. Harding HP*, et al.* (2003) An integrated stress response regulates amino acid metabolism and resistance to oxidative stress. *Mol Cell* 11(3):619-633.

15. Ron D & Harding HP (2012) Protein-folding homeostasis in the endoplasmic reticulum and nutritional regulation. *Cold Spring Harb Perspect Biol* 4(12).

16. Donnelly N, Gorman AM, Gupta S, & Samali A (2013) The eIF2alpha kinases: their structures and functions. *Cell Mol Life Sci* 70(19):3493-3511.

17. Hinnebusch AG, Ivanov IP, & Sonenberg N (2016) Translational control by 5'-untranslated regions of eukaryotic mRNAs. *Science* 352(6292):1413-1416.

18. Sonenberg N & Hinnebusch AG (2009) Regulation of translation initiation in eukaryotes: mechanisms and biological targets. *Cell* 136(4):731-745.

19. Costa-Mattioli M*, et al.* (2007) eIF2alpha phosphorylation bidirectionally regulates the switch from short- to long-term synaptic plasticity and memory. *Cell* 129(1):195-206.

20. Costa-Mattioli M, Sossin WS, Klann E, & Sonenberg N (2009) Translational control of long-lasting synaptic plasticity and memory. *Neuron* 61(1):10-26.

21. Buffington SA, Huang W, & Costa-Mattioli M (2014) Translational control in synaptic plasticity and cognitive dysfunction. *Annu Rev Neurosci* 37:17-38.

22. Zhu PJ*, et al.* (2011) Suppression of PKR promotes network excitability and enhanced cognition by interferon-gamma-mediated disinhibition. *Cell* 147(6):1384-1396.

23. Stern E, Chinnakkaruppan A, David O, Sonenberg N, & Rosenblum K (2013) Blocking the eIF2alpha kinase (PKR) enhances positive and negative forms of cortex-dependent taste memory. *J Neurosci* 33(6):2517-2525.

24. Batista G, Johnson JL, Dominguez E, Costa-Mattioli M, & Pena JL (2016) Translational control of auditory imprinting and structural plasticity by eIF2alpha. *Elife* 5.

25. Jiang Z*, et al.* (2010) eIF2alpha Phosphorylation-dependent translation in CA1 pyramidal cells impairs hippocampal memory consolidation without affecting general translation. *J Neurosci* 30(7):2582-2594.

26. Scheper W & Hoozemans JJ (2015) The unfolded protein response in neurodegenerative diseases: a neuropathological perspective. *Acta Neuropathol* 130(3):315-331.

27. Petrov T, Underwood BD, Braun B, Alousi SS, & Rafols JA (2001) Upregulation of iNOS expression and phosphorylation of eIF-2alpha are paralleled by suppression of protein synthesis in rat hypothalamus in a closed head trauma model. *J Neurotrauma* 18(8):799-812.

28. Begum G*, et al.* (2014) Docosahexaenoic acid reduces ER stress and abnormal protein accumulation and improves neuronal function following traumatic brain injury. *J Neurosci* 34(10):3743-3755.

29. Sidrauski C*, et al.* (2013) Pharmacological brake-release of mRNA translation enhances cognitive memory. *Elife* 2:e00498.

30. Sidrauski C, *et al.* (2015) Pharmacological dimerization and activation of the exchange factor eIF2B antagonizes the integrated stress response. *Elife* 4:e07314.

31. Sekine Y, *et al.* (2015) Stress responses. Mutations in a translation initiation factor identify the target of a memory-enhancing compound. *Science* 348(6238):1027-1030.

32. Sidrauski C, McGeachy AM, Ingolia NT, & Walter P (2015) The small molecule ISRIB reverses the effects of eIF2alpha phosphorylation on translation and stress granule assembly. *Elife* 4.

33. Di Prisco GV, *et al.* (2014) Translational control of mGluR-dependent long-term depression and object-place learning by eIF2alpha. *Nat Neurosci* 17(8):1073-1082.

34. Morganti JM, *et al.* (2015) CCR2 Antagonism Alters Brain Macrophage Polarization and Ameliorates Cognitive Dysfunction Induced by Traumatic Brain Injury. *J Neurosci* 35(2):748-760.

35. Xiong Y, Mahmood A, & Chopp M (2013) Animal models of traumatic brain injury. *Nat Rev Neurosci* 14(2):128-142.

36. Neves G, Cooke SF, & Bliss TV (2008) Synaptic plasticity, memory and the hippocampus: a neural network approach to causality. *Nat Rev Neurosci* 9(1):65-75.

37. Schwarzbach E, Bonislawski DP, Xiong G, & Cohen AS (2006) Mechanisms underlying the inability to induce area CA1 LTP in the mouse after traumatic brain injury. *Hippocampus* 16(6):541-550.

38. Webster SJ, Van Eldik LJ, Watterson DM, & Bachstetter AD (2015) Closed head injury in an age-related Alzheimer mouse model leads to an altered neuroinflammatory response and persistent cognitive impairment. *J Neurosci* 35(16):6554-6569.

39. Bachstetter AD*, et al.* (2015) Attenuation of traumatic brain injury-induced cognitive impairment in mice by targeting increased cytokine levels with a small molecule experimental therapeutic. *J Neuroinflammation* 12:69.

40. Lloyd E, Somera-Molina K, Van Eldik LJ, Watterson DM, & Wainwright MS (2008) Suppression of acute proinflammatory cytokine and chemokine upregulation by post-injury administration of a novel small molecule improves long-term neurologic outcome in a mouse model of traumatic brain injury. *J Neuroinflammation* 5:28.

41. Faizi M*, et al.* (2012) Thy1-hAPP(Lond/Swe+) mouse model of Alzheimer's disease displays broad behavioral deficits in sensorimotor, cognitive and social function. *Brain Behav* 2(2):142-154.

42. Dixon CE*, et al.* (1999) One-year study of spatial memory performance, brain morphology, and cholinergic markers after moderate controlled cortical impact in rats. *J Neurotrauma* 16(2):109-122.

43. Kumar A, Alvarez-Croda DM, Stoica BA, Faden AI, & Loane DJ (2015) Microglial/Macrophage Polarization Dynamics following Traumatic Brain Injury. *J Neurotrauma*.

44. Choi BY*, et al.* (2012) Prevention of traumatic brain injury-induced neuronal death by inhibition of NADPH oxidase activation. *Brain Res* 1481:49-58.

45. Hsieh CL*, et al.* (2014) CCR2 deficiency impairs macrophage infiltration and improves cognitive function after traumatic brain injury. *J Neurotrauma* 31(20):1677-1688.

46. Carlos TM, Clark RS, Franicola-Higgins D, Schiding JK, & Kochanek PM (1997) Expression of endothelial adhesion molecules and recruitment of neutrophils after traumatic brain injury in rats. *J Leukoc Biol* 61(3):279-285.

47. Szmydynger-Chodobska J, Strazielle N, Zink BJ, Ghersi-Egea JF, & Chodobski A (2009) The role of the choroid plexus in neutrophil invasion after traumatic brain injury. *J Cereb Blood Flow Metab* 29(9):1503-1516.

48. Acosta SA, Tajiri N, Sanberg PR, Kaneko Y, & Borlongan CV (2017) Increased Amyloid Precursor Protein and Tau Expression Manifests as Key Secondary Cell Death in Chronic Traumatic Brain Injury. *J Cell Physiol* 232(3):665-677.

49. Acosta SA*, et al.* (2015) Alpha-synuclein as a pathological link between chronic traumatic brain injury and Parkinson's disease. *J Cell Physiol* 230(5):1024-1032.

50. Song S*, et al.* (2016) Granulocyte colony-stimulating factor promotes behavioral recovery in a mouse model of traumatic brain injury. *J Neurosci Res* 94(5):409-423.

51. Kontos HA (1989) Oxygen radicals in CNS damage. *Chem Biol Interact* 72(3):229-255.

52. Roth TL*, et al.* (2014) Transcranial amelioration of inflammation and cell death after brain injury. *Nature* 505(7482):223-228.

53. Morganti JM*, et al.* (2016) Age exacerbates the CCR2/5-mediated neuroinflammatory response to traumatic brain injury. *J Neuroinflammation* 13(1):80.

54. Wang GH*, et al.* (2011) Free-radical scavenger edaravone treatment confers neuroprotection against traumatic brain injury in rats. *J Neurotrauma* 28(10):2123-2134.

55. Homsi S*, et al.* (2010) Blockade of acute microglial activation by minocycline promotes neuroprotection and reduces locomotor hyperactivity after closed head injury in mice: a twelve-week follow-up study. *J Neurotrauma* 27(5):911-921.

56. Acosta SA*, et al.* (2014) Combination therapy of human umbilical cord blood cells and granulocyte colony stimulating factor reduces histopathological and motor impairments in an experimental model of chronic traumatic brain injury. *PLoS One* 9(3):e90953.

57. Jacotte-Simancas A*, et al.* (2015) Effects of voluntary physical exercise, citicoline, and combined treatment on object recognition memory, neurogenesis, and neuroprotection after traumatic brain injury in rats. *J Neurotrauma* 32(10):739-751.

58. Chen A*, et al.* (2003) Inducible enhancement of memory storage and synaptic plasticity in transgenic mice expressing an inhibitor of ATF4 (CREB-2) and C/EBP proteins. *Neuron* 39(4):655-669.

59. Pasini S, Corona C, Liu J, Greene LA, & Shelanski ML (2015) Specific downregulation of hippocampal ATF4 reveals a necessary role in synaptic plasticity and memory. *Cell Rep* 11(2):183-191.

60. Nadif Kasri N, Nakano-Kobayashi A, & Van Aelst L (2011) Rapid synthesis of the X-linked mental retardation protein OPHN1 mediates mGluR-dependent LTD through interaction with the endocytic machinery. *Neuron* 72(2):300-315.

61. Huang W*, et al.* (2016) Translational control by eIF2alpha phosphorylation regulates vulnerability to the synaptic and behavioral effects of cocaine. *Elife* 5.

62. Placzek AN*, et al.* (2016) eIF2alpha-mediated translational control regulates the persistence of cocaine-induced LTP in midbrain dopamine neurons. *Elife* 5.

63. Gao X, Deng P, Xu ZC, & Chen J (2011) Moderate traumatic brain injury causes acute dendritic and synaptic degeneration in the hippocampal dentate gyrus. *PLoS One* 6(9):e24566.

64. Erturk A*, et al.* (2016) Interfering with the Chronic Immune Response Rescues Chronic Degeneration After Traumatic Brain Injury. *J Neurosci* 36(38):9962-9975.

65. Kelleher RJ, 3rd, Govindarajan A, & Tonegawa S (2004) Translational regulatory mechanisms in persistent forms of synaptic plasticity. *Neuron* 44(1):59-73.

66. Maletic-Savatic M, Malinow R, & Svoboda K (1999) Rapid dendritic morphogenesis in CA1 hippocampal dendrites induced by synaptic activity. *Science* 283(5409):1923-1927.

67. Engert F & Bonhoeffer T (1999) Dendritic spine changes associated with hippocampal long-term synaptic plasticity. *Nature* 399(6731):66-70.

68. Deng J*, et al.* (2004) Translational repression mediates activation of nuclear factor kappa B by phosphorylated translation initiation factor 2. *Mol Cell Biol* 24(23):10161-10168.

69. Zhang K & Kaufman RJ (2008) From endoplasmic-reticulum stress to the inflammatory response. *Nature* 454(7203):455-462.

70. Freeman OJ & Mallucci GR (2016) The UPR and synaptic dysfunction in neurodegeneration. *Brain Res* 1648(Pt B):530-537.

71. Stoica L*, et al.* (2011) Selective pharmacogenetic inhibition of mammalian target of Rapamycin complex I (mTORC1) blocks long-term synaptic plasticity and memory storage. *Proc Natl Acad Sci U S A* 108(9):3791-3796.

72. Huang W, *et al.* (2013) mTORC2 controls actin polymerization required for consolidation of long-term memory. *Nat Neurosci* 16(4):441-448.

Chapter 4: Frontal Lobe Contusion in Mice Chronically Impairs Prefrontal-Dependent Behavior

Abstract

Traumatic brain injury (TBI) is a major cause of chronic disability in the world. Moderate to severe TBI often results in damage to the frontal lobe region and leads to cognitive, emotional, and social behavioral sequelae that negatively affect quality of life. More specifically, TBI patients often develop persistent deficits in social behavior, anxiety, and executive functions such as attention, mental flexibility, and task switching. These deficits are intrinsically associated with prefrontal cortex (PFC) functionality. Currently, there is a lack of analogous, behaviorally characterized TBI models for investigating frontal lobe injuries despite the prevalence of focal contusions to the frontal lobe in TBI patients. We used the controlled cortical impact (CCI) model in mice to generate a frontal lobe contusion and studied behavioral changes associated with PFC function. We found that unilateral frontal lobe contusion in mice produced long-term impairments to social recognition and reversal learning while having only a minor effect on anxiety and completely sparing rule shifting and hippocampal-dependent behavior.

Introduction

Traumatic Brain Injury (TBI) is a leading cause of long-term neurological disability in the world with over 3 million TBI-related emergency and outpatient visits a year in the United States alone [1, 2]. While the fatality rate after TBIs has declined in the last two decades, the incidence of TBIs continues to climb, and the majority of TBI patients experience prolonged neurocognitive dysfunctions that substantially impact their quality

of life [3, 4]. Clinically, most TBIs are mild to moderate in severity, result in damage to frontal lobe areas due to cortical contusion, and affect prefrontal cortex (PFC)-dependent functions [5-7].

The PFC is responsible for executive function and is most susceptible to injury [5, 8]. Deficits in executive function in TBI patients include poor sociability [9], loss of cognitive flexibility [10, 11] and increased anxiety [12, 13]. The vulnerability of the PFC to TBI is further highlighted by studies correlating behavioral impairment to the severity of TBI characterized by MRI scans [5, 14]. Yet despite the relevance of PFC function in TBI patients, limited attention has been devoted to understanding and modeling the damage processes in the PFC at a chronic time point after a TBI event.

To more closely recapitulate injuries observed in human patients, we applied the controlled cortical impact (CCI) method to induce a frontal cortex TBI and measured PFC function at chronic time points post injury. Using the three-chamber sociability task [15, 16], the rule shift paradigm [17], and the elevated plus maze [18], we determined the injury's effect on social behavior, cognitive flexibility, and anxiety respectively. Furthermore, we utilized the novel object recognition task [19] to determine whether frontal lobe injury would affect hippocampal-dependent function given the anatomical and functional link between the two regions [20]. Our results demonstrate that frontal lobe contusion impairs social recognition and orbitofrontal cortex (OFC)-dependent rule reversal behavior. Conversely, the model displays only a trend for increased anxiety and no impairment on medial prefrontal cortex (mPFC)-dependent rule shifting or hippocampal-dependent memory.

Results

Frontal CCI produces a protracted contusion in the dorsal frontal cortex

Approximately 40 days after injury and following behavioral assessment, we perfused animals from each treatment group for volumetric analysis. Qualitative images for NeuN staining showed formation of a cavitation at the site of injury (Fig 1A). Quantification through stereological analysis of the frontal lobe revealed approximately 25% loss of cortical volume in injured animals compared to sham (Fig 1B; $p < 0.01$).

Social recognition but not sociability is impaired by frontal TBI

Since social behavior is often altered after TBI events in human patients [14, 24], we utilized the three-chamber social approach task to investigate sociability and social recognition of the mice one month after injury. Mice were tested on two aspects of social behavior: their preference for socializing with a mouse over exploring a novel object (sociability; Fig 2A) and their preference for interacting with a novel mouse over a familiar mouse (social recognition; Fig 2B). There were no differences in total exploration time between treatment groups during either phase (Figs 2C and 2D). Frontal TBI did not affect the sociability of the injured mice; both experimental groups showed strong preferences for interacting with a mouse over an empty cage (Preference Ratio>1; Figs 2A and 2E). Although both groups exhibited preference for the novel stranger over the familiar mouse, however, TBI-injured animals had significantly less preference compared to sham (Figs 2B and 2F; $p < 0.05$).

Frontal TBI selectively impairs OFC-dependent reversal learning but spares mPFC-dependent rule shift behavior

To determine whether frontal lobe TBI would produce region-specific behavioral deficits, we employed the rule shift assay to identify differences in OFC-mediated or mPFC-mediated behavior after injury [17]. Mice first learned to associate one of four cues (Texture 1, Texture 2, Odor 1, Odor 2) with a food reward and then were tested on their ability to reverse the association (e.g. Texture 1 to Texture 2) or perform a rule shift (e.g. Texture 1 to Odor 1; Figs 3A and 3B). There were no differences between experimental groups in learning to associate either odor or digging media to the food reward during the initial association (Fig 3C). During the OFC-dependent reversal task, TBI animals committed significantly more errors before they successfully unlearned the initial rule and associated the new stimulus with the food reward (Fig 3D; $p < 0.05$). Conversely, there was no effect of TBI on the animals' ability to learn a new initial association the following day (data not shown) or perform the mPFC-dependent rule shift (Fig 3E).

Furthermore, because TBI-induced symptoms in human patients persist years after injury [3, 4], we examined a separate cohort of mice at 5.5 months after TBI surgery to determine whether OFC function would be chronically impaired. Similar to the first group of TBI animals, the second TBI cohort was also impaired on OFC-dependent reversal and unaffected on initial association and mPFC-dependent rule shifting (Figs 3C and 3D; $p < 0.05$).

Anxiety and hippocampal-dependent memory are unaffected by frontal TBI

To determine whether a frontal TBI would affect anxiety, we tested animals a month after injury on the EPM which measures anxiety as the time animals spend in the closed and open arms of the maze. Frontal contusion did not reduce the distance traveled or affect the average velocity of the animal compared to sham surgery controls, indicating no loss of motivation to explore or impairment in motor control (Figs 4A and B). There was no significant difference on the time spent in the closed arms of the EPM between sham and injured mice (Fig 4C; p=0.112). We did observe a trend for TBI animals to spend less time in the open arm of the EPM compared to sham although the result was not statistically significant (Fig 4D; p=0.065).

Additionally, to assess whether frontal lobe TBI would affect hippocampal-dependent memory, the animals were tested on the hippocampal-dependent novel object recognition assay. During the training trial, animals were exposed to two identical objects. On the test trial 24 hours after, animals were presented with one familiar object from the training trial and a novel object. Sham and TBI animals explored for the same amount of time during both training and testing trials (Figs 5A and 5B). Animals from both groups explored the identical objects equally during the training trial (Fig 5C). Furthermore, both sham and TBI animals exhibited similarly significant preference for the novel object over the familiar object during the test trial, suggesting hippocampal function was unaffected by the injury (Fig 5D; p<0.01).

Discussion

Currently, there is a lack of analogous, behaviorally characterized TBI models investigating frontal lobe injuries despite the prevalence of focal contusions to the frontal

lobe in TBI patients [5, 25, 26]. Utilizing the CCI model to simulate a frontal contusion, we evaluated three frontal lobe dependent behaviors to determine whether TBI symptoms observed in human patients could be recapitulated in mice. Given the functional and anatomical connection between PFC and hippocampus [20], we also assessed performance on a hippocampal-dependent assay.

Social behavior is commonly affected among human patients leading to impairment of social cognition such as emotion recognition, theory of mind, and empathy [24, 27]. Furthermore, the degree of social behavioral deficits has been correlated to severity of injury based on duration of post-TBI amnesia and formation of lesion [14]. Recent studies have shown that blast TBI and pediatric TBI rodent models demonstrate impairments in sociability and social recognition, recapitulating changes in social behavior seen in human patients with analogous injuries [16, 28]. While our frontal contusion model exhibits normal sociability, the injured mice have a decreased preference for social novelty. The result warrants further investigation as the impairment in social recognition could be due to social anxiety, diminished response to novelty, or deficits in forming social memory [22, 29, 30]. Our data from the EPM and the novel object recognition assay, however, suggests that any effect of TBI to anxiety or preference for novelty may be specific to social interactions.

In addition to social behavior, the frontal lobe is also responsible for maintenance of attention and the ability to reverse recently acquired behavioral rules [31, 32]. TBI patients often exhibit deficits in cognitive flexibility as reflected by poor performance on the Wisconsin Card Sorting Test in which participants learn initial rules for matching cards into sets and then have to unlearn previous associations in subsequent trials that

follow new rules for organization [33, 34]. This diagnostic test has been adopted for rodents in the form of the rule shift and attentional set shift assays, allowing for quantification of an animal's ability to reverse out of a previously learned behavioral rule and its ability to switch attention from one stimulus to another [17, 31, 35]. A previous study found that a severe parietal CCI injury that resulted in substantial loss of brain tissue could induce deficits in both reversal and set shifting ability three weeks post-injury [36]. Our frontal lobe contusion model, however, produced moderate cortical tissue loss and exhibited deficits only on rule reversal and not on rule shift behavior which suggests that reversal ability may be more vulnerable to frontal lobe TBIs in mice. Furthermore, the impairment in reversal learning persisted past 5 months after injury, suggesting the effect of injury is chronic as it is in human patients.

Patients also often develop chronic anxiety and comorbid anxiety-related disorders after TBI events [12, 37, 38]. Various models of TBI on the parietal lobe however have produced conflicting effects of injury in rodents; some models report increased anxiety while others exhibit reduced anxiety or no significant changes in behavior [39-41]. Further complicating the matter, our current data shows a trend for anxiogenic effect of injury which may suggest this injury model is insufficient to induce significant anxiety-like behavior. This is supported by data in human survivors of TBI showing that severity of injury is more highly correlated with anxiety disorders [42].

The behavioral sequelae observed in this study suggest an OFC-specific vulnerability to frontal TBI. This is primarily supported by the deficit on reversal learning observed in the injured mice. Lesion studies and optogenetic manipulations on mice performing the rule shift assay have shown that the OFC is necessary for reversal

learning while rule shifting depends on mPFC function [17, 31]. The region-specificity of the behavioral assay is further supported by models for schizophrenia and aging that display deficits in OFC neuronal function and reversal learning only [31] or mPFC function and rule shifting only [43, 44]. In humans, the OFC is commonly injured after severe trauma and the TBI patients often display behavioral symptoms, such as poor performance on the Wisconsin Card Sorting Test, similar to those with explicitly degenerated or lesioned OFCs [5, 10, 33]. Moreover, OFC involvement has also been documented in social recognition impairment and development of anxiety in patients with anxiety disorders [45, 46].

The specificity of impairment to the OFC further distinguishes the frontal CCI model from parietal CCI models. Numerous studies on the network between the hippocampus and frontal cortex have established that the ventral hippocampus (posterior parietal cortex; PPC) projects to the frontal cortex and vice versa [47]. The necessity of the hippocampus in reversal learning and rule shifting has been highlighted in two studies via chemical lesioning of the ventral hippocampus or PPC [48, 49]. Taken with the fact that the CCI lesion in the Bondi et al 2014 paper is an extremely severe injury that essentially ablates the hippocampus in one hemisphere, it follows that the parietal CCI can affect both reversal and set shift. In contrast, our frontal CCI model does not lesion either the OFC or mPFC, and hippocampal function is unaffected as measured by the novel object recognition assay. Furthermore, since mPFC-dependent rule shifting is unimpaired, our data implies that the frontal CCI only affects OFC-involved pathways. It is also possible that OFC-specific function is particularly vulnerable to frontal CCI independent of projections to the region. Investigating the OFC

further may allow us to identify cell populations and the underlying mechanisms affected by injury that lead to development of behavioral dysfunction.

The frontal CCI mouse model provides a behavioral foundation for exploring the effect of TBI on frontal lobe regions and their functionalities. The model recapitulates OFC-dependent deficits seen in human patients while sparing the function of the mPFC and hippocampus [11, 50, 51]. The specificity of the model's behavioral outcome distinguishes the OFC as a region of interest for future studies to differentiate the effects of parietal and frontal contusions and identify potential mechanisms that may not be affected in parietal injury models without severe damage to the brain. Further investigation of the physiological effects of frontal TBI in the OFC could help elucidate particularly vulnerable cell type populations and molecular targets to improve treatment for human TBI patients.

Materials and Methods

Animals. All experiments were conducted in accordance with National Institutes of Health *Guide for the Care and Use of Laboratory Animals* and were approved by the Institutional Animal Care and Use Committee of University of California (San Francisco). All C57B6/J wildtype (WT) male mice were purchased from Jackson Laboratory (Bar Harbor, ME) and used for experiments at approximately 12 weeks of age. Mice were group housed in environmentally controlled conditions with reverse light cycle (12:12h light:dark cycle at 21 ± 1°C) and provided food and water *ad libitum.*

Surgical Procedure. All animals were randomly assigned to TBI or sham surgeries. Animals were anesthetized and maintained at 2% isoflurane and secured to a stereotaxic frame with non-traumatic ear bars. The hair on their scalp was removed, and eye ointment and betadine were applied to their eyes and scalp respectively. A midline incision was made to expose the skull. TBI was induced in the frontal lobe using the controlled cortical impact (CCI) model [21]. Mice received a craniectomy ~2.5 mm in diameter using an electric microdrill. The coordinates of the craniectomy were: anteroposterior, +2.34 mm and mediolateral, +1.62 mm with respect to bregma. Any animal that experienced excessive bleeding due to disruption of the dura was removed from the study. After the craniectomy, the contusion was induced using a 2 mm convex tip attached to an electromagnetic impactor (Leica). The contusion depth was set to 1.25 mm from dura with a velocity of 4.0 m/s sustained for 300 ms. These injury parameters were chosen to target, but not penetrate, the medial and orbitofrontal regions of the PFC. After injury, the scalp was sutured and the animal was allowed to recover in an incubation chamber set to 37°C. Animals were returned to their home cage after showing normal walking and grooming behavior. Sham animals received craniectomy surgeries but without the CCI injury. On average animals recovered and were ambulatory within 10 minutes of removal from isoflurane exposure. After surgery animals were weighed weekly and monitored for indications of poor health including ambulation, muscle atrophy and emaciation, lethargy, infection of surgery site, anorexia, difficulty breathing, and difficulty remaining upright. Any animals that displayed such signs were monitored closely, treated if possible, and humanely euthanized based on

veterinarian recommendation. Animals fully recovered from the surgical procedures as exhibited by normal behavior and weight maintenance.

Behavioral Assays

Social Approach Task. At 29 d after surgery, a group of animals(n=16-17/group) were tested for sociability and social recognition behavior on the three-chamber social approach task as previously described [22]. Animals were placed individually into the center of a three-chamber environment and their behavior was recorded during three consecutive phases: habituation, sociability, and social recognition. During habituation phase, mice were allowed to explore the entirety of the empty environment for 10 minutes. Following habituation, mice were guided to the center chamber, and access to the chambers was blocked.

During the sociability phase, animals were tested for their preference for a novel mouse over a novel object. A stranger mouse from a different cage was placed into a small cylindrical cage on either the left or right chamber while a similar, but empty, cage was placed in the opposite chamber. Placement of stranger mouse into the right or left cage was chosen semi-randomly for each trial. Test mice were allowed to explore the stranger mouse and an empty cage for 10 minutes before being restricted in the center chamber again. During the social recognition phase, animals were tested for their preference for a novel mouse over a familiar mouse they previously encountered. In this phase, a new stranger animal from a third cage was placed into the previously empty cage. Test mice were allowed 5 minutes to explore the environment again, this time with the familiar mouse (from the sociability phase) and the new stranger mouse. The

environment and cage objects were cleaned with 0.025% bleach between test animals. Exploration was recorded using the previously mentioned video tracking and analysis setup (Ethovision XT 8.5, Noldus Information Technology) and analyzed for time spent interacting with the stimuli during the first three minutes of each phase. The Preference Ratio was calculated as the percent of time exploring the mouse vs percent of time exploring the object (empty cage) for phase 2 and as percent of time exploring the novel mouse vs percent of time exploring the familiar mouse for phase 3.

Rule Shift Assay. At 35-40 days post injury, animals (n=7/group) were tested for cognitive flexibility using the rule shift assay based upon the set shift paradigm as described by Bissonette et al. (2008) and the rule-shifting assay as described by Cho et al. (2015). Mice were housed either individually or in pairs and placed under food restriction for two days such that mice reached 80-85% of their starting body weights. During food restriction, mice were exposed to all assay components (e.g. bowls, textures, odors). The provided food during the assay consisted of normal chow and the food reward – pieces of Honey Nut Cheerios (General Mills). Both were placed in the bowls to associate the bowls with food and covered with prepared digging media.

The bowls used for the assay were purple, small Lixit Nibble Food Bowls (Amazon). The digging media consisted of two dimensions: odor and texture. The olfactory cues consisted of dried, ground spices: garlic powder, onion powder, paprika, and coriander (Simply Organic). Unscented digging media were obtained from local hardware and pet stores and the animal facility (Mosser Lee decorative white sand, unbranded unscented cat litter, alpha-dry bedding, or hardwood). The digging media and odors were utilized in two different combinations (e.g. Combination 1: sand and

litter with garlic and coriander. Combination 2: alpha-dry bedding and hardwood with paprika and coriander). Pairing of digging media and odors were made with 0.7% odor and 0.1% ground Cheerios by volume.

During habituation and test trials, mice were placed into a holding cage while the home cage was used as the test chamber [17]. In the test chamber, mice were presented with two bowls, each filled with a different texture-odor pair from a single combination. Only one of the bowls contained the food reward. During habituation, mice were given 10 consecutive trials. Mice were allowed three minutes to dig in both bowls to learn that only one bowl contained food on each trial. The animals were considered to have timed out of a trial if they failed to dig within the three minutes. Any animals that timed out of five trials on a single day were excluded from the study. The animals were exposed to every pair from both media combinations, and the food reward and cues had no correlation during habituation to prevent animals from forming any associations prior to the test days.

During test days, the mice were exposed to only a single media combination. They were allowed three minutes to explore the two bowls until they began digging, signifying a choice. If they correctly chose the rewarded bowl, they were returned to the holding cage after they had found and consumed the food reward. If they chose the incorrect bowl, they were returned to the holding cage after they had given up digging in the selected bowl without a chance to dig in the bowl with the reward and the trial was marked as an error. If they did not dig within the three minutes, they were returned to the holding cage and the trial was marked as a timed out trial.

Animals first had to learn an initial association where the food reward was associated with one of the four cues presented. The learning criterion was defined as eight successful choices in the last ten consecutive attempts. After the animal had learned the initial association, the rule was either reversed (e.g. texture to texture) or shifted (e.g. texture to odor). The animals continued with the trials until they met the learning criterion again for the new association. The reward was presented equally on the left and right of the test chamber and the order of the possible media pairs were pseudo-randomized through the assay such that animals were exposed to a media pair up to a maximum of three consecutive trials. The animals did not exhibit a preference for any cue over the others before forming initial associations (data not shown).

Animals were given three test days. On day 1, media combination 1 was used with a rule reversal after Initial Association. On day 2, media combination 2 was used with a rule reversal. On day 3, media combination 2 was used again but with a rule shift. The total errors to reach criterion were analyzed.

Animals were divided into two groups and tested on the rule shift assay either 35-40 days (n=7/group) or 5.5 months post-injury (n=10-11/group).

Elevated Plus Maze. At 28 d after surgery, animals were tested for anxiety on the elevated plus maze (EPM; n=21-22). The EPM consists of two exposed, open arms (35cm) opposite each other and two enclosed arms (30.5cm) also across from each other. The four arms are attached to a center platform (4.5 cm square) and the entire maze elevated 40cm off the floor [23]. Mice were placed individually onto the center of the maze and allowed to explore the maze for 5 minutes. Their activity was recorded using an overhead camera connected to a video tracking and analysis system

107

(Ethovision XT 8.5, Noldus Information Technology). The maze was cleaned with 0.025% bleach between animals.

Novel Object Recognition. At 31 d after surgery, a separate cohort of animals (n=9) from those that ran the previous assays were tested for hippocampal-dependent memory function using a mouse novel object recognition assay [19]. The test environment consists of an open field arena in a dimly lit behavioral testing room. Mice were allowed to explore the arena for two 10 minute periods for two consecutive days (habituation phase). On day three (training phase), two identical objects (red lego blocks) were secured to the floor in opposite corners of the arena using magnets and mice were allowed to explore the arena and objects for 5 minutes. 24hours later on day four (testing phase), one of the objects was replaced with a novel object (orange lego flower) of similar dimensions and texture. Mice were reintroduced in to the arena and allowed to explore for 5 minutes. The objects and arena were cleaned with 0.025% bleach between trials and animals. Trials were recorded using the video tracking and analysis setup (Ethovision XT 8.5, Noldus Information Technology) and manually scored. Exploratory behavior was defined as time the animals spent directing its nose towards an object within 3 cm of the object. Data was expressed as percent of time mice spent exploring each object. Mice that had less than 5 seconds of exploration time during either training or testing were excluded from analysis.

Tissue Collection. All mice were lethally overdosed using a mixture of ketamine (150mg/kg) and xylaxine (15mg/kg). Once animals were completely anesthetized, the chest cavity was opened and each animal was transcardially perfused with ice-cold

Hank's balanced salt without calcium and magnesium (HBSS; Gibco) followed by 4% paraformaldehyde (PFA) in buffered saline. Immediately after perfusion, brains were post-fixed in 4% PFA before being transferred to 30% sucrose and stored at 4°C.

Brain Tissue Sectioning and Imaging. All brain tissues used for imaging was sectioned as previously described (Morganti 2014). 40 µm free-floating sections were stained for neuronal nuclei (NeuN, MAB377, Millipore) with biotinylated secondary antibodies (Biotinylated anti-mouse IgG, BA-2001, Vector) and revealed with DAB (Sigmafast DAB tablets, Sigma-Aldrich). Sections were mounted onto Superfrost Plus slides (Fisher #12-550-15). All imaging was achieved using a Zeiss Imager.Z1 Apotome microscope controlled by ZEN software (Zeiss 2012).

Lesion Analysis. To calculate cortical volume for each animal, six sections evenly spaced at 240 um apart and centered at the epicenter of impact were analyzed utilizing a Zeiss Imager.M1 Apotome microscope at 2.5x magnification and the Cavalieri estimator in StereoInvestigator 10.0. Grid spacing was set to 200 um with slice cut thickness of 40 um for the Cavalieri estimator. Tissue loss was quantified as the percentage of ipsilateral volume over contralateral volume.

Data Analysis. Results were analyzed using Prism software (v6.05, GraphPad; La Jolla, CA) and expressed as mean ± standard error of the mean (SEM). Statistical analyses were performed using Student's t-test with p values of <0.05 considered as significant.
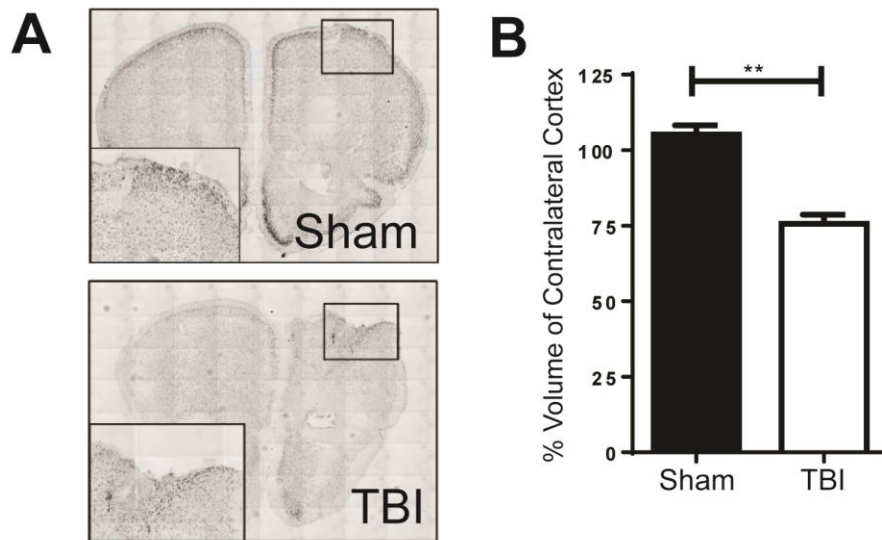
Figures

Figure 1. Frontal Lobe CCI results in a cavitation at site of injury. A. 40 days post-injury, qualitative NeuN staining reveal normal morphology in sham control animals (top) and a cavitation at site of injury in animals that had received a TBI (bottom). **B.** Injured animals showed approximately 25% cortical tissue loss (n=3/group; Student's t-Test; **p < 0.01).
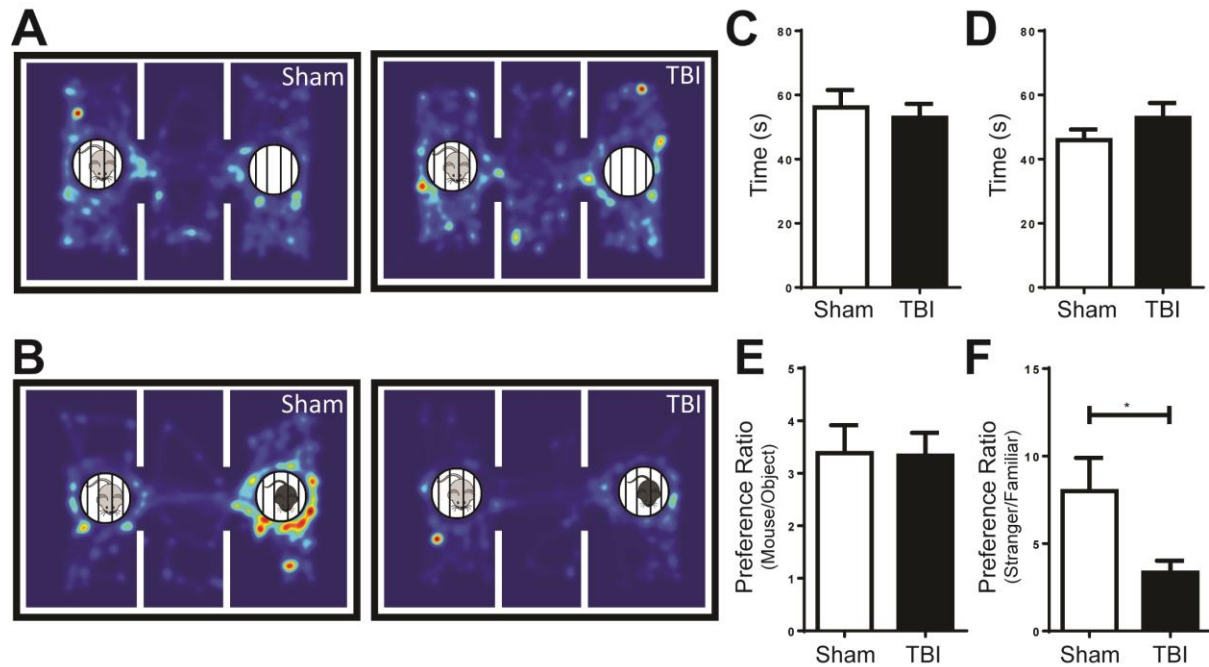
Figure 2. Injured mice demonstrate impairment in social recognition but not sociability on the three-chamber social approach task 1 month post-injury. A, B. Top-down heat map of the animal's nose point location during each phase cumulatively. During sociability (A), animals were exposed to a stranger mouse (left side, light grey) and an empty cage (right chamber). During social recognition (B), animals were exposed to the familiar mouse from the sociability phase (left chamber, light grey) and a new stranger mouse (right chamber, black). **C, D.** There were no differences in time spent exploring the stimuli during sociability (C) or social recognition (D) phases (Student's t-Test; $p > 0.05$). **E.** Animals that received a frontal lobe CCI did not exhibit any difference in preference for the mouse over the empty cage (object) during the sociability phase (Preference Ratio>1; Student's t-Test; $p > 0.05$). **F.** Animals that received a frontal lobe CCI had significantly less preference for the stranger over the familiar mouse during the social recognition phase (n=16-17/group; Student's t-Test; *$p < 0.05$).
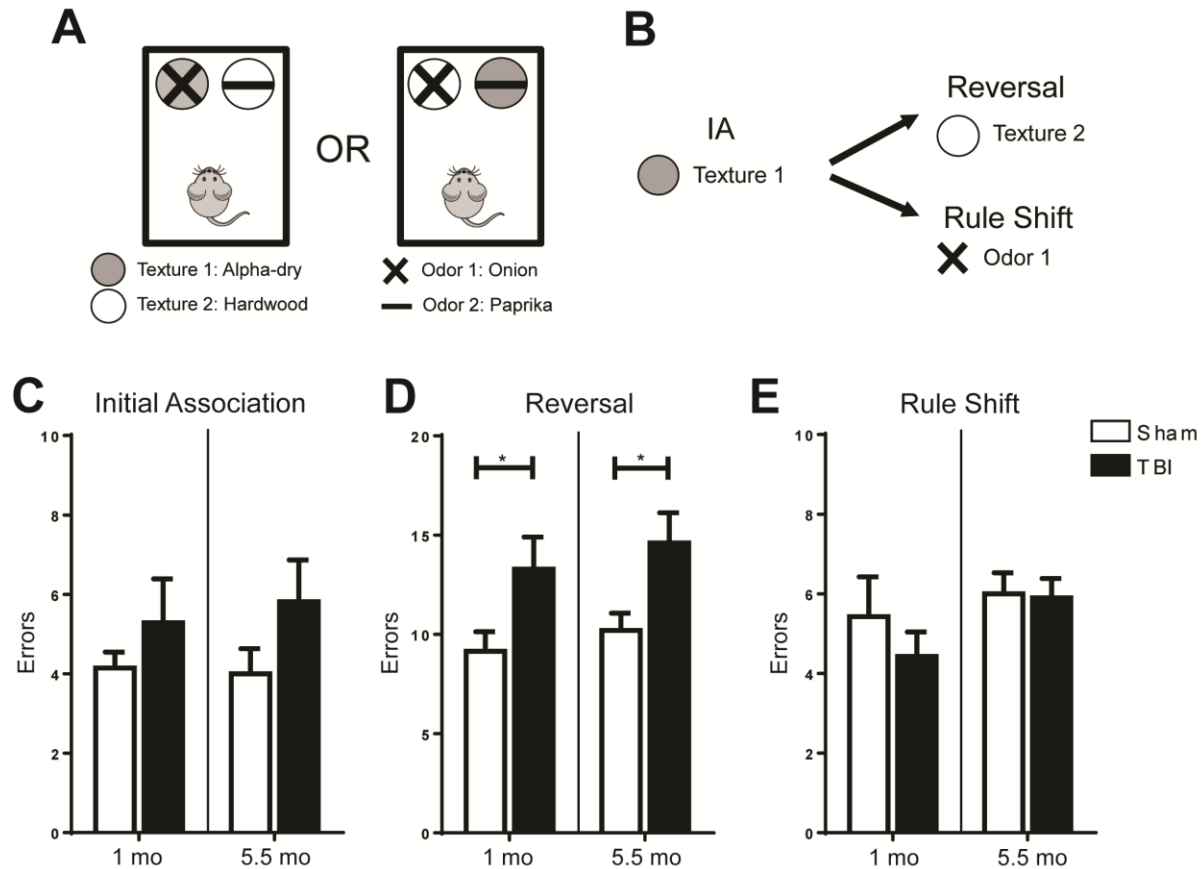
Figure 3. Frontal lobe TBI impairs reversal learning but not rule shifting at 1 month post-injury and the deficit persist at 5.5 months after injury. A. Animals were presented with a combination of two textures and two odors during each test day. **B.** Animals first learned to associate a single cue with a food reward. After successfully learning the initial association (IA), animals were tested on either reversal learning or rule shifting which changed the association to a cue within the same or second dimension respectively. **C.** There was no difference between sham and TBI animals on forming an initial association (1mo: n=7/group; 5.5mo: n=9-10/group; Student's t-Test; p > 0.05). **D.** Animals with frontal lobe TBIs made significantly more errors during the reversal task than their sham controls at 1 month after injury. A second cohort exhibited

112

the same effect at 5.5 months after injury (Student's t-Test; *p < 0.05). **E.** Frontal lobe

TBI did not significantly affect rule shifting performance at either 1 month or 5.5 months
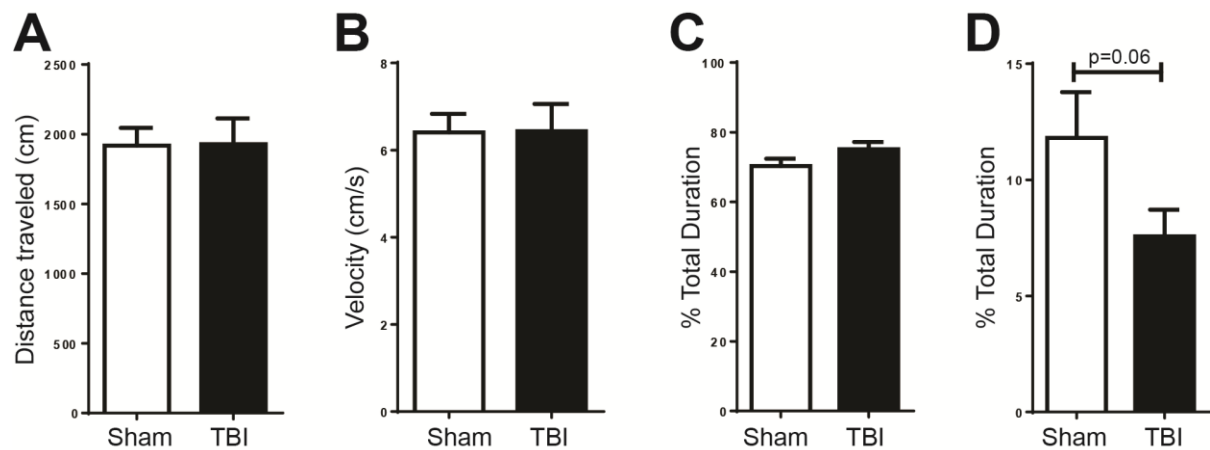
after injury (Student's t-Test; p > 0.05).

Figure 4. Animals with frontal lobe TBIs exhibit a trend for increased anxiety on the elevated plus maze at 1 month post-injury. A. Injured animals traversed as much distance as sham animals did (Student's t-Test; p>0.05) and **B.** displayed no difference in movement speed (Student's t-Test; p > 0.05). **C.** Injured animals did not spend more time in the closed arms (Student's t-Test; p = 0.11), but **D.** did have a trend for less time spent exploring the open arms of the maze (n=21-22/group; Student's t-Test; p = 0.06).
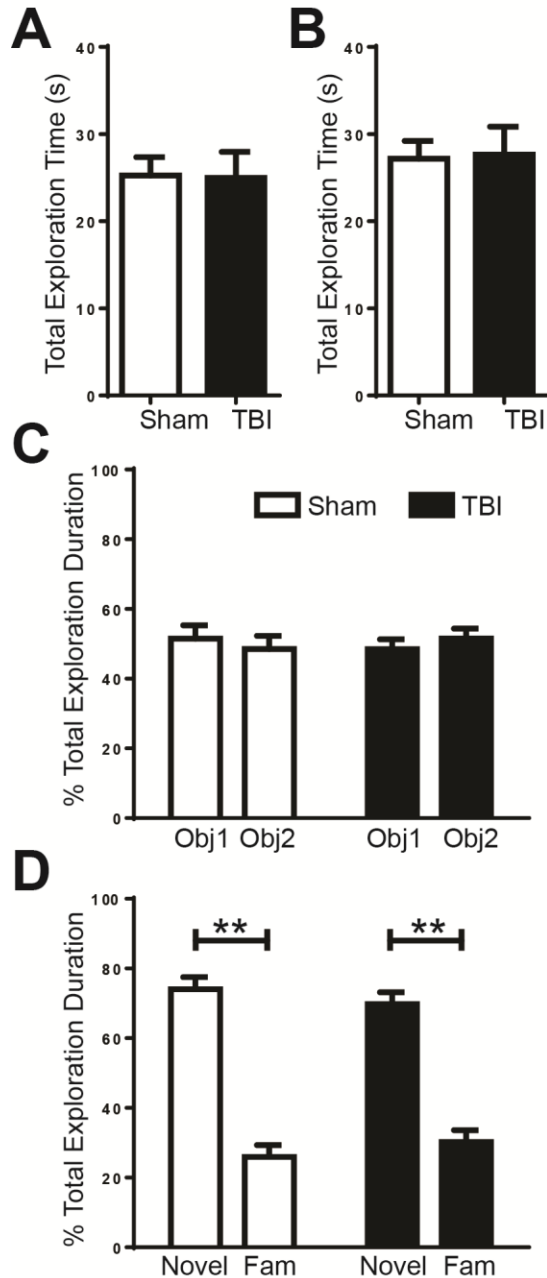
Figure 5. Frontal lobe TBI does not affect recognition memory on hippocampal-dependent novel object recognition task. A, B. Sham and TBI animals did not differ significantly on their exploration time during training (A) or test (B) trials (Student's t-Test; $p > 0.05$). **C.** There was no preference for either of the two identical objects (Obj1, Obj2) in sham (white) and TBI (black) animals (Student's t-Test; $p > 0.05$). **D.** Animals were tested 24 hours after the initial training and both sham (white) and TBI (black)

animals significantly preferred to explore the novel object (Novel) over the familiar object (Fam) (n=9/group; Student's t-Test; **$p < 0.01$).

References

1. Coronado VG, McGuire LC, Sarmiento K, Bell J, Lionbarger MR, Jones CD, et al. Trends in Traumatic Brain Injury in the U.S. and the public health response: 1995-2009. J Safety Res. 2012;43(4):299-307. doi: 10.1016/j.jsr.2012.08.011. PubMed PMID: 23127680.

2. Corrigan JD, Selassie AW, Orman JA. The epidemiology of traumatic brain injury. J Head Trauma Rehabil. 2010;25(2):72-80. doi: 10.1097/HTR.0b013e3181ccc8b4. PubMed PMID: 20234226.

3. Ponsford J, Draper K, Schonberger M. Functional outcome 10 years after traumatic brain injury: its relationship with demographic, injury severity, and cognitive and emotional status. J Int Neuropsychol Soc. 2008;14(2):233-42. doi: 10.1017/S1355617708080272. PubMed PMID: 18282321.

4. Engberg AW, Teasdale TW. Psychosocial outcome following traumatic brain injury in adults: a long-term population-based follow-up. Brain Inj. 2004;18(6):533-45. doi: 10.1080/02699050310001645829. PubMed PMID: 15204335.

5. Fujiwara E, Schwartz ML, Gao F, Black SE, Levine B. Ventral frontal cortex functions and quantified MRI in traumatic brain injury. Neuropsychologia. 2008;46(2):461-74. doi: 10.1016/j.neuropsychologia.2007.08.027. PubMed PMID: 17976665; PubMed Central PMCID: PMCPMC2287189.

6. Wallesch CW, Curio N, Galazky I, Jost S, Synowitz H. The neuropsychology of blunt head injury in the early postacute stage: effects of focal lesions and diffuse axonal injury. J Neurotrauma. 2001;18(1):11-20. doi: 10.1089/089771501750055730. PubMed PMID: 11200246.

7. Stuss DT. Traumatic brain injury: relation to executive dysfunction and the frontal lobes. Curr Opin Neurol. 2011;24(6):584-9. doi: 10.1097/WCO.0b013e32834c7eb9. PubMed PMID: 21968550.

8. McAllister TW. Neurobehavioral sequelae of traumatic brain injury: evaluation and management. World Psychiatry. 2008;7(1):3-10. PubMed PMID: 18458777; PubMed Central PMCID: PMCPMC2327235.

9. Cicerone KD, Tanenbaum LN. Disturbance of social cognition after traumatic orbitofrontal brain injury. Arch Clin Neuropsychol. 1997;12(2):173-88. PubMed PMID: 14588429.

10. Stuss DT, Levine B, Alexander MP, Hong J, Palumbo C, Hamer L, et al. Wisconsin Card Sorting Test performance in patients with focal frontal and posterior brain damage: effects of lesion location and test structure on separable cognitive processes. Neuropsychologia. 2000;38(4):388-402. PubMed PMID: 10683390.

11. Levin HS, Goldstein FC, High WM, Jr., Eisenberg HM. Disproportionately severe memory deficit in relation to normal intellectual functioning after closed head injury. J Neurol Neurosurg Psychiatry. 1988;51(10):1294-301. PubMed PMID: 3225586; PubMed Central PMCID: PMCPMC1032918.

12. Warden DL, Gordon B, McAllister TW, Silver JM, Barth JT, Bruns J, et al. Guidelines for the pharmacologic treatment of neurobehavioral sequelae of traumatic

brain injury. J Neurotrauma. 2006;23(10):1468-501. doi: 10.1089/neu.2006.23.1468. PubMed PMID: 17020483.

13. Harvey AG, Bryant RA. Predictors of acute stress following mild traumatic brain injury. Brain Injury. 1998;12(2):147-54. doi: 10.1080/026990598122773.

14. Spikman JM, Timmerman ME, Milders MV, Veenstra WS, van der Naalt J. Social cognition impairments in relation to general cognitive deficits, injury severity, and prefrontal lesions in traumatic brain injury patients. J Neurotrauma. 2012;29(1):101-11. doi: 10.1089/neu.2011.2084. PubMed PMID: 21933011.

15. Yang M, Silverman JL, Crawley JN. Automated three-chambered social approach task for mice. Curr Protoc Neurosci. 2011;Chapter 8:Unit 8 26. doi: 10.1002/0471142301.ns0826s56. PubMed PMID: 21732314.

16. Semple BD, Canchola SA, Noble-Haeusslein LJ. Deficits in social behavior emerge during development after pediatric traumatic brain injury in mice. J Neurotrauma. 2012;29(17):2672-83. doi: 10.1089/neu.2012.2595. PubMed PMID: 22888909; PubMed Central PMCID: PMCPMC3510450.

17. Cho KK, Hoch R, Lee AT, Patel T, Rubenstein JL, Sohal VS. Gamma rhythms link prefrontal interneuron dysfunction with cognitive inflexibility in Dlx5/6(+/-) mice. Neuron. 2015;85(6):1332-43. doi: 10.1016/j.neuron.2015.02.019. PubMed PMID: 25754826; PubMed Central PMCID: PMCPMC4503262.

18. Rogers JT, Morganti JM, Bachstetter AD, Hudson CE, Peters MM, Grimmig BA, et al. CX3CR1 deficiency leads to impairment of hippocampal cognitive function and synaptic plasticity. J Neurosci. 2011;31(45):16241-50. doi: 10.1523/JNEUROSCI.3667-11.2011. PubMed PMID: 22072675; PubMed Central PMCID: PMCPMC3236509.

19. Mumby DG, Gaskin S, Glenn MJ, Schramek TE, Lehmann H. Hippocampal damage and exploratory preferences in rats: memory for objects, places, and contexts. Learn Mem. 2002;9(2):49-57. doi: 10.1101/lm.41302. PubMed PMID: 11992015; PubMed Central PMCID: PMCPMC155935.

20. Thierry AM, Gioanni Y, Degenetais E, Glowinski J. Hippocampo-prefrontal cortex pathway: anatomical and electrophysiological characteristics. Hippocampus. 2000;10(4):411-9. doi: 10.1002/1098-1063(2000)10:4<411::AID-HIPO7>3.0.CO;2-A. PubMed PMID: 10985280.

21. Morganti JM, Jopson TD, Liu S, Riparip LK, Guandique CK, Gupta N, et al. CCR2 antagonism alters brain macrophage polarization and ameliorates cognitive dysfunction induced by traumatic brain injury. J Neurosci. 2015;35(2):748-60. doi: 10.1523/JNEUROSCI.2405-14.2015. PubMed PMID: 25589768; PubMed Central PMCID: PMCPMC4293420.

22. Moy SS, Nadler JJ, Perez A, Barbaro RP, Johns JM, Magnuson TR, et al. Sociability and preference for social novelty in five inbred strains: an approach to assess autistic-like behavior in mice. Genes Brain Behav. 2004;3(5):287-302. doi: 10.1111/j.1601-1848.2004.00076.x. PubMed PMID: 15344922.

23. Lister RG. The use of a plus-maze to measure anxiety in the mouse. Psychopharmacology (Berl). 1987;92(2):180-5. PubMed PMID: 3110839.

24. McDonald S. Impairments in social cognition following severe traumatic brain injury. J Int Neuropsychol Soc. 2013;19(3):231-46. doi: 10.1017/S1355617712001506. PubMed PMID: 23351330.

25. Gentry LR, Godersky JC, Thompson B. MR imaging of head trauma: review of the distribution and radiopathologic features of traumatic lesions. AJR Am J Roentgenol. 1988;150(3):663-72. doi: 10.2214/ajr.150.3.663. PubMed PMID: 3257624.

26. Kinnunen KM, Greenwood R, Powell JH, Leech R, Hawkins PC, Bonnelle V, et al. White matter damage and cognitive impairment after traumatic brain injury. Brain. 2011;134(Pt 2):449-63. doi: 10.1093/brain/awq347. PubMed PMID: 21193486; PubMed Central PMCID: PMCPMC3030764.

27. Robinson KE, Fountain-Zaragoza S, Dennis M, Taylor HG, Bigler ED, Rubin K, et al. Executive functions and theory of mind as predictors of social adjustment in childhood traumatic brain injury. J Neurotrauma. 2014;31(22):1835-42. doi: 10.1089/neu.2014.3422. PubMed PMID: 25003478; PubMed Central PMCID: PMCPMC4224037.

28. Klemenhagen KC, O'Brien SP, Brody DL. Repetitive concussive traumatic brain injury interacts with post-injury foot shock stress to worsen social and depression-like behavior in mice. PLoS One. 2013;8(9):e74510. doi: 10.1371/journal.pone.0074510. PubMed PMID: 24058581; PubMed Central PMCID: PMCPMC3776826.

29. Sobota R, Mihara T, Forrest A, Featherstone RE, Siegel SJ. Oxytocin reduces amygdala activity, increases social interactions, and reduces anxiety-like behavior irrespective of NMDAR antagonism. Behav Neurosci. 2015;129(4):389-98. doi: 10.1037/bne0000074. PubMed PMID: 26214213; PubMed Central PMCID: PMCPMC4518468.

30. Allsop SA, Vander Weele CM, Wichmann R, Tye KM. Optogenetic insights on the relationship between anxiety-related behaviors and social deficits. Front Behav

Neurosci. 2014;8:241. doi: 10.3389/fnbeh.2014.00241. PubMed PMID: 25076878; PubMed Central PMCID: PMCPMC4099964.

31. Bissonette GB, Martins GJ, Franz TM, Harper ES, Schoenbaum G, Powell EM. Double dissociation of the effects of medial and orbital prefrontal cortical lesions on attentional and affective shifts in mice. J Neurosci. 2008;28(44):11124-30. doi: 10.1523/JNEUROSCI.2820-08.2008. PubMed PMID: 18971455; PubMed Central PMCID: PMCPMC2657142.

32. Schoenbaum G, Setlow B, Nugent SL, Saddoris MP, Gallagher M. Lesions of orbitofrontal cortex and basolateral amygdala complex disrupt acquisition of odor-guided discriminations and reversals. Learn Mem. 2003;10(2):129-40. doi: 10.1101/lm.55203. PubMed PMID: 12663751; PubMed Central PMCID: PMCPMC196660.

33. Greve KW, Love JM, Sherwin E, Mathias CW, Ramzinski P, Levy J. Wisconsin Card Sorting Test in chronic severe traumatic brain injury: factor structure and performance subgroups. Brain Inj. 2002;16(1):29-40. doi: 10.1080/0269905011008803. PubMed PMID: 11796097.

34. Wiegner S, Donders J. Performance on the Wisconsin Card Sorting Test after traumatic brain injury. Assessment. 1999;6(2):179-87. PubMed PMID: 10335020.

35. McAlonan K, Brown VJ. Orbital prefrontal cortex mediates reversal learning and not attentional set shifting in the rat. Behavioural Brain Research. 2003;146(1-2):97-103. doi: 10.1016/j.bbr.2003.09.019.

36. Bondi CO, Cheng JP, Tennant HM, Monaco CM, Kline AE. Old dog, new tricks: the attentional set-shifting test as a novel cognitive behavioral task after controlled cortical

impact injury. J Neurotrauma. 2014;31(10):926-37. doi: 10.1089/neu.2013.3295. PubMed PMID: 24397572; PubMed Central PMCID: PMCPMC4012626.

37. Schwarzbold ML, Rial D, De Bem T, Machado DG, Cunha MP, dos Santos AA, et al. Effects of traumatic brain injury of different severities on emotional, cognitive, and oxidative stress-related parameters in mice. J Neurotrauma. 2010;27(10):1883-93. doi: 10.1089/neu.2010.1318. PubMed PMID: 20649482.

38. Prasad KN, Bondy SC. Common biochemical defects linkage between post-traumatic stress disorders, mild traumatic brain injury (TBI) and penetrating TBI. Brain Res. 2015;1599:103-14. doi: 10.1016/j.brainres.2014.12.038. PubMed PMID: 25553619.

39. Siopi E, Llufriu-Daben G, Fanucchi F, Plotkine M, Marchand-Leroux C, Jafarian-Tehrani M. Evaluation of late cognitive impairment and anxiety states following traumatic brain injury in mice: the effect of minocycline. Neurosci Lett. 2012;511(2):110-5. doi: 10.1016/j.neulet.2012.01.051. PubMed PMID: 22314279.

40. Pandey DK, Yadav SK, Mahesh R, Rajkumar R. Depression-like and anxiety-like behavioural aftermaths of impact accelerated traumatic brain injury in rats: a model of comorbid depression and anxiety? Behav Brain Res. 2009;205(2):436-42. doi: 10.1016/j.bbr.2009.07.027. PubMed PMID: 19660499.

41. Rodgers KM, Bercum FM, McCallum DL, Rudy JW, Frey LC, Johnson KW, et al. Acute neuroimmune modulation attenuates the development of anxiety-like freezing behavior in an animal model of traumatic brain injury. J Neurotrauma. 2012;29(10):1886-97. doi: 10.1089/neu.2011.2273. PubMed PMID: 22435644; PubMed Central PMCID: PMCPMC3390983.

42. Mauri MC, Paletta S, Colasanti A, Miserocchi G, Altamura AC. Clinical and neuropsychological correlates of major depression following post-traumatic brain injury, a prospective study. Asian J Psychiatr. 2014;12:118-24. doi: 10.1016/j.ajp.2014.07.003. PubMed PMID: 25193507.

43. Young JW, Powell SB, Geyer MA, Jeste DV, Risbrough VB. The mouse attentional-set-shifting task: a method for assaying successful cognitive aging? Cogn Affect Behav Neurosci. 2010;10(2):243-51. doi: 10.3758/CABN.10.2.243. PubMed PMID: 20498348; PubMed Central PMCID: PMCPMC2877277.

44. Placek K, Dippel WC, Jones S, Brady AM. Impairments in set-shifting but not reversal learning in the neonatal ventral hippocampal lesion model of schizophrenia: further evidence for medial prefrontal deficits. Behav Brain Res. 2013;256:405-13. doi: 10.1016/j.bbr.2013.08.034. PubMed PMID: 23994544.

45. Milad MR, Rauch SL. The role of the orbitofrontal cortex in anxiety disorders. Ann N Y Acad Sci. 2007;1121:546-61. doi: 10.1196/annals.1401.006. PubMed PMID: 17698998.

46. Wood JN. Social cognition and the prefrontal cortex. Behav Cogn Neurosci Rev. 2003;2(2):97-114. doi: 10.1177/1534582303253625. PubMed PMID: 13678518.

47. Preston AR, Eichenbaum H. Interplay of hippocampus and prefrontal cortex in memory. Curr Biol. 2013;23(17):R764-73. doi: 10.1016/j.cub.2013.05.041. PubMed PMID: 24028960; PubMed Central PMCID: PMCPMC3789138.

48. Fox MT, Barense MD, Baxter MG. Perceptual attentional set-shifting is impaired in rats with neurotoxic lesions of posterior parietal cortex. J Neurosci. 2003;23(2):676-81. PubMed PMID: 12533627.

49. Brooks JM, Pershing ML, Thomsen MS, Mikkelsen JD, Sarter M, Bruno JP. Transient inactivation of the neonatal ventral hippocampus impairs attentional set-shifting behavior: reversal with an alpha7 nicotinic agonist. Neuropsychopharmacology. 2012;37(11):2476-86. doi: 10.1038/npp.2012.106. PubMed PMID: 22781844; PubMed Central PMCID: PMCPMC3442342.

50. Catroppa C, Crossley L, Hearps SJ, Yeates KO, Beauchamp M, Rogers K, et al. Social and behavioral outcomes: pre-injury to six months following childhood traumatic brain injury. J Neurotrauma. 2015;32(2):109-15. doi: 10.1089/neu.2013.3276. PubMed PMID: 24773028.

51. Rudebeck PH, Murray EA. The orbitofrontal oracle: cortical mechanisms for the prediction and evaluation of specific behavioral outcomes. Neuron. 2014;84(6):1143-56. doi: 10.1016/j.neuron.2014.10.049. PubMed PMID: 25521376; PubMed Central PMCID: PMCPMC4271193.

Publishing Agreement

It is the policy of the University to encourage the distribution of all theses, dissertations, and manuscripts. Copies of all UCSF theses, dissertations, and manuscripts will be routed to the library via the Graduate Division. The library will make all theses, dissertations, and manuscripts accessible to the public and will preserve these to the best of their abilities, in perpetuity.

Please sign the following statement:

I hereby grant permission to the Graduate Division of the University of California, San Francisco to release copies of my thesis, dissertation, or manuscript to the Campus Library to provide access and preservation, in whole or in part, in perpetuity.

_____   8/16/17
Author Signature   _____
                                     Date